

**Molecular genetic characterization of the  
mouse truncate (*tc*) mutation**

Von Der Naturwissenschaftlichen Fakultät der Universität Hannover

Zur Erlangung des Grades

Doktorin der Naturwissenschaften

**Dr.rer.nat**

Genehmigte Dissertation

Von

Lic.Biol. **Hanaa Ben Abdelkhalek**

Geboren am 14.12.1970 in Ksar El Kebir, Marokko

**2006**

Referent: Prof.Dr.rer.nat. Achim Gossler

Koreferentin: Prof.Dr.rer.nat. Rita Gerardy-Schahn

Tag der Disputation: 7.02.2006

**Keywords:** truncate mutation, notochord development, node, *Not* gene,  
homeodomain protein, *Foxa2*, *T*, left-right asymmetry

**Schlagworte:** Truncate Mutation, Entwicklung des Notochords, Node, *Not* gen,  
Homeodomäne protein, *Foxa2*, *T*, Links-Rechts Asymetrie

## Abstract

The aim of the present PhD thesis is to identify and characterize the gene responsible for the mouse truncate (*tc*) mutation. Truncate is an autosomal recessive spontaneous mutation perturbing the development of the caudal notochord during embryogenesis. We have identified a homeobox gene, which based on sequence and expression pattern represents a murine member of the vertebrate *Not* gene family. We demonstrate that the truncate phenotype is due to a mutation in the coding sequence of *Not* gene. The truncate allele (*Not*<sup>*tc/tc*</sup>) contains a point mutation in the homeobox of *Not* that changes a conserved Phenylalanine residue in helix 1 to a Cysteine (F20C), and significantly destabilizes the homeodomain. Reversion of F20C in one allele of homozygous *tc* embryonic stem (ES) cells is sufficient to restore normal notochord formation in completely ES cell-derived Embryos.

The phenotype of the *Not*<sup>*tc/tc*</sup> allele and the expression domain of *Not* indicates that during mouse embryonic development proper *Not* function is essential for posterior notogenesis. We report here that *Foxa2* and *T* acts upstream of *Not* in the genetic cascade governing notogenesis, since *Not* expression is abolished in *Foxa2* and *T* mutant embryos. This is in contrast to zebrafish embryos, in which *flh* (zebrafish *Not*) acts upstream of *ntl* (zebrafish *T*) and interacting in a regulatory loop, and is essential for the development of the entire notochord, suggesting that the genetic control of notochord development in different vertebrate species has diverged during evolution. Additionally, we demonstrate in transactivation Luciferase assays that *Foxa2* is most likely a direct regulator of *Not*. An approximate 12kb upstream genomic region of *Not* spanning the first exon and intron fused to a *lacZ* reporter gene, and containing the *cis*-regulatory sequences, are able to drive the expression in the notochord, however not sufficient to reproduce the endogenous expression pattern of *Not* in transgenic embryos. This finding suggests that regulatory elements for the restriction of expression to notochord are located either upstream or downstream of the genomic region tested in the transgene.

We also report that truncate mutation affects laterality leading to a positional randomization of the organs in mice, suggesting that proper *Not* function is required for the normal establishment of the left-right determination. The expression of L-R marker *Nodal* is altered in *Not*<sup>*tc/tc*</sup> mutants, suggesting that *Not* regulates *Nodal* expression either directly or indirectly. Our analysis support the previously proposed idea which suggests that laterality defects are associated to abnormal midline tissue such as notochord. The identification of novel, so far unknown mutants with impaired laterality is essential for the further understanding of LR-axis formation in vertebrates.

## Zusammenfassung

Diese Promotionsarbeit hatte das Ziel, das in der truncate (*tc*) Mutation der Maus betroffene Gen zu identifizieren und zu charakterisieren. Bei *tc* handelt es sich um eine autosomale rezessive Mutation, welche die Entwicklung des kaudalen Notochords während der frühen Embryogenese stört. Als ein möglicher Kandidat wurde ein murines homeobox Gen identifiziert, welches aufgrund der Sequenzhomologie und des Expressionsmusters im Vergleich zu anderen Vertebraten (Zebrafisch, *Xenopus* und chick) dem zu diesem Zeitpunkt noch unbekanntem murinen *Not* Gen entspricht. Im Gegensatz zum Zebrafisch zeigte das murine *Not* eine Restriktion der Expression im kaudalen Notochord. Als Ursache des Phänotyps in den Mutanten wurde eine Punktmutation in der Homeobox vom *Not* identifiziert. Diese wandelt einen erhaltenen Phenylalanin-rest in der Helix 1 zu Cystein (F20C) um und destabilisiert die Homeodomäne in vitro merklich. Die durchgeführte Restauration der F20C-Punktmutation in einem Allel homozygotischer *tc* embryonischer Stammzellen war für eine normale Notochord-Bildung in allen von diesen embryonalen Stammzellen abgeleiteten Embryonen ausreichend.

Eine Analyse der Genregulation zeigte, daß die Transkriptionsfaktoren *Foxa2* und *T* genetisch oberhalb von *Not* agieren. *Foxa2* (-/-) und *T* (-/-) mutante Embryos wiesen den vollständigen Verlust der *Not* Expression auf. Dies steht im Gegensatz zu den Embryonen des Zebrafischs, in denen *flh* (Zebrafisch *Not*) mit *ntl* (Zebrafisch *T*) in einer regulatorischen Schleife wechselwirkt und für die Entwicklung des gesamten Notochords wichtig ist. Dies legt die Vermutung nahe, daß eine unterschiedliche genetische Kontrolle der Notochord Bildung in unterschiedlichen vertebraten Spezies stattfindet. In *trans*-aktivierenden Luciferase-Assays konnte eine direkte Regulation einer 12kb upstream Region von *Not* einschließlich des ersten Exons und Introns durch *Foxa2* nachgewiesen werden. Die Promoter Analyse weist darauf hin, dass diese mit dem *lac Z* Reporter Gen fusionierte 12kb Sequenz in der Lage ist, die Expression im Notochord anzuregen, aber für die Reproduktion des endogenen Expressionsmusters von *Not* in transgenen Embryonen nicht ausreichend ist. Dieser Zusammenhang führt zu dem Schluß, daß sich zusätzliche die Restriktion der Expression des Notochord regulierende Elemente entweder upstream oder downstream außerhalb der untersuchten genomischen Region im Transgen befinden.

Weiterhin konnte gezeigt werden, daß die truncate Mutation auch die Rechts-Links Ausrichtung der inneren Organe stört. Zusätzlich wurde eine gestörte Expression des Rechts-Links Markers *Nodal* in truncate mutierten Embryos als Hinweis darauf gefunden, daß die *Nodal* Expression direkt oder indirekt durch *Not* beeinflusst wird. Dieses ist ein weiterer Beleg dafür, daß abnorme Mittelliniengewebe wie Notochord die Rechts-Links Ausrichtung beeinflussen.

# Projektskizze

Die truncate (*tc*) Mutation der Maus stört die Entwicklung des kaudalen Notochords. Im Rahmen der Doktorarbeit sollen verschiedene Untersuchungen durchgeführt werden:

1. Identifizierung des betroffenen Gens der “truncate Mutation”
2. Expressionsanalyse des betroffenen Gens
  - In wild-typ Embryonen
  - In truncate mutanten Embryonen
3. Identifizierung der Natur der “truncate Mutation”
4. Funktionelle Analyse der “truncate Mutation”
  - In vitro
  - In vivo
5. Regulation des *tc* Gens
  - Position des *tc* Gens in der Genetischen Kaskade der Notocherdentwicklung
  - Identifizierung von potentiellen direkten Regulatoren des *tc* Gens
  - Promoter Analyse des *tc* Gens in Reporter *lacZ* transgene
6. Analyse des Phänotyps von truncate Mutanten
  - Histologisch / Makroskopisch
  - Marker gen Analyse in truncate mutanten Embryonen.

# Contents

<i>Abstract</i> .....	
<i>Zusammenfassung</i> .....	
<i>Projektskizze</i> .....	
<b>1. Introduction</b> .....	<b>1</b>
1.1 <i>Some aspects of notochord development</i> .....	1
1.2 <i>Notochord Significance in tissues patterning</i> .....	3
1.2.1 <i>NOTOCHORD SIGNALLING TO MESODERM</i> .....	4
1.2.1.1 <i>The role of the notochord in somite differentiation</i> .....	4
1.2.1.2 <i>The role of the notochord in vertebral chondrogenesis</i> .....	6
1.2.1.3 <i>The role of the notochord in vertebral column segmentation</i> .....	6
1.2.1.4 <i>Notochord Patterning of Other Mesodermal Tissues</i> .....	8
1.2.2 <i>NOTOCHORD SIGNALLING TO ECTODERM</i> .....	9
1.2.2.1 <i>Notochord Patterning of the Neural Tube</i> .....	9
1.2.2.2 <i>Notochord Patterning of Other Ectoderm Derivatives</i> .....	10
1.2.3 <i>NOTOCHORD SIGNALLING TO THE ENDODERM</i> .....	10
1.2.3.1 <i>Proximity of Notochord and Endoderm</i> .....	11
1.2.3.2 <i>Medical Examples Implicating the Notochord in Endodermal Development</i> .....	11
1.2.3.3 <i>Notochord signals are required for pancreas development</i> .....	12
1.2.3.4 <i>Notochord signals are required for hypochord formation</i> .....	12
1.2.3.5 <i>Possible nature of notochord signals</i> .....	13
1.3 <i>Notochord and the organizer "node"</i> .....	14
1.4 <i>Genetic control of notochord development</i> .....	16
1.5 <i>Truncate mutation (tc)</i> .....	18
<b>2. Materials and methods</b> .....	<b>22</b>
2.1 <i>Chemicals</i> .....	22
2.2 <i>Apparatus</i> .....	24
2.3 <i>Oligonucleotides</i> .....	25
2.4 <i>Vectors</i> .....	27
2.4.1 <i>Cloning vectors</i> .....	27
2.4.2 <i>Expression vectors</i> .....	27
2.5 <i>E.Coli strains</i> .....	27
2.6 <i>E.Coli medium</i> .....	27
2.7 <i>Cell culture medium</i> .....	28
2.8 <i>Cell line</i> .....	29
2.9 <i>Molecular Biology Methods</i> .....	29
2.9.1 <i>DNA-Methods</i> .....	29
2.9.1.1 <i>Agarose gel Electrophoresis</i> .....	29
2.9.1.2 <i>Quantitation of DNA with absorption spectroscopy</i> .....	30
2.9.1.3 <i>Digestion of DNA with restriction endonucleases</i> .....	30
2.9.1.4 <i>Isolation and purification of DNA restriction fragments from agarose gels</i> .....	30
2.9.1.5 <i>Dephosphorylation of vector DNA by alkaline-phosphatase</i> .....	31
2.9.1.6 <i>Transformation of E.coli competent cells with plasmid DNA by electroporation</i>	31

2.9.1.7	<i>Plasmid isolation using alkaline lysis miniprep</i> .....	32
2.9.1.8	<i>Plasmid isolation using NucleoSpin Kit</i> .....	32
2.9.1.9	<i>Isolation of Genomic DNA from mouse tissue</i> .....	33
2.9.1.10	<i>Enzymatic amplification of genomic DNA by PCR reaction</i> .....	33
2.9.1.11	<i>Cloning techniques</i> .....	34
2.9.1.11.1	<i>Subcloning into pGEMT-Easy vector</i> .....	34
2.9.1.11.2	<i>Subcloning into TOPO-XL-PCR vector</i> .....	35
2.9.1.11.3	<i>Ligation of DNA and (Vector: Insert) Ratio</i> .....	35
2.9.1.12	<i>Southern blot analysis</i> .....	36
2.9.1.12.1	<i>Labeling of DNA by Random Oligonucleotide-Primed synthesis</i> .....	36
2.9.1.12.2	<i>DNA Blotting onto a nylon membrane using an alkaline buffer</i> .....	36
2.9.1.12.3	<i>Hybridization analysis of DNA blot with radiolabeled DNA probe</i> .....	37
2.9.2	<i>RNA-Methods</i> .....	38
2.9.2.1	<i>Isolation of total RNA from mouse tissue</i> .....	38
2.9.2.2	<i>Quantitation of RNA with absorption spectroscopy</i> .....	38
2.9.2.3	<i>Amplification of cDNA by RT-PCR</i> .....	38
2.9.2.4	<i>Synthesis of digoxigenin-labeled riboprobes</i> .....	39
2.9.2.5	<i>Whole-Mount in Situ Hybridization and detection of RNAs in mouse embryos</i> ...	40
2.10	<i>Cell Biology Methods</i> .....	43
2.10.1	<i>Cell culture conditions</i> .....	43
2.10.2	<i>Trypsinizing and subculturing cells</i> .....	43
2.10.3	<i>Freezing cells</i> .....	43
2.10.4	<i>Thawing and recovering cells</i> .....	44
2.10.5	<i>Calcium-Phosphate-mediated transfection of HEK293 cells</i> .....	44
2.11	<i>Biochemical Methods</i> .....	45
2.11.1	<i>Transactivation Assay</i> .....	45
2.11.1.1	<i>Measurement of Luciferase activity</i> .....	45
2.11.1.2	<i>Measurement of <math>\beta</math>-galactosidase activity</i> .....	46
2.11.2	<i>Whole-Mount histochemical detection of <math>\beta</math>-galactosidase activity</i> .....	46
2.12	<i>Histology Methods</i> .....	47
2.12.1	<i>Analysis of WISH-Paraffin-Sections after Eosin-staining</i> .....	47
2.12.2	<i>Skeleton preparation</i> .....	47
2.13	<i>Embryology Methods</i> .....	48
2.13.1	<i>Embryo generation</i> .....	48
2.13.2	<i>Fixation and storage of embryos</i> .....	48
2.14	<i>Gene targeting by homologous recombination in ES cells</i> .....	49
2.14.1	<i>Construction of the Targeting vector</i> .....	49
2.14.2	<i>Isolation of genomic DNA from ES cells after electroporation</i> .....	49
2.14.3	<i>Screen for the right targeted ES cells before cre expression</i> .....	50
2.14.4	<i>Screen for the correct targeted ES cells after cre expression</i> .....	50
2.14.5	<i>Generation of tetraploid embryos</i> .....	51
2.15	<i>Transgene methods</i> .....	51
2.15.1	<i>Construction of the promoter-LacZ reporter plasmid</i> .....	51
2.15.2	<i>Transgene generation by pronuclear injection</i> .....	52
2.15.3	<i>Genotyping of LacZ transgene</i> .....	52



<b>3.</b>	<b>Results.....</b>	<b>53</b>
3.1	<i>Truncate phenotype.....</i>	53
3.1.1	<i>Skeletal defects in truncate mutant mice.....</i>	53
3.1.2	<i>Notochord defects in truncate mutant embryos.....</i>	54
3.2	<i>Identification of Not as a candidate gene for truncate mutation.....</i>	55
3.2.1	<i>Expression pattern of the candidate gene Not.....</i>	55
3.2.2	<i>Cloning of Not cDNAs.....</i>	56
3.2.3	<i>Not genomic organization, cDNA, encoded protein and similarity to other vertebrate Not genes.....</i>	57
3.3	<i>Expression of Not.....</i>	59
3.3.1	<i>Not expression in the wild type during embryogenesis.....</i>	59
3.3.2	<i>Not expression in the truncate mutants during embryogenesis.....</i>	61
3.4	<i>Transcription of Not.....</i>	62
3.5	<i>Truncate allele is a point mutation in the homeobox of Not.....</i>	63
3.5.1	<i>Identification of a point mutation in the tc allele.....</i>	63
3.5.2	<i>Stability of Not homeodomain.....</i>	65
3.5.3	<i>Generation of Not<sup>tc/tc</sup> ES cells and reversion of the tc mutation.....</i>	67
3.6	<i>Regulation of Not.....</i>	70
3.6.1	<i>Not act downstream of both Foxa2 and T.....</i>	70
3.6.2	<i>Not is most likely a direct target of Foxa2.....</i>	72
3.6.3	<i>Analysis of the significance of predicted binding sites of Not promoter.....</i>	75
3.6.4	<i>Analysis of the regulatory region required for Not expression in vivo in transgenic embryos.....</i>	77
3.7	<i>Left-right determination defects in truncate mutants.....</i>	79
3.7.1	<i>Randomization of embryonic turning in truncate mutants.....</i>	79
3.7.2	<i>Left-right positional defects in visceral and thoracic organs in truncate mutants.....</i>	80
3.7.3	<i>Randomized expression of Nodal as L-R marker in truncate mutants.....</i>	83
<b>4.</b>	<b>Discussion.....</b>	<b>85</b>
4.1	<i>Murine Not represents a new member of Not genes family.....</i>	85
4.2	<i>The truncate mutation and Not function.....</i>	86
4.3	<i>The role of Not in notochord development.....</i>	88
4.4	<i>The regulation of Not gene.....</i>	88
4.5	<i>The truncate mutation and L-R determination.....</i>	91
<b>5.</b>	<b>References.....</b>	<b>93</b>
<b>6.</b>	<b>Appendix.....</b>	<b>106</b>
6.1	<i>Abbreviations.....</i>	106
6.2	<i>List of cloned constructs.....</i>	108
	<i>Acknowledgements.....</i>	112
	<i>A token of appreciation.....</i>	113
	<i>Curriculum Vitae.....</i>	114

# **1. Introduction**

The notochord is an embryonic midline structure common to all members of the phylum Chordata. It serves as a source of midline signals that pattern the surrounding tissues such as mesoderm, endoderm and ectoderm. Also, notochord plays an important structural role and is essential for normal skeletal element formation. In vertebrates, the notochord arises from the organizer. Functionally the significance of the notochord is well established, but molecularly only few genetic elements that control its development are characterized such as *T* and *Foxa2* genes. Genetic screens in mice have identified several mutations that affect notochord development. One of these mutations is the truncate mutation, where the involved gene was not identified so far.

## **1.1 Some aspects of notochord development**

Notochord development has been extensively investigated since the nineteenth century. The notochord is an axial structure of mesodermal origin (Fig.A) and its presence during embryonic development defines members of the Chordate phylum. Notochord precursors emerge during gastrulation from the organizer region of embryos, such as the blastopore lip of the amphibian embryo, Hensen's node of the chick and node of the mouse. The notochord is one of the earliest embryonic structures to be formed and functions as a structural support for the entire organism, either transiently (as in higher vertebrates) or persistently (as in some lower vertebrates). The rigidity of the notochord maintains alignment of embryonic tissues during development and allows axis elongation (Spemann, 1938; Adams *et al.*, 1990).

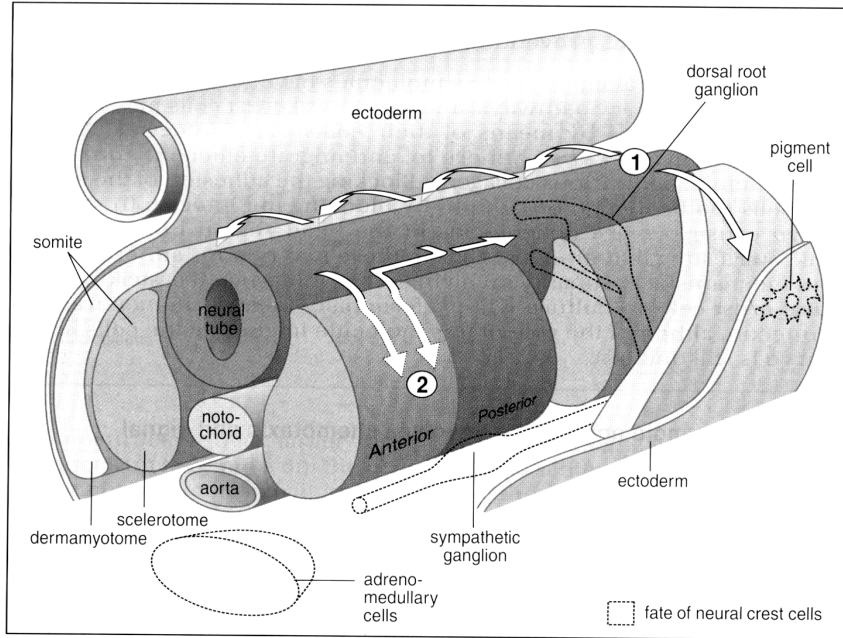


**Figure A.** Sagittal section of a chordate embryo. The notochord is a rod-like structure, located ventral to the neural tube in the midline of the embryo. Signals from the notochord are involved in sclerotome differentiation in the somites and floorplate induction in the neural tube during embryogenesis. (Photography From: Wolpert et al. 2002).

In mice, notochord development starts around embryonic stage E7 and notochord precursors are located in the organizer region “node“. At embryonic stage E8, notochordal cells derived from axial mesendodermal cells that migrate through the node along the midline of the embryo, forming the notochordal plate (Lawson et al. 1991; Lawson and Pedersen 1992; Tam et al. 1997; Kinder et al. 2001). During subsequent development the notochord arises from the tail bud posteriorly to the hind limb buds, the mechanistic features and topographical fate maps being similar to that of the formation of anterior notochord (Schoenwolf 1984; Gajovic et al.1993; Gajovic and Kostovic Knezevic 1995; Wilson and Beddington 1996). At embryonic stage E9, the chordal plate is elongated anteriorly and the notochord develops as a distinct anatomical entity where the cells fold off and form a solid continuous rod tissue that detaches from the underlying endoderm, surrounded first by a basal lamina and later by a notochordal sheath along the antero-posterior body axis. The notochord detaches itself from the endoderm, first at the level of the cardiac primordium, then gradually in the caudal direction to come into contact with the ventral surface of the neural tube. At this embryonic stage the notochord, as it detaches from the endoderm, bends like a wave towards the neural tube and attaches itself to the ventral surface of the latter. At embryonic stage E11, the entire trunk portion of the notochord is attached to the

neural tube, and remains attached to the endoderm only at the extreme cephalic and caudal ends. At this and later stages all the changes in the notochord occur in antero-posterior gradient. From E11 onwards the notochord is circular in transverse section, and its diameter is 20  $\mu\text{m}$ . At the cephalic end it is slightly thinner (about 15  $\mu\text{m}$  in diameter). Eventually, at embryonic stage E11.5, the notochord leaves the endoderm along almost all its length, and except for the hindbrain area, adheres to the ventral side of the neural tube. At embryonic stage E12, the notochord detaches also from the neural tube, apparently because mesenchyme cells penetrate between the neural tube and the notochord. This process also follows an antero-posterior gradient. The activity of the mesenchyme cells detaches the notochord completely from the axial organs and it becomes surrounded by the mesenchyme. Thus in a central position, parallel to and about 100  $\mu\text{m}$  ventral from the neural tube, it indicates the site of the future vertebral column. It is now a uniform cylindrical rod, 25  $\mu\text{m}$  in diameter, extending from a point close to Rathke's pocket to the end of the tail. At embryonic stage E13, the notochord is surrounded by evenly scattered mesenchyme cells, which are denser than previously. At this stage, in the lumbo-sacral area the notochord shows 10-15 slight short flexures, which are as long as the future vertebral segments. The rest of the notochord does not show such flexures. Ventral convexities are opposite to the future intervertebral discs, and dorsal ones opposite to the future vertebral centra. During the next 36 hours the mesenchyme around the notochord undergoes segmentation and forms more distinct vertebral cartilage condensations, while segmental bends in the lumbo-sacral region disappear. At embryonic stage E14, the notochord first shows dilations opposite the prospective intervertebral discs, and corresponding constrictions at the level of the vertebral centra.

## **1.2 Notochord Significance in tissues patterning**

Many different studies have shown that in addition to its structural function, the notochord plays a critical role in the patterning of ectodermal, endodermal, and mesodermal tissues, such as the neural tube and the somitic derivatives. Thus, the notochord is a source of signalling molecules that influence the developmental fate of ectodermal, endodermal and mesodermally derived tissues.

## **1.2.1 NOTOCHORD SIGNALLING TO MESODERM**

### **1.2.1.1 The role of the notochord in somite differentiation**

Numerous studies show that the notochord is involved in patterning of the paraxial mesoderm. Somites are epithelial spheres within the paraxial mesoderm in a craniocaudal (anteroposterior) sequence. In amniote embryos, the ventromedial portion of the somite undergoes an epithelial to mesenchymal transition to form the sclerotome. The dorsolateral portion remains epithelial, forming the dermomyotome, which subsequently gives rise to the dermatome (presumptive dermis) and the myotome (presumptive muscle). In the chick embryo, removal of the notochord results in the failure of sclerotome formation and a corresponding enlargement of the dermomyotome (Goulding *et al.*, 1994). The molecular control of somite differentiation has been elucidated in both chick and mouse models (Dockter, 2000). Shortly after somite formation, signals from the notochord induce the expression of the transcription factors *Pax1* and *Mfh1* within the somite (Fan and Tessier-Lavigne, 1994; Furumoto et al. 1999). *Pax1* expression subsequently becomes localized to the ventral portion of the sclerotome, while in the dorsal sclerotome *Pax9* expression is initiated (Peters et al. 1995). *Pax1* and *Mfh1* are essential for maintaining sclerotomal proliferation and are dependent on signals from the notochord for their continued expression (Furumoto et al. 1999). In vitro experiments have demonstrated that coculture of presomitic mesoderm with notochord or floorplate can induce expression of *Pax1* and that Sonic Hedgehog (SHH) mimics this effect, suggesting that SHH directs sclerotome induction (Fan and Tessier-Lavigne, 1994). It is therefore somewhat surprising that *Pax1* is expressed, albeit at a low level, in *Shh*-deficient mice. This expression, however, is not maintained at later developmental stages (Chiang et al. 1996). This finding suggests that the notochord may express other molecules capable of inducing sclerotome. Noggin appears to be such a candidate in that it is expressed by the notochord at the time of sclerotome formation and also because it can induce *Pax1* expression in cultured somites (McMahon et al. 1998). On the other hand, sclerotome forms in *Noggin*-deficient mice, although this is delayed (McMahon et al. 1998). It appears, therefore, that sclerotome induction requires both Noggin and SHH from the notochord for the initiation and maintenance of *Pax1* expression in the sclerotome lineage.

In zebrafish, the myotome forms the bulk of the differentiated somite, while the sclerotome comprises a very minor portion of the somite. In addition, a distinct population of presumptive

muscle cells, the adaxial cells, develops medially between the notochord and sclerotome (Holley and Nusslein-Volhard, 2000; Stickney et al. 2000). In the zebrafish mutant *ntl* and *flh*, both of which lack a notochord, exhibit fused somites which are characterized by disrupted somite chevron formation and by the lack of muscle pioneer cells (Halpern *et al.*, 1993, 1995). The somites of *ntl* mutant embryos correspondingly exhibit incorrect spatiotemporal expression of the muscle determination gene, *myoD* (Weinberg *et al.*, 1996). While it is clear that development and differentiation of the zebrafish myotome is dependent on signals from the notochord (reviewed by Holley and Nusslein-Volhard, 2000), it is less clear whether sclerotome differentiation and survival depends on such signals. Since attenuation and overactivation of Hedgehog signalling both result in inhibition of sclerotome differentiation, the precise role of Hedgehog proteins remains to be determined (Hammerschmidt and McMahon, 1998). Noggin may also play a role in sclerotome induction, as *Noggin2* is expressed in the zebrafish notochord (Furthauer et al. 1999). Although the factors that induce the sclerotome remain to be elucidated, more is known about the molecular differentiation of these cells in the zebrafish. A distinct cluster of mesenchymal cells is first apparent within each somite 2-3h after the somite individuates from the presomitic mesoderm (Morin-Kensicki and Eisen, 1997). These cells lie adjacent to the notochord, occupying a ventromedial position within the somite. Lineage tracing of these cells have revealed that anterior (cranial) cells of the cluster are committed to the sclerotome lineage, while posterior (caudal) cells are capable of forming both sclerotome and muscle (Morin-Kensicki and Eisen, 1997). At the molecular level, the zebrafish sclerotome appears similar to amniote embryos in that the expression of *Pax9* and *Twist* is conserved (Devoto et al. 1996; Nornes et al. 1996). Although the influence of the notochord on cartilage formation from sclerotome is firmly established, the precise role of the notochord on myogenic specification appears to be complex and is not completely understood (reviewed in Hall, 1977; Halpern, 1997). Nevertheless, both *in vitro* and *in vivo* studies provide strong evidence that the notochord does exert an important influence on muscle development and that, once again, this signalling may be mediated by SHH (Kenny-Mobbs and Thorogood, 1987; Bober *et al.*, 1994; Munsterberg *et al.*, 1995; Bumcrot and McMahon, 1995; Lassar and Munsterberg, 1996; Pownall *et al.*, 1996; Xue and Xue, 1996).

### **1.2.1.2 The role of the notochord in vertebral chondrogenesis**

In addition to its role in inducing and maintaining sclerotome, the notochord acts in the vertebral chondrogenic pathway by promoting the development of ventral structures (e.g. vertebral bodies) and repressing dorsal structures (e.g. spinous processes). Grafting studies in chick embryos have shown that when an ectopic notochord is implanted dorsal to the neural tube, formation of dorsal structures is inhibited (Monsoro-Burq et al. 1994). In contrast, ectopic notochord grafts to the ventrolateral region result in an increase in the size of ventral structures (Pourquie et al. 1993). The molecular control of this dorsoventral patterning is based upon the action of BMPs dorsally and their inhibition ventrally (Watanabe et al. 1998). Application of BMP2 or BMP4 protein dorsal to the neural tube results in an increased expression of dorsal markers such as *Msx1* and *Msx2*, together with the subsequent enlargement of dorsal structures (Monsoro-Burq et al. 1996). Conversely, application of BMP2 or BMP4 lateral to the neural tube results in the inhibition of chondrogenesis in the ventrolateral region (Monsoro-Burq et al. 1996; Tonegawa et al. 1997).

The dorsoventral patterning of the vertebral column is coordinated by the interaction of SHH from the notochord/floor plate with BMP4 from the roof plate and overlaying ectoderm. The actions of these proteins are mutually antagonistic: grafting ectopic sources of either protein disturbs the balance of this interaction and disrupts dorsoventral patterning (reviewed in Monsoro-Burq and Le Douarin, 2000). For example, SHH ventralises paraxial mesoderm by promoting the expression of *Pax1*, while dorsally migrating cells downregulate *Pax1* and express *Msx1* and *Msx2* under the influence of BMP signals. When SHH-expressing cells are grafted dorsally, BMP4/BMP2 molecular pathways are antagonized and subsequent chondrogenesis is prevented (Watanabe et al. 1998). Although these aspects of dorsoventral sclerotome patterning are less well characterized in zebrafish, it is known that Smad1 expression in the sclerotome is required to transduce BMP2/BMP4 signals and positively regulated by Hedgehog proteins (Dick et al. 1999).

### **1.2.1.3 The role of the notochord in vertebral column segmentation**

While recent studies have confirmed the role of the notochord in early vertebral development, the potential later functions of the notochord have also been investigated. Many experiments designed to examine the mechanisms of vertebral segmentation have focused on the reorganisation of somite derivatives according to the 'resegmentation theory', a single vertebra forms from the recombination of the anterior and posterior halves of two adjacent sclerotomes on

both sides of the embryo. In zebrafish, it has been reported that vertebral bodies (centra) arise by secretion of bone matrix from the notochord rather than somites; centra do not form via a cartilage intermediate stage, nor do they contain osteoblasts (Fleming et al., 2003). Moreover, isolated, cultured notochords secrete bone matrix in vitro and ablation of notochord cells at segmentally reiterated positions in vivo prevents the formation of centra. Analysis of *fss* mutant embryos, in which sclerotome segmentation is disrupted, shows that whereas neural arch segmentation is also disrupted, centrum development proceeds normally. These suggest that the notochord plays a key, perhaps ancient, role in the segmental patterning of the vertebrae.

The 'resegmentation theory' that states that a single vertebra is formed from a combination of the anterior (cranial) half of one sclerotome with the posterior (caudal) half of the next-anterior sclerotome (Remak, 1850; reviewed in Verbout, 1976; Brand-Saberi and Christ, 2000), however it remains uncertain whether it applies to all vertebrates. Since, histological analysis has suggested that this may not be the case, at least for the ventral sclerotome, as these cells are seen to form a uniform, apparently non-segmented tube around the notochord. This tube later segments to give rise to the vertebral bodies and, together with the notochord, forms the intervertebral discs (Dalglish, 1985; Verbout, 1985). This suggests that the metameric patterning is lost in the ventral sclerotomes, with the implication that segmentation of the vertebral bodies is imparted instead by another mechanism.

Ablation experiments in amphibian embryos have lent some support to this view. Removal of the notochord from neural plate-stage urodele embryos results in the formation of a fused rod of vertebral cartilage ventral to the neural tube (Kitchin, 1949; Holtzer, 1952; Holtzer and Detwiler, 1953). In avian embryos, the notochord excision experiments of Strudel have produced similar results. Excision of the notochord from embryos at the 12-30 somite-stage leads to the formation of an unsegmented cartilagenous rod ventral to the neural tube (Strudel, 1955). On the other hand, experiments by Watterson et al. (1954) at the same embryonic stages have shown that removal of the notochord results in the formation of normal neural arches but a total absence of ventral cartilagenous tissue. These apparently conflicting observations may have arisen due to variations in the precise stage and location of notochord excision.



#### **1.2.1.4 Notochord Patterning of Other Mesodermal Tissues**

A number of independent studies provide evidence that notochord signalling is also important for the development of the cardiovascular system and for establishing the laterality of organs. Studies in zebrafish show a role for the notochord in regulation of early cardiac development (Goldstein and Fishman, 1998). More specifically, laser ablation of the anterior extremity of the notochord causes expansion of the expression domain of the homeobox gene *Nkx2-5*, a marker for the presumptive heart field. This suggests that the notochord might normally function to suppress cardiogenic fate in the underlying splanchnic mesoderm. Notochord signals have also been associated with the formation of the dorsal aorta. The zebrafish mutants *ntl* and *flh*, both of which lack a notochord, also fail to form the dorsal aorta (Fouquet *et al.*, 1997; Sumoy *et al.*, 1997). When wild type notochord cells are transplanted into *flh* mutants, some notochord development is restored and an aortic primordium forms. Finally, the notochord may be involved in the assignment or maintenance of left–right asymmetry. When the notochord is experimentally ablated or when it is absent in mutant embryos, asymmetric markers of lateral plate mesoderm are either randomized or expressed bilaterally. In *Xenopus* embryos, either surgical extirpation of the notochord or suppression of its development using UV irradiation leads to cardiac reversals and bilateral expression of the laterality marker *nodal* in the lateral plate mesoderm (Danos and Yost, 1995; Lohr *et al.*, 1997). Similar reversals are seen in notochord-deficient zebrafish mutants such as *ntl* and *flh* (Danos and Yost, 1996; Bisgrove *et al.*, 2000). Furthermore, in mice homozygous for the *no turning* mutation, both the notochord and the floor plate degenerate, and these embryos exhibit randomized cardiac looping and bilateral expression of the laterality markers *nodal* and *lefty* (Melloy *et al.*, 1998). Equivalent results are obtained when the node is surgically ablated in mouse embryos, resulting in the failure of notochord development and subsequent randomization of expression of *Pitx2*, a regulatory gene in the laterality pathway (Davidson *et al.*, 1999).

## **1.2.2 NOTOCHORD SIGNALLING TO ECTODERM**

### **1.2.2.1 Notochord Patterning of the Neural Tube**

The developing neural tube exhibits a distinct dorsoventral (DV) polarity, characterized by differences in cell morphology and by the position of specific classes of neurons. In the early embryo, the notochord lies immediately beneath the floor plate, a specialized group of neuroepithelial cells in the ventral portion of the spinal chord. The role of the notochord in the induction of the floor plate has been studied intensively in a number of different organisms (for review see Jessell and Dodd, 1990–1991; Placzek *et al.*, 1991; Placzek, 1995; Dodd *et al.*, 1998). For example in *Xenopus laevis*, ultraviolet irradiation of fertilized eggs causes dose-dependent deficits in notochord development (Cooke, 1985). In these experiments, embryos which fail to form a notochord also show severe disruption of proper floor-plate formation in the neural tube (Youn and Malacinski, 1981; Clarke *et al.*, 1991). In chick embryos, when an ectopic notochord is grafted adjacent to the neural tube, cells in the lateral walls of the neural tube are ventralized and induced to exhibit the morphological and functional properties of the floor plate, including its associated motor neurons and bundles of efferent axons (van Straaten *et al.*, 1985, 1988; Smith and Shoenwolf, 1989; Placzek *et al.*, 1990; Yamada *et al.*, 1991, 1993). Dorsal neural tube markers such as *Pax-3*, *Pax-6*, and *dorsalin* are repressed in the vicinity of the grafted notochord (Goulding *et al.*, 1993; Basler *et al.*, 1993). Conversely, notochord extirpation in chick embryos results in the absence of the floor plate and of the adjacent motor neuron pools (van Straaten and Drukker, 1987; Placzek *et al.*, 1990; Hirano *et al.*, 1991; van Straaten and Hekking, 1991; Yamada *et al.*, 1991). As expected, this is accompanied by a ventral shift in the domain of expression of dorsal neural tube markers (Goulding *et al.*, 1993; Basler *et al.*, 1993). The induction of the floor plate by the notochord is thought to be mediated by the secreted protein Sonic Hedgehog (SHH), which is expressed in the notochord and can induce floor-plate markers both *in vivo* and *in vitro* (Echelard *et al.*, 1993; Fan and Tessier-Lavigne, 1994; Johnson *et al.*, 1994; Roelink *et al.*, 1994; Marti *et al.*, 1995; Munsterberg *et al.*, 1995; Ericson *et al.*, 1996). When discussing the role of patterning by the notochord, it is impossible to ignore some recent studies that call into question the importance of notochord signalling for the development of the floor plate (LeDouarin *et al.*, 1998; Teillet *et al.*, 1998). Specifically, it is argued that the observed failure of floor-plate development, following the removal of the notochord, results from

inadvertent removal of floor-plate cells, rather than the absence of inductive notochord signals. In addition, these investigators point to a number of zebrafish mutants, such as *flh*, *ntl*, *cyclops*, and *oep* mutants, which can develop either a notochord or a floor plate, apparently independent of each other. However, while these studies have raised some interesting questions about lineage relationships of axial tissues and certain aspects of notochord signalling, the ability of notochord to induce an ectopic floor plate in the lateral walls of the neural tube remains unquestioned and strongly implies an important role for the notochord signals in neurectoderm patterning. Discussion of these arguments can be followed in the specialized literature (Vogel, 1998; Placzek *et al.*, 2000; LeDouarin and Halpern, 2000).

### **1.2.2.2 Notochord Patterning of Other Ectoderm Derivatives**

In addition to neural tube patterning, the notochord appears to influence development of other ectodermal structures. It has been observed that the tip of the notochord contacts head ectoderm fated to become the anterior pituitary, thereby raising the possibility that the notochord might be involved in pituitary growth and development (Eyal-Giladi, 1958; Barteczko and Jacob, 1999). In support of this hypothesis, the transplantation of anterior notochord into a lateral region of the head causes the stomodeal ectoderm to invaginate and form a pocket structure reminiscent of the early appearance of Rathke's pouch, the precursor of the anterior pituitary (Gleiberman *et al.*, 1999). Although notochord is not sufficient to induce complete formation of the anterior pituitary, these experiments clearly implicate the impact of the notochord in the early stages of development of an independent, ectodermally derived tissue.

### **1.2.3 NOTOCHORD SIGNALLING TO THE ENDODERM**

The biological mechanisms responsible for patterning the endoderm are less explored relative to those underlying ectoderm and mesoderm development. However, in order to generate organ primordia at appropriate locations along the gut tube, the endodermal epithelium must receive correct anterior–posterior and dorsoventral patterning signals derived from the adjacent tissues such as notochord. Coordination of these signals results in the formation of the respiratory system, the tympanic cavities, the thymus and thyroid gland, and the digestive system, including the esophagus, stomach, liver, pancreas, intestines, and colon.

### **1.2.3.1 Proximity of Notochord and Endoderm**

It is plausible to argue that the notochord is involved in endodermal patterning. In all species examined, the notochord is first formed in close association with the endoderm, and notochord precursors remain embedded in the dorsal endoderm as they coalesce into a rod-shaped structure. As development proceeds, the notochord resolves into an independent structure but continues to adhere to the underlying endoderm, even sharing a common basal lamina for a time (Jurand, 1974; Lamers *et al.*, 1987). The notochord remains in contact with the endoderm from gastrulation until about E8 in mice (13-somite stage), stage 14 in chickens (22-somite stage) and stage 32 in frogs (26-somite stage). Subsequently, the notochord becomes separated from the endoderm by intervening endothelial tissue. This occurs during the fusion of the dorsal aortae at the midline ventral to the notochord (in mice and chickens) or during the *in situ* formation of a single dorsal aorta (in frogs and fish). The direct contact between the notochord and the endoderm is therefore sustained for much of early development, from gastrulation to well beyond the end of neurulation.

It is interesting to note that, although the spatial relationship between notochord and endoderm is effectively identical in different organisms, the relative size of the notochord varies dramatically. In frogs, the notochord is large and almost as wide as the neural tube, while the murine notochord is extremely narrow compared to adjacent structures. In both cases, however, the notochord is only a few cells in diameter. At present it is unclear whether these structural differences have any functional impact on the inductive signalling properties of the notochord.

### **1.2.3.2 Medical Examples Implicating the Notochord in Endodermal Development**

There are a number of compelling observations in the medical literature illustrating a correlation between notochord defects and problems with development of endodermal tissues. For instance, human patients exhibiting developmental abnormalities in the vertebral bone, apparently due to defects in notochord development, also show congenital gastrointestinal defects (Elliott *et al.*, 1970). This suggests that notochord signalling influences both sclerotome and endodermal patterning during human development. In another example, anomalous overgrowth of the notochord leads to foregut and hindgut abnormalities, such as duplications of the pharynx,

esophageal and gastric cysts, rectovesical fistula, and rectal agenesis (Fallon, 1954). These observations imply that prolonged exposure to notochord signals is inhibitory to proper endoderm development. Overall, these observations are consistent with a role for the notochord in endoderm patterning and moreover, they suggest that the timing of notochord signalling must be closely regulated for correct development of the gut tube.

### **1.2.3.3 Notochord signals are required for pancreas development**

Recent experiments using the chick embryo have provided strong evidence that the notochord plays a role in development of the pancreas. Removal of the notochord from chick embryos, at a stage when the notochord is in contact with the endoderm, eliminates subsequent expression of several markers of dorsal pancreas bud development, including both endocrine and exocrine cell markers, such as insulin, glucagon, and carboxypeptidase A (Kim *et al.*, 1997).

A specific molecular consequence of notochord signalling is repression of SHH expression in the endoderm (Kim *et al.*, 1997; Hebrok *et al.*, 1998). SHH is expressed in most portions of the gut tube except for those juxtaposed to the notochord (Hebrok *et al.*, 1998). In addition, the SHH receptor, Patched (Ptc), is expressed in all visceral mesoderm, except for pancreatic mesenchyme. When notochord tissue is grafted ventral to the gut tube, SHH expression is repressed in tissues in close proximity to the notochord. Conversely, removal of the notochord leads to expression of SHH in the pancreatic endoderm, to Ptc expression in the surrounding mesenchyme, and to the concomitant loss of pancreatic genes. Using *in vitro* culture of embryonic tissue, it was shown that activin-bB and FGF2 could effectively mimic the notochord signal by inhibiting SHH expression in endoderm and allowing pancreatic marker expression (Hebrok *et al.*, 1998).

### **1.2.3.4 Notochord signals are required for hypochord formation**

Given the close juxtaposition of the notochord and the hypochord in the frog embryo, it is certainly plausible that the notochord might be involved in the regulation of the hypochord development. Using the *Xenopus* embryo, both notochord extirpations and transplantations had been carried out to address this question (Cleaver *et al.*, 2000). When the notochord is removed during early neurulation (stage 13–14), the hypochord fails to develop. However, if the notochord is removed later during neurulation (stage 17–18), hypochord development proceeds unhindered. These observations suggest that the notochord is necessary for the formation of the hypochord, but that this requirement is complete by the late neurula stages. It also appears that no

maintenance signals from the notochord are required for hypochord development, after the initial signalling period. In notochord transplantation experiments, addition of a second notochord to the midline of the embryo results in enlarged hypochord tissue at the location of the graft. However, notochord transplantation ventrolateral to the somites does not induce the formation of an ectopic hypochord. By transplanting notochords next to the endoderm at different dorsolateral positions, it was demonstrated that competence to form hypochord is loosely restricted to the dorsalmost portion of the endoderm. As with the studies of pancreatic development, these results imply that a dorsoventral prepattern already exists in the amphibian endoderm by the early neurula stage.

### **1.2.3.5 Possible nature of notochord signals**

The evidence that the notochord is an important source of patterning signals is undeniable, although the nature of these signals is only beginning to be understood. During floor-plate induction and somite patterning, an excellent candidate molecule for the notochord signal is SHH. This is supported by a number of *in vitro* and *in vivo* experiments in which SHH is shown to directly affect floor-plate and somite development. For example, cells transfected with SHH can mimic the effect of the notochord and ventralize paraxial mesoderm or spinal cord (Johnson *et al.*, 1994; Fan *et al.*, 1995; Tanabe *et al.*, 1995).

In addition to SHH, activin-bB and FGF2, are potential signals in the notochord, which have been implicated in the development of the underlying endoderm (Hebrock *et al.*, 1998); study of different organisms provides a long list of growth factors and secreted signalling molecules expressed in the notochord, including BMP7, BMP2, BMP3, follistatin, BMP1/tolloid, TGF-b3, TGF-b5, eFGF, FGF4, activin (Xatv), nodal-related 2 (ndr2), Xnr4, noggin, chordin, and Hip (Echelard *et al.*, 1993; Dudley and Robertson, 1997; Dale *et al.*, 1999; Hemmati-Brivanlou *et al.*, 1994; Marti, 2000; Yamagishi *et al.*, 1999; Kondaiah *et al.*, 2000; Isaacs *et al.*, 1995; Shamim *et al.*, 1999; Cheng *et al.*, 2000; Rebagliati *et al.*, 1998; Joseph and Melton, 1997; Smith and Harland, 1992; Sasai *et al.*, 1994; Chuang and McMahon, 1999). Although the precise roles of these potent signalling molecules during embryonic patterning events are not completely understood, it seems likely that some at least will be important for the development of adjacent tissues, including endodermal derivatives.

### 1.3 Notochord and the organizer “node“

The notochord is a rod-like structure which arises during gastrulation from axial mesendodermal cells located in the organizer “node“ (Wilson et al. 1996; Selleck et al. 1992). The organizer is a group of cells necessary and sufficient to initiate a complex program of spatial organization in competent embryonic tissue (Spemann, 1938).

The organizer “node“ is generally considered to be the most important region of the very early, gastrulating embryo. Not only does it generate the midline organs of the body (such as notochord, prechordal region, gut), but is also responsible for inducing and patterning the whole of the central nervous system. Like its amphibian counterpart (the dorsal lip of the blastopore), Hensen’s node can be characterized by a well-defined set of cellular and molecular properties. In amniote embryos, the node is a bulb-like thickening lying at the cranial tip of the primitive streak during gastrulation (Fig.B). In the chick, where most studies have been conducted because of its ease of manipulation, the node is some 100  $\mu\text{m}$  in diameter and contains about 2,000 cells (Gallera, 1971; Nicolet, 1971; Leikola, 1976; Hara, 1978; Stern, 1994; Streit et al., 1994).

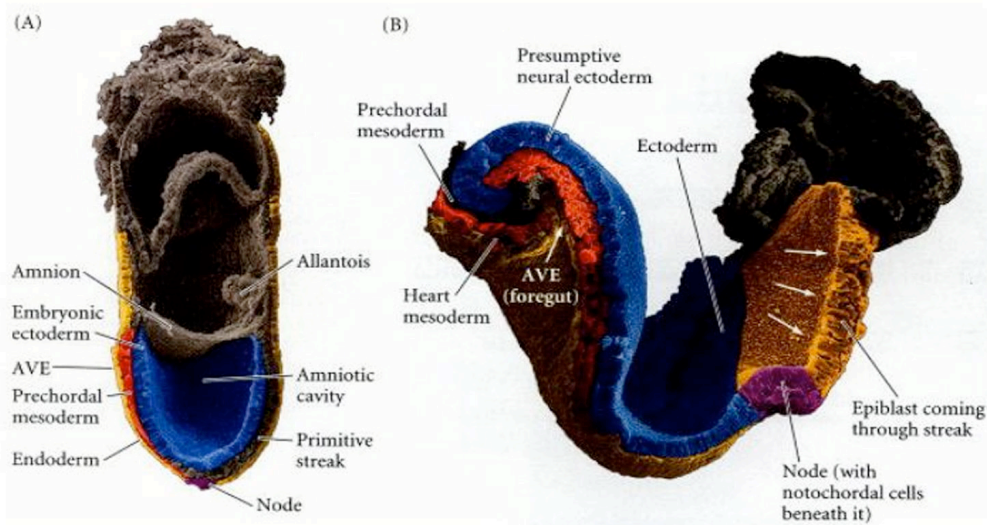


**Figure B.** The mouse embryo. (A) At embryonic stage E7, the dorsal surface of the epiblast (embryonic ectoderm) is in contact with the amniotic cavity. The ventral surface of the epiblast contacts the newly formed mesoderm. In this cuplike arrangement, the endoderm covers the surface of the embryo, the node is located at the distal tip. (B) At embryonic stage E8, the cells in the midline of the epiblast migrate through the primitive streak (white arrows). Notochord cells are generated from the axial mesendodermal cells that migrate through the node. (Photography From: Wolpert et al. 2002).

Among the salient features of the chick node are:

(a) *the fate of its cells*: the node gives rise to the notochord/head process, the prechordal mesendoderm, the definitive (gut) endoderm, the medial halves of the somites and contributes to the midline (floor plate, or notoplate) of the future spinal cord (see Spratt, 1955; Rosenquist, 1966; 1983; Nicolet, 1970; Hara, 1978; Selleck and Stern, 1991; 1992; Schoenwolf, 1992).

(b) *its expression of a number genes in a stage- and regionspecific manner*: these include the homeobox genes *gooseoid* (Izpisúa-Belmonte et al., 1993) and *cNot* (Stein and Kessel, 1995; Knezevic et al., 1995), the secreted factors HGF/SF (Streit et al., 1995), *Sonic hedgehog* (*Shh*; Riddle et al., 1993; Roelink et al., 1994) and *c-NR1* (Levin et al., 1995), the activin receptors *cActR-IIA* and *cActRIIB* (Stern et al., 1995), and the transcription factor *HNF-3 b* (Ruiz i Altaba et al., 1995).

(c) *its role in the establishment of left/right asymmetry*: four of the above genes, *Shh*, *cActRIIA*, *cNR-1* and *HNF-3 b* are expressed in or near the node in an asymmetric fashion and their misexpression alters the left-right polarity of heart looping (Levin et al., 1995).

(d) *its ability to induce an ectopic nervous system*: when grafted into an ectopic site (including regions fated to contribute only to extraembryonic membranes) at an appropriate stage of development (up to about stage 5), the node is able to change the fates of neighbouring epiblast cells by inducing them to form a complete nervous system (Waddington, 1932; 1933; Gallera, 1971; Hara, 1978; Dias and Schoenwolf, 1990; Storey et al., 1992).

(e) *its ability to pattern the neural plate of a host embryo*: when grafted to appropriate position adjacent to the neural plate of a host embryo, even older nodes are able to organize a second axis from the neuralized cells of the host (Gallera, 1971; Storey et al., 1992; Izpisúa-Belmonte et al., 1993). Perhaps surprisingly, this ability operates across species and even across vertebrate classes (see Kintner and Dodd, 1991; Streit et al., 1994).

(f) *its ability to induce extra digits in the limb bud of a host embryo*: when grafted to the anterior margin of the limb bud of a host embryo, the node can induce digit duplications, mimicking the activity of the polarizing region of the limb (Hornbruch and Wolpert, 1986). However, this activity is different from neural inducing ability: the node starts to lose neural inducing activity from stage 4 up to stage 5 (Storey et al., 1992), but it continues to induce extra digits until the 7 somite stage (stage 9; Hornbruch and Wolpert, 1986).



## **1.4 Genetic control of notochord development**

Functionally, notochord significance is largely explored and well defined. However the genetic elements involved in controlling notochord development and integrity are less known, and are still an open field to be investigated. Therefore, the isolation and functional characterization of more mutations that disrupt notochord development is fundamental for the identification of new genes involved in these processes with the purpose of offering more understanding concerning the molecular mechanisms that control notochord formation.

In the mouse, mutations at several loci required in notochord development process have been identified in genes such as *T* and *Foxa2*, which encode for transcription factors. *T* was isolated by positional cloning (Herrmann et al. 1990) and *Foxa2* was characterized through targeted mutagenesis analysis (Ang and Rossant 1994; Weinstein et al. 1994).

*Foxa2*, a member of the fork head family of transcription factors is expressed in the node, notochord, floor plate and gut in mouse embryos. A null mutation of this gene leads to embryonic lethality. The earliest detectable defects in *Foxa2* mutant embryos are the lack of a distinct node, the absence of the notochord and the truncation of the primitive streak. In addition, at later stages mutant embryos show marked defects in the organization of somites and neural tube, which exhibits overt anteroposterior polarity but lacks a floor plate and motor neurons. Endodermal cells are present but fail to form a gut tube in mutant embryos.

Structural analysis has shown that the DNA-binding domain of *Foxa2* gene has a winged-helix conformation (Clark et al., 1993). Winged-helix genes share a highly conserved DNA-binding domain, encoded a protein of about 110 amino acids and have been shown to function as transcription factors (reviewed by Kaufmann and Knoechel, 1996).

*T*, a gene encoding for a transcription factor, is normally expressed in early mesoderm and primitive ectoderm next to the primitive streak and then becomes restricted to the notochord and to the tailbud. *T* (*Brachyury*) mutant embryos show a truncation of the primitive streak so that gastrulating *T* embryos generate insufficient mesoderm, whereas the number of ectodermal cells is increased. The chordamesoderm is most strongly affected and although the notochordal plate is formed initially, it later degenerates and no notochord is established. The posterior region of the embryo is entirely missing, probably owing to a failure of primitive streak regression. Finally, the allantois, a derivative of the mesoderm, is not formed, resulting in embryonic death at around embryonic stage E10. Lack of the somites and the neural tube in *T* mutants are secondary effects presumably reflecting the absence of inductive influence of the notochord on these tissues.

*T*-box genes also show a high degree of conservation in their sequence among vertebrates. It encodes a 436 amino acid residue, contains six putative glycosylation sites of the canonical sequence Asn-X-Ser/Thr, and is rich in serine (13%) and proline (9%) residues.

The zebrafish *floating head* (*flh*) is another transcription factor gene expressed in the organizer at the beginning of gastrulation, and later in the developing notochord (Halpern et al., 1995; Talbot et al. 1995). *Flh*, which is essential for notochord formation, acts upstream of *T* in notochord precursors. *Floating head* is an embryonic lethal mutation, which disrupts axial mesoderm development. *Flh* mutant embryos lack entirely a differentiated notochord and instead have muscle in the midline under the neural tube since in the trunk somites are fused medially beneath the spinal cord; these mutants also have defects in ventral cell types within the neural tube that are induced by the notochord.

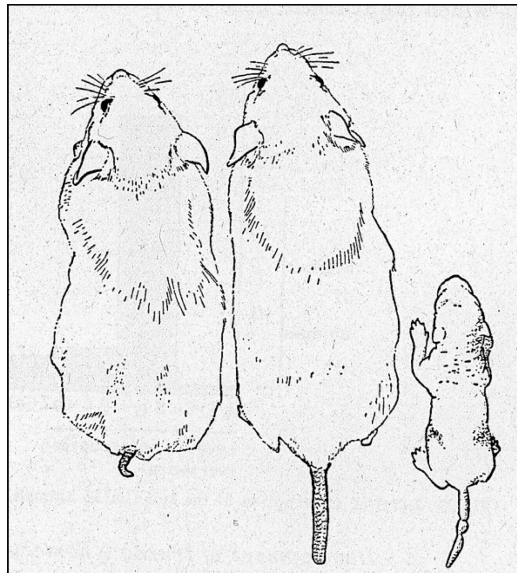
*Flh* represents a null allele. *Flh* is a mutation containing a deletion of two base pairs in the sequence. This deletion causes a frameshift in the ORF and leads to truncation of the Flh polypeptide upstream of the homeodomain. *Flh* gene sequence analysis revealed an open reading frame (ORF) of 241 amino acids that contains a homeobox sequence. The homeodomain sequence places the gene in the *ems* subfamily, which includes *Xnot* (*Xenopus*), *Cnot1* and *Cnot2* (Chicken), *ems* (*Drosophila*), and *Emx-1* and *Emx-2* genes (of mouse and human), however no mammalian *Not* gene has been identified so far.

In the mouse, several mutations that disrupt notochord formation have been identified such as Danforth's short tail (*Sd*), pintail (*Pt*), curly tail (*ct*), and truncate (*tc*); the specific genes affected in these mutations are still unknown (for review, see Johnson 1986; Theiler 1988).

## **1.5 Truncate mutation (*tc*)**

Theiler described this mutation and reported that the phenotype can be explained by a primary defect in the formation of the notochord-mesoderm in the caudal body region. The primary visible effect is a block in the out-growth of the notochord. The block is not always complete; sometimes the notochord reappears posteriorly for a short stretch, but disappears again. It is not simply an inability of the notochordal cells to multiply; on the contrary, some mitosis is regularly found in the terminal part of the notochord. However, the cells do not form a rod there, but assemble to form a solid knob which soon shows degenerating cells in the center. The possibility suggests itself that the supply of notochordal cells from the undifferentiated blastema is interrupted. The cells which have already differentiated are not disturbed and multiply, except those in the center of the knob which degenerate perhaps because of metabolic difficulties. In the region lacking a notochord, the somites generally develop normally up to the point where the epithelial alignment of somite cells is lost; the sclerotomic cells migrate medially until they meet in the mid-line beneath the neural tube. The sclerotomic cells degenerate and more and more cell fragments are visible in microscopic preparations. Pycnosis sometimes can be observed in normal embryos too but never in this degree. In a more posterior region, opposite somites sometimes fuse across the middle from the beginning, but cell degeneration always starts later. The alteration of the spinal cord in *tc/tc* embryos is easy to explain. It is secondary in nature. In *tc/tc* embryos a floor plate fails to appear whenever the notochord is missing. The median ventral fissure of the spinal cord does not develop, and both motor columns unite to form a single cell mass on the ventral border. In the defective tail, the blood vessels are enlarged and sometimes give origin to a blood-filled and centrally located bleb. Another type of bleb appears earlier, is situated subepidermally and is filled with clear fluid. Both phenomena are only temporarily visible and may be regarded as a toxic effect caused by the extensive breakdown of sclerotomic cells. The neural tube may be involved too, exhibiting marked cell disintegration, which is, however, not always present and originates later than the disturbance of the sclerotome. Macroscopically, the defect of the neural tube causes a sharp depression in the dorsal contour of the body. Truncate embryos shows sometimes a transitory subepidermal bleb and extensive degeneration of sclerotomic cells in the caudal body region. In addition, the caudal part of the notochord often retains connection with the neural tube. This peculiarity may occur in wild type mice too, but is rare.

In summary, truncate (*tc*) is a recessive spontaneous mutation with incomplete penetrance and variable expressivity affecting exclusively the posterior portion of the notochord (Theiler 1959; Dietrich et al. 1993). In homozygous d9.5-d10 embryos, the notochord fails to grow caudally and abruptly ends, usually in the sacral region. In the region lacking the notochord, no floor plate develops in the overlying neural tube, somites fuse across the midline, and sclerotome development is impaired. These abnormalities lead to malformations and/or agenesis of the vertebral column in the tail, the sacrum and/or the lumbar region of homozygous *tc* mutants (Fig.C). In the most severe cases, the hind legs are paralyzed and the floor plate and the median ventral fissure of the spinal cord is absent. The anterior notochord remains fully intact and is not affected by this mutation.



**Theiler, 1959**

**Figure C.** Truncate mice, exhibiting varying degrees of tail reduction. A newborn with constrictions (right) and two adults (left).

The specific defects in homozygous *tc* mutant embryos suggest that truncate is an essential gene required for normal notochord formation, specifically in the caudal region of the body axis. Thus, the isolation and molecular characterization of the *tc* gene is likely to elucidate the mechanisms governing notochord development.

The truncate mutation is located at map position 38 on mouse chromosome 6 (The Mouse Genome Database; [URL:http://www.informatics.jax.org/map.html](http://www.informatics.jax.org/map.html)). Previously, a fine genetic map has been constructed (Fig. D), by analysis of a number of simple sequence length

polymorphism (SSLP) markers from this region with respect to *tc*, which placed *tc* locus between the markers *D6R4Arb5* and *D6Mit6* (Pavlova et al. 1998). Further analysis narrowed the *tc* region down to approximately 180 kb. This region was entirely sequenced, and then by computational analysis (as described in Frishman et al. 1998; Altschul et al. 1997; Apweiler et al. 2001) all known and predicted genes in this region were identified (table A).

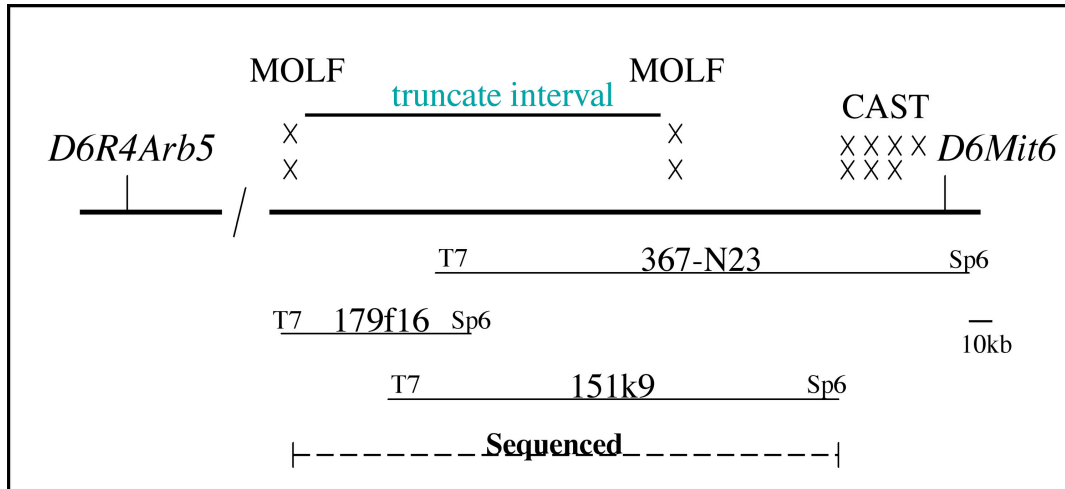


**Figure D.** Fine genetic and physical map around the critical interval containing *tc*. Truncate region was sequenced, and predicted genes were identified by computational analysis.

**Table A.** Predicted genes in the truncate interval identified by computational analysis

Sideroflexin 5 ( <i>Mus musculus</i> )
KIAA0857 protein ( <i>Homo sapiens</i> )
<b>Gnot1 homeodomain protein</b> ( <i>Gallus Gallus</i> )
NN8-4AG-human ( <i>Homo sapiens</i> )
putative ( <i>Mus musculus</i> )
chaperonin subunit 7 (eta) Cct7 ( <i>Mus musculus</i> )
mCG17168 unknown gene
early growth response 4 , Egr4 ( <i>Mus musculus</i> )
KIAA0328 protein ( <i>Homo sapiens</i> )

Interestingly, in this *tc* interval, one of the predicted genes encoded a polypeptide of 240 amino acids containing a homeodomain protein which belongs to the *ems* subfamily, including zebrafish *flh* (Talbot et al. 1995), chick *Cnot1*, *Cnot2* (Stein and Kessel 1995; Stein et al. 1996), *Xenopus* *Xnot1*, *Xnot2* (Gont et al. 1993; von Dassow et al. 1993), *Drosophila* genes empty spirales *ems* (Dalton et al. 1989), and mouse *Emx-1* and *Emx-2* human genes (Simeone et al. 1992). Based on the pattern of the *Not* family genes such as *flh*, *Xnot1*, *Xnot2*, *Cnot1* and *Cnot2* which are specifically expressed in the notochord during embryonic development and known to be essential for notogenesis, this predicted gene represented a potential candidate gene for the *tc* mutation. Therefore, to explore this possibility, this mouse gene hereafter designated as *Not*, was further investigated.

The aims of the present PhD thesis are to identify the gene mutated in the truncate mice, to investigate the nature of this mutation, to determine the position of this gene in the genetic hierarchy governing notochord development, to characterize some aspects of its regulation in the notogenesis process and to further analyse the *tc* phenotype. Together, the results of this work should help to elucidate the role of this gene, which is essential for caudal notochord formation and integrity and further our understanding of the molecular mechanisms controlling notochord development and laterality process.

## 2. Materials and methods

### 2.1 Chemicals

All chemicals that are not included in this table were provided from manufacturers such as AppliChem, Calbiochem, Fluka, Merck or Roth.

<b>Product</b>	<b>Manufacturer</b>
1 kb DNA Ladder, 100 bp DNA Ladder markers	NEB, Invitrogen
Lambda DNA- <i>HindIII</i> digest marker	NEB
10x PCR-Buffer	Sigma
DMEM Powder (#52100)	Gibco BRL
DMSO	Sigma
dNTPs	PEQLAB Biotechnologie GmbH
FCS	Gibco BRL
Agarose	Sigma, Invitrogen
NucleoSpin® Extract Kit	Macherey-Nagel
NucleoSpin® Plasmid Kit	Macherey-Nagel
RNeasy Mini Kit	QIAGEN
Expand Hight Fidelity PCR Kit	Roche
Prime-It II Random Primer Labeling Kit	Stratagene
TOPO-XL-PCR Cloning Kit	Invitrogen
Dig RNA labeling kit	Boehringer
Dynabeads mRNA Direct Kit	Dynal
Omnifix ®-F 1-5 ml Syringes	Braun
Penicillin (10000 U/ml)/Streptomycin (10000 U/ml)	Gibco BRL
pGEMT easy System Kit	Promega
QIAshredder column Kit	QIAGEN
RNA Ladder marker	Invitrogen
Restriction Endonucleases	NEB, Boehringer
Superscript II Reverse Transcriptase	Invitrogen
Mung Bean Nuclease	Boehringer, NEB
T4 DNA polymerase	Boehringer
Exo (-) Klenow	Stratagene
Shrimp Alkaline Phosphatase	Boehringer
Sterican Ø 0,90 x 40 mm	Braun
T4 DNA Ligase	Boehringer, NEB

<b>Product</b>	<b>Manufacturer</b>
Oligo(dT) primers	Invitrogen
0,1M DTT	Invitrogen
RNA polymerase (SP6, T7 or T3)	Boehringer
tRNA	Boehringer
RNase A	Sigma
NTPs (Dig RNA labeling mix)	Boehringer
RNase inhibitor	Boehringer
BM purple AP substrate	Roche
anti-digoxigenin antibodies	Roche
Blocking reagent 5 % (w/v)	Boehringer
alcian blue 8GX	Sigma
alizarin red S	Sigma
Eosin Y-Certified	Sigma
VectaMount (H-5000)	Vector Laboratories
Expand Hight Fidelity Enzyme mix kit	Roche
HybondN-Plus, HybondN membranes	Amersham Pharmacia biotech
Hyperfilm-MP	Amersham Pharmacia biotech
Luciferin	Roche
ATP	Roche
Tritonx-100	Applichem
IPTG	Applichem
X-gal	Applichem
Antibiotics	Sigma
Ethidiumbromide	Merck
Tween20	Applichem, Sigma
Paraffin	Roth
Rotihistol	Roth
glycogen	Applichem
$\beta$ -Mercaptoethanol	Merck
glycerol	Applichem
Orange G	Sigma
RNA later	Ambion
Tissue culture dishes	Cellstar
Gloves	Kimberly-Clark
DEPC	Applichem
Glutaraldehyde	Fluka



<b>Product</b>	<b>Manufacturer</b>
Nonidet 40P	Applichem
Agar	Applichem
Proteinase K	Merck
Taq Polymerase	Sigma

## 2.2 Apparatus

<b>Apparatus</b>	<b>Name</b>	<b>Manufacturer</b>
Electroporation apparatus	MicroPulser	BioRad
Film developing system	Hyper Processor	Amersham
Electrophoresis Equipment	Electrophoresis Equipment	BioRad
PCR thermal cycler	Primus96 plus	MWG-Biotech
Laminar-Flow Hood	LaminAir ®	Heraeus
Humidified CO <sub>2</sub> incubator	Humidified CO <sub>2</sub> incubator	GFL
Power supplies	Power Pac 300	Bio Rad
Microcentrifuge	Centrifuge 5415D	Eppendorf
Cold centrifuge	Centrifuge 5810R	Eppendorf
Vacuum centrifuge	SpeedVac SVC 100	Savant
Cell Culture centrifuge	Megafuge 1.0	Heraeus
Centrifuge (200-2000ml)	J-6B-Centrifuge	Beckmann
Centrifuge (up to 1000 ml)	J2-21 Centrifuge	Beckmann
Microcentrifuge 4°C-Room	Biofuge 13	Heraeus
PH meter	PH meter	Inolab
Vortex mixer	Reax 2000	Heidolph
Balance	Balance	Sartorius
Water bath with adjustable T°	Water bath with adjustable T°	GFL
Spectrophotometer	Biophotometer	Eppendorf
Refrigerator 4°C	Refrigerator 4°C	Leibherr
Freezer -20°C	Freezer -20°C	Leibherr
Freezer -80°C	Freezer -80°C (low flow)	Sanyo
Macroscope	Macroscope Leica M420	Leica
Microscope (for cells)	Microscope Axiovert 35	Zeiss
Microscope (for sections)	Microscope Axioplan	Zeiss
Microscope	DMLB	Leica
Thermomixer	Thermomixer comfort	Eppendorf

<b>Apparatus</b>	<b>Name</b>	<b>Manufacturer</b>
Phosphoimager	Phosphoimager Bas 1000	Fujix
UV crosslink	Stratalinker 1200J	Stratagene
Microwave	Microwave	Bosch
Heating block	Heating block	Eppendorf
Shaker	Duomax 1030	Heidolph
Sections apparatus	Sections apparatus	Leica
Timer	Timer	Oregon scientific
Pipettors	Pipettors	Eppendorf
Gel photography/documentation system	Gel photo./docu. system	BioRad
Hybridization Oven/Shaker	Hybridization Oven/Shaker	Amersham
UV transilluminator	UV transilluminator	IBN, Biozym, Uvis
Scintillation counter	Scintillation counter LS 6000 SE	Beckmann
Luminometer	Apparatus Lumat Berthold, LB 9501	Berthold
Photometer	Titertek-Multiskan-Plus-apparat	Citizen

## 2.3 Oligonucleotides

All primers used for different purposes in this study were synthesized by MWG ([www.ecom.mwgdna.com](http://www.ecom.mwgdna.com)). The oligonucleotide sequences are shown in the following table:

<b>Oligonucleotide</b>	<b>Sequence 5' -- -- --&gt; 3'</b>
1008LacZ-B2	CCATGGAAGCTTTACCGCTGGACGCCCTTGCT
1008LacZ-F1	CTCGAGACTAGTTCTAGAGCGGCCGGCA
BG081305-B2	ACCCTGCGATTTTGAAC
BG081305-B10	CATTTGGTGTCTTTGACC
BG081305-F1	CCTCTCTCTCCCATTGAG
BG081305-F7	ACCAGTCTGAACCTCCTCG
En2-B1	GTCGACATCGATCCTCGCTGTCCGACTTGCC
En2-F1	GGATCCATGGAGGAGAAGGATTCCAAGCC
Exon1-B3	GGAAAAGTCAGGGGGATGTGAAG
Exon1-F2	CAAGGTCCAGGATAGCCAGAGTTAC
Exon2-B4	CCACACACATAAAAAGGAGGAAGC
Exon2-F2	TTGCTGGCTGAAGTCTGCTCTTGG

Exon3-B6	TTTGAAGCCAATCTGTGCCAC
Exon3-F4	TGTGCGGTGACTGAGAACTTAGG
Foxa2-B1	GTCGACATCGATCGGATGAGTTCATAATAGGCCTGGA
Foxa2-F1	GGATCCATGCTGGGAGCCGTGAAGATGG
Geno Dpuro-not-B3	CAACCCACACACATAAAAAGGAGG
Geno Dpuro-not-F3	TGACGGAGAATCAGGTGAGAGCAG
Geno puro-3'not1-B1	TTTGCCACATAGCACGAG
Geno puro-3'not1-B2	GAAGAGCCTGACTCAAAGG
Geno puro-3'not1-F1	GGGATTAGATAAATGCCTGC
LacZ4	CCAGATAACTGCCGTCCTCC
nHD-B1	TCTAGACAATTTTCAGTTTTTGCTGCTTCTG
nHD-F1	CTCGAGACAAAGAGGGTTCGCACAACG
nHD-F2	ACTAGTACAAAGAGGGTTCGCACAACG
not intron1-B1	ATGCCCTCTTCTGGTGTGTGTCTG
not intron1-F1	GATGGTGTATGCCTGTAATCACTGC
not LRg-B2	AAGAGGCTGGGTATGATGG
not LRg-F2	TGTGTGTGTGTGTGTGTGCG
not ORF-B1	TTGAATCTTAACTGCCAATTCCTCAACTCAGCA
not ORF-B3	GTCGACATCGATCACTGCCAATTCCTCAACTCAGC
not ORF-F1	GGGGATCCATGTCCAGCCCTGCTCCCTCA
not ORF-F3	GGATCCATGTCCAGCCCTGCTCCCTCAG
not-homeo-B1	TTGAATCTTACAATTTTCAGTTTTTGCTGCTTC
not-homeo-F1	GGGGATCCACAAAGAGGGTTCGCACAACG
not1LacZ-B3	CTCGAGACTAGTTGCGCGACCCTGAGGGGACCT
not1LacZ-B4	CTCGAGAAGCTTCGGTGGGTGCCCATTTTCAGAGG
not1LacZ-F1	GTCCCAGCTGCAGTGAGGAAGTGCACAAAT
PGK puro-B1	TGGATGTGGAATGTGTGCG
VP16-B1	CTCGAGCCCACCGTACTCGTCAATTCCAAG
VP16-F1	GAATTCATGACCGATGTCAGCCTGGGGGAC

## 2.4 Vectors

### 2.4.1 Cloning vectors

Cloning vectors used during cloning procedures such as pGEM-Teasy, TOPO-XL-PCR, pUC19, pLitmus28, pLitmus29, pBluescript, pNEB193 and others were provided from companies such as Stratagene, New England Biolab, Invitrogen and Promega.

### 2.4.2 Expression vectors

Expression vectors used during cloning procedures such as pGEX4T-1, pQE30, pCS2MT, pCS2 and pGL3-Basic were provided from companies such as Stratagene, Invitrogen and Promega.

## 2.5 *E. Coli* strains

All *Escherichia coli* strains used to make Competent bacterias for DNA transformation are shown in the following table:

Strain	Genotype	Source
XL1-Blue	recA1 endA1 gyrA96 thi-1 hsdR17 supE44 relA1 lac [F <sup>-</sup> proAB lacIqZΔM15 Tn10 (TetR)]	Stratagene
SURE	E14 <sup>-</sup> (McrA <sup>-</sup> )Δ(mcrCB-hsdSMR-mrr)171 endA1 supE44thi-1 gyrA96 relA1 lac recB recJ sbcC umuC::Tn5(kanR) uvrC [F <sup>'</sup> proAB lacI <sup>q</sup> ZΔM15Tn10(TetR)]	Stratagene
SCS110	RpsL (strR) thr leu endA thi-1 lacY galK galT ara tonA tsx dam dcm supE44Δ(lac-proAB) [F <sup>'</sup> traD36 proAB lacI <sup>q</sup> ZΔM15]	Stratagene

## 2.6 *E. Coli* medium

*E. Coli* was grown in LB rich medium. Ingredients for this medium were added to water and the pH was adjusted to near 7 with 1N NaOH. Finally, the medium was sterilized by autoclaving. Liquid media can be solidified with Agar.

---

<b>Medium</b>	<b>Ingredients</b>	<b>Concentration</b>
LB	Tryptone	10 g/l
(Luria-Bertani)	Yeast Extract	5 g/l
	Sodiumchlorid	10 g/l
	(Agar)	(15 g/l)

---

If required, antibiotics and supplements with the appropriate concentration were added to the previously autoclaved LB medium. But the antibiotics and supplements were added to the medium until it cooled to <50 °C. IPTG and X-gal were used for white/blue colonies selection in the plates with LB solid medium.

---

<b>Antibiotics &amp; supplements</b>	<b>Stock solution</b>	<b>Final concentration</b>
Ampicillin	50 mg/ml in 70% EtOH (500x)	20-100 µg/ml
Kanamycin	50 mg/ml in H <sub>2</sub> O (1000x)	10-50 µg/ml
Chloramphenicol	34 mg/ml in 70% EtOH (1000x)	25-170 µg/ml
Tetracyclin	12 mg/ml in 70% EtOH (1000x)	10-50 µg/ml
Streptomycin	12 mg/ml in 70% EtOH (1000x)	10-50 µg/ml
IPTG	1 M (1000x)	1 mM
X-Gal	50 mg/ml (1000x)	50 µg/ml

---

## 2.7 Cell culture medium

Culture Medium used for HEK293 cell line, consists of two parts: a basal nutrient medium DMEM (Dulbecco's modified Eagle's medium) and supplements. The DMEM medium was sterilized by filtration using 0.1µm filter membranes. The fetal calf serum (FCS) was inactivated for 30 min at 56°C before adding it to the medium.

---

<b>HEK293-Medium:</b>	400ml DMEM (133.8 g DMEM-powder+ 37g NaHCO <sub>3</sub> ; pH7.4)
	45 ml FCS (fetal calf serum)
	5 ml 100x Penicillin/ Streptomycin (10000iU/ml)

---

## 2.8 Cell line

The cell line used for the transactivation assays was HEK293.

Name	Organism	Tissue
HEK293	Human	Embryonic kidney

## 2.9 Molecular Biology Methods

### 2.9.1 DNA-Methods

#### 2.9.1.1 Agarose gel Electrophoresis

Agarose gel electrophoresis was used as a standard method for separating, identifying and purifying 0.2kb to 30kb DNA fragments. The protocol can be divided into three stages: (1) a gel was prepared with an agarose concentration appropriate for the size of DNA fragments to be separated; (2) the DNA samples were loaded into the sample wells and the gel was runned at a voltage and for a time period that will achieve optimal separation; and (3) the gel was stained or, if ethidium bromide has been incorporated into the gel and electrophoresis buffer, was visualized directly upon illumination with UV light.

The appropriate Agarose concentrations for separating DNA fragments of various sizes are indicated in the following table:

Agarose (%)	Effective range of resolution of linear DNA fragments (kb)
0.5	30 to 1
0.7	12 to 0.8
1.0	10 to 0.5
1.2	7 to 0.4
1.5	3 to 0.2

### **2.9.1.2 Quantitation of DNA with absorption spectroscopy**

To quantify the DNA, an aliquot was measured by UV absorbance at 260 nm ( $A_{260}$ ) and 280 nm ( $A_{280}$ ) where the absorbance of 1 in a 1 cm path length corresponds to a DNA concentration of 50 $\mu$ g/ml (1 OD<sub>260</sub> dDNA = 50  $\mu$ g/ml). The absorbance ratio of 260 nm and 280 nm gave an estimate of the purity of the solution. Pure DNA solutions had  $A_{260}/A_{280}$  values between 1.7-2.

### **2.9.1.3 Digestion of DNA with restriction endonucleases**

Restriction endonuclease cleavage was accomplished simply by incubating the enzyme(s) with the DNA in appropriate reaction conditions. The amounts of enzyme and DNA, the buffer and ionic concentrations and the temperature and duration of the reaction vary depending upon the specific application.

#### Reaction mixture

x $\mu$ l	DNA (0.1-4 $\mu$ g DNA in H <sub>2</sub> O or TE buffer)
2 $\mu$ l	10X restriction buffer
x $\mu$ l	enzyme (1-5 U/ $\mu$ g DNA)
x $\mu$ l	H <sub>2</sub> O (to 20 $\mu$ l total volume)

In general, the reaction mixture was incubated for 1-2h at the recommended temperature (in general, 37 °C). The reaction was stopped by incubating for 10 min at 65°C (for most enzymes) or for 15 min at 75°C (for particular enzymes) to inactivate the enzyme.

### **2.9.1.4 Isolation and purification of DNA restriction fragments from agarose gels**

The recovery of DNA from agarose was performed using a silica membrane column purification method. The Kits, that include silica membrane spin columns and all appropriate buffers necessary for DNA purification, were provided from companies such as Macherey-Nagel or Qiagen. The procedure consist of: (1) a gel slice, containing DNA fractionated through an agarose gel, is melted and passed through a silica membrane column in the presence of high salt. Under these conditions, DNA is adsorbed onto the silica membrane. (2) The gel contaminants are subsequently washed away and (3) DNA is eluted in a low-salt buffer.

Therefore, DNA sample was digested with the appropriate restriction enzymes, loaded in agarose gel (with ethidium bromide) and subjected to electrophoresis. The target band was cut out with a clean scalpel and transferred to a 1.5-ml microcentrifuge tube. The volume of the agarose was estimated ( $\pm 100\mu\text{l}$ ), 2.5 to 3.0 vol of 6M sodium iodide was added and the contents were incubated for 5-10 min at 50°C to dissolve the agarose. 2vol of binding buffer were added, the contents were mixed well and the supernatant was applied to the silica membrane spin column. The spin column together with its collection tube were microcentrifugated for 1 min at maximum speed and the flowthrough was discarded. The spin column was washed with 750  $\mu\text{l}$  of wash buffer, microcentrifugated for 1 min at maximum speed and the flowthrough was discarded. The spin column was microcentrifugated for 1 min at maximum speed to remove any residual wash buffer (ethanol) from the column membrane. The spin column was transferred to a new 1.5-ml microcentrifuge tube and the DNA was eluted by adding 75-100  $\mu\text{l}$  nuclease-free water to the membrane, incubated for 10 min followed by microcentrifugation for 1 min at maximum speed. The DNA was collected and stored at 4°C or -20°C until use.

#### **2.9.1.5 Dephosphorylation of vector DNA by alkaline-phosphatase**

Dephosphorylation of DNA was achieved simply by incubating the shrimp alkaline-phosphatase enzyme with the DNA in appropriate reaction conditions. This procedure was used to dephosphorylate 5' termini of vector DNA in order to prevent self-ligation of the vector termini, thereby to decrease the vector background in cloning strategies. In general, the phosphatase treatment can be done directly following cleavage by restriction endonuclease. The reaction mixture was incubated for 1-2h at 37°C.

#### **2.9.1.6 Transformation of *E.coli* competent cells with plasmid DNA by electroporation**

Electroporation with high voltage was used for transforming *E.coli* with plasmid DNA. This procedure routinely gives more than  $10^9$  bacterial transformants per micro-gram of input plasmid DNA. The electroporation apparatus was set to 2.5 kv, 25  $\mu\text{F}$  and the pulse controller to 200 or 400 ohms. The plasmid DNA or ligation reactions was electroporated together with Competent bacteria cells (XL-blue, SURE, or SCS110 *E.coli*) and 1ml LB was added followed by an



incubation for 1h at 37°C. The bacterias were harvested and plated onto plates containing (LB / antibiotics / ±IPTG/X-Gal) and incubated at 37°C overnight.

### **2.9.1.7 Plasmid isolation using alkaline lysis miniprep**

The isolation of plasmid DNA from *E.coli* was performed using the alkaline lysis method. This procedure is appropriate to extract plasmid DNA from small amounts of many different cultures of plasmid-containing bacteria. 1-2 ml of *E.coli* LB culture was harvested by 3-5 min centrifugation (11.000 x g) and the pellet was resuspended with 200 µl buffer P1, lysated with 200 µl buffer P2 and neutralized with 200 µl buffer P3. After 10 min centrifugation at 14000 rpm, the supernatant (400-500µl) was transferred into a new tube, precipitated with 600-650 µl isopropanol and incubated for 10 min at RT. After 15 min centrifugation at 14000 rpm, the pellet was washed with 400 µl of 70% ethanol and the DNA was eluted with 50 TE buffer. For the enzymatic reaction, 5 µl of DNA were used to check the clone.

<b>Solution</b>	<b>composition</b>
Buffer P1	50 mM Tris.Cl, 10 mM EDTA, adjust to pH8 with HCl, add 100µg/ml RNaseA
Buffer P2	200 mM NaOH, 1% SDS
Buffer P3	3M potassium acetate, adjust to pH5.5 with glacial acetic acid

### **2.9.1.8 Plasmid isolation using NucleoSpin Kit**

The isolation of plasmid DNA from *E.coli* was performed by using a NucleoSpin Plasmid kit (Macherey-Nagel) for clones that were later sent for sequencing. 5 ml of *E.coli* LB culture was harvested by 3-5 min centrifugation (14000 rpm) and the pellet was resuspended with 250 µl lysis A1 buffer, lysated with 250µl buffer A2 and 300µl buffer A3 was added. After 10 min centrifugation at 11,000x g, the supernatant was loaded into a NucleoSpin Plasmid column with collection tube. The flow through was discarded after centrifugation for 1 min at 11,000x g. The NucleoSpin Plasmid column was washed two times with 600µl buffer A4 containing ethanol and after 2 min incubation, the DNA was eluted with 50µl H<sub>2</sub>O or EB (elution buffer) by centrifugation. The DNA was stored at 4°C or -20°C until use.

### **2.9.1.9 Isolation of Genomic DNA from mouse tissue**

Genomic DNA was extracted from fresh tissue of a (1/3) liver of an adult mouse. The tissue was cut in small pieces and incubated in 50 ml-Falcon overnight at 56 °C with 25 ml proteinase K buffer and 1 ml proteinase K (10mg/ml) in order to digest the tissue (after lysis and digestion the solution should appear clear and homogeneous). After 10 min centrifugation, 1 volume of Phenol/ Chloroform (equilibrated with TE) 25 ml was added to the supernatant and mixed by rotating the falcon up and down (this step is important to remove the protein). The phases are separated by 15 min centrifugation at 4000 rpm. The aqueous phase was removed by pipetting and transferred to a new plastic-Falcon. The DNA was precipitated by adding 0.8-1volume of isopropanol (25 ml), mixed gently and centrifugated for 10 min at 4000 rpm. The precipitate was washed with 70 % ethanol, the pellet was dried at RT and DNA was resuspended in 2 ml of TE buffer until dissolved (in general, 1mg DNA/ml TE buffer) by rotating on a vertical rotator 30rpm overnight at room temperature. The DNA was collected and stored at 4°C or –20°C until use.

<b>Solution</b>	<b>composition</b>
Proteinase K buffer	50mM Tris-HCL pH8, 100mM EDTA pH8, 100mM NaCL, 1% SDS
TE Buffer	10mM Tris, pH 8.0, 1mM EDTA

### **2.9.1.10 Enzymatic amplification of genomic DNA by PCR reaction**

The exons of *Not* were amplified by PCR using genomic DNA of wild type or mutant strains, as templates. The primers were Exon1-F2 and Exon1-B3 flanking exon1, Exon2-F2 and Exon2-B4 flanking exon2, and Exon3-F4 and Exon3-B6 flanking exon3. The PCR cycling parameters were: 1 initial cycle 94°C for 3 min (for pre-denaturation), 40 cycles (94°C for 30sec for denaturation, 57°C for 30 sec annealing temperature for the primers and 72 °C for 1 min for elongation) and 1 cycle 72°C for 7 min (for the final extension).

PCR reaction mixture

1-2µl	genomic DNA (250-500 ng)
25µl	1x Lysis buffer
2.5µl	10x PCR buffer
1.5µl	40mM Mg Cl <sub>2</sub>
1µl	10mM dNTPs
2µl	10µM forward primer
2µl	10µM backward primer
1µl	Taq polymerase (5U/µl)
14µl	H <sub>2</sub> O

<b>Solution</b>	<b>composition</b>
1x Lysis buffer	50mM KCL, 10mM Tris-CL ph8.3, 2mM MgCl <sub>2</sub> , 0.45% tween 20, 0.45% NP40
10x PCR buffer	166mM (NH <sub>4</sub> ) <sub>2</sub> SO <sub>4</sub> , 670mM Tris-Cl PH8.8, 1mg/ml BSA fractionV

PCR products were subcloned in a pGem-TEasy vector (Promega) and then verified by sequencing.

### **2.9.1.11 Cloning techniques**

#### **2.9.1.11.1 Subcloning into pGEMT-Easy vector**

The PCR or RT-PCR products were ligated to a pGEM-TEasy Vector (Promega Kit) in the following reaction mixture at 16 °C overnight:

Ligation reaction mixture

10-200 ng	PCR product
5µl	10x ligation Buffer
0.5µl	25ng pGEM-T Easy Vector (3kb)
1µl	T4 DNA Ligase (3 U/µl)
10µl	total volume

### **2.9.1.11.2 Subcloning into TOPO-XL-PCR vector**

The TOPO-XL-PCR Cloning Kit (Invitrogen) is designed for cloning 3-10kb PCR products. The PCR products were ligated to a TOPO-XL-PCR Vector in the following reaction mixture:

#### Ligation reaction mixture

4 µl          PCR product (2-40 ng/ µl)  
1µl          25ng TOPO-XL-PCR Vector (3.5kb)

The reaction mixture was incubated for 5 min at RT, 1µl 6xT0PO Cloning stop solution was then added, mixed for 10 sec at RT and placed on ice. The transformation was performed with TOP10 *E.coli* cells.

### **2.9.1.11.3 Ligation of DNA and (Vector: Insert) Ratio**

T4 DNA Ligase catalyses the joining of two strands of DNA between the 5'-phosphate and 3'-hydroxyl groups of adjacent nucleotides in either a cohesive-ended or blunt-ended configuration. As standard procedure to ligate insert(s) DNA and vector DNA by using T4 DNA Ligase (Promega), the templates were previously linearized with the appropriate enzyme(s) and sticky-ends or blunt-ends were generated. The vector DNA fragment was dephosphorylated and the ligation was set up in the following proportion :

$$\frac{\text{ng of vector} \times \text{Kb size of insert}}{\text{Kb size of vector}} \times \text{molar ratio insert} = \text{ng of insert}$$

#### Ligation reaction mixture

x ng          insert DNA  
x ng          vector DNA  
1µl          10x ligation Buffer  
1-2µl        T4 DNA Ligase (3 U/µl)  
10µl        total volume

The ligation reaction mixture was incubated at 16 °C overnight.

## **2.9.1.12 Southern blot analysis**

### **2.9.1.12.1 Labeling of DNA by Random Oligonucleotide-Primed synthesis**

The DNA probes were labeled by using Prime-It II Random Primer Labeling Kit from Stratagene (#300385). The following components were added to a sterile microcentrifuge tube: 25-50 ng of linearized Double stranded DNA, 0-23  $\mu$ l of water, and 10  $\mu$ l of random oligonucleotide primers and then heated at 95°C for 5 min. The contents of the tube were collected by a brief centrifugation at room temperature; where 10  $\mu$ l of 5x buffer, 5  $\mu$ l of radioactive labeled nucleotides (32P-dCTP) and 1  $\mu$ l of Exo(-) Klenow Enzyme (5 U) were added and incubated for 1-2 h at 37°C. The reaction was stopped by adding 2  $\mu$ l of stop mix. The probe was then purified as follow: the labeled DNA was precipitated by adding 50  $\mu$ l H<sub>2</sub>O, 50  $\mu$ l 7.5M NH<sub>4</sub> Ac, 2  $\mu$ l of glycogen (20 mg/ml), and 400 $\mu$ l ethanol 100%, incubated for 15 –30 min at -20°C, centrifugated for 10-15 min at 4000 rpm and washed with 400  $\mu$ l of 70% ethanol. The labeled probe was eluted in 100  $\mu$ l H<sub>2</sub>O. The radioactivity was measured by using a Scintillation counter apparatus.

### **2.9.1.12.2 DNA Blotting onto a nylon membrane using an alkaline buffer**

The DNA blotting was performed using the alkaline transfer for HybondN-Plus membrane protocol (Amersham Pharmacia biotech). The genomic DNA from ES cells or from mouse tissue was previously digested in 50  $\mu$ l total volume with 30-40 U of the appropriate enzyme(s), and incubated overnight at 37°C. The digested DNA was loaded in 1% Agarose gel and runned slowly to achieve good separation. After electrophoresis, the gel was incubated in 0.2N HCl (use 4x volume of gel) for 15 min while shaking gently and 2 times in a denaturation solution for 20 min. The gel was transferred carefully back on gel tray and overlaid with two Whatman 3MM cut to gel size and were wetted in denaturation solution. The gel and Whatman were flipped around and the set was put down on a spread out Saran wrap (fold in Saran wrap so that the transfer only goes via the gel). HybondN-Plus membrane was wetted first in water, then in denaturation solution and placed neatly on gel. The nylon membrane was covered with two layers of Whatman 3MM wetted in denaturation solution and then a large stack of paper towels was put on top, finished up with the gel tray which held the paper towels together. After blotting overnight, the membrane was neutralized for 5 min in 500 ml 50mM NaPi, placed between two Whatman layers, baked for 20 min at 80°C and subjected to UV crosslink in a Stratalinker 1200J.

<b>Solution</b>	<b>composition</b>
Denaturation solution	0.5M NaOH, 1.5M NaCl
Neutralization solution	50mM NaPi (pH6.7)
0.2N HCl	20 ml conc.HCl in 1L water

### **2.9.1.12.3 Hybridization analysis of DNA blot with radiolabeled DNA probe**

The hybridization was performed as follows: The solutions WashII and Church were pre-warmed at 65°C. The membrane was shortly incubated in WashII at 65°C. 20 ml of Church were filled into hybridization tube, the membrane was added and incubated for at least 30 min at 65°C (pre-hybridization). The labeled probe was denatured at 95°C for 10 min and the membrane was hybridized overnight in 20 ml Church containing the labeled probe (Radioactivity 100000-200000 cpm of 32P-dCTP per ml). The membrane was washed 3x 20 min with WashII at 65°C and dried between Whatman layers 3MM. The membrane was exposed at -80 °C to Hyperfilm-MP (Amersham).

<b>Solution</b>	<b>composition</b>
Church Buffer	BSA10 g, 0.5M EDTA 2 ml, 1 M NaHPO <sub>4</sub> (pH7.2) 500 ml, 20% SDS 350 mL, H <sub>2</sub> O to 1 liter
Wash I	BSA 10 gm, 0.5M EDTA 2 ml, 1 M NaHPO <sub>4</sub> (pH7.2) 80 ml, 20% SDS 500ml, H <sub>2</sub> O to 2 liters
Wash II	0.5M EDTA 8 ml, 1 M NaHPO <sub>4</sub> (pH7.2) 160 ml, 20 % SDS 200 ml, H <sub>2</sub> O to 4 liters

## **2.9.2 RNA-Methods**

### **2.9.2.1 Isolation of total RNA from mouse tissue**

The isolation of total RNA was performed following the protocol from RNeasy Mini Kit (QIAGEN). Approximately, 20 mg of fresh tissues from wild type or mutant mouse embryos at stage E9.5 were disrupted with a mortar and a pestle and the lysate was homogenized in 350  $\mu$ l RLT buffer. The lysate was pipetted onto a QIAshredder column, sitting in a 2-ml collection tube, and centrifuged for 2 min at maximum speed ( $8000 \times g = 10,000$  rpm). 1 volume of 70% ethanol (350  $\mu$ l) was added to the supernatant (cleared lysate), mixed well by pipetting, 700  $\mu$ l of the sample was applied onto a RNeasy mini spin column, sitting in a 2-ml collection tube, and centrifuged for 15 sec. The column was washed with 700  $\mu$ l of RW1 buffer and washed two times with 500  $\mu$ l of RPE buffer. To ensure that no ethanol is carried over during elution, it is important to dry the RNeasy membrane by performing an additional centrifugation for 2min; since residual ethanol may interfere with subsequent reactions. RNase-free water (30-50  $\mu$ l) was added directly onto the RNeasy membrane to elute total RNA by performing a centrifugation for 1min. The total RNA quality was confirmed by checking the integrity of 18S (1900bp) and 28S (4800bp) RNA molecules using the 1% agarose gel stained with ethidiumbromide.

### **2.9.2.2 Quantitation of RNA with absorption spectroscopy**

To quantify the total RNA, an aliquot was measured by UV absorbance at 260 nm ( $A_{260}$ ) and 280 nm ( $A_{280}$ ) where the absorbance of 1 in a 1 cm path length corresponds to a RNA concentration of 40  $\mu$ g/ml (1 OD<sub>260</sub> RNA = 40  $\mu$ g/ml). The absorbance ratio of 260 nm and 280 nm gave an estimate of the purity of the solution. Pure RNA solutions had  $A_{260}/A_{280}$  values between 1.7-2.

### **2.9.2.3 Amplification of cDNA by RT-PCR**

First-strand cDNA was synthesized from 5  $\mu$ g of total RNA using the Superscript II Reverse Transcriptase (Invitrogen) and the oligo(dT) primers. The total volume reaction was 20  $\mu$ l.

The following components were added to a nuclease-free microcentrifuge tube: 5  $\mu$ g of total RNA, 1  $\mu$ l Oligo (dT)<sub>12-18</sub> (500  $\mu$ g/ml) and x  $\mu$ l sterile distilled water to 12  $\mu$ l. The mixture was heated at 70 °C for 10 min (to denature the secondary structure of RNA) and quicked chill on ice. The contents of the tube were collected by a brief centrifugation and the following components were

added to the tube: 4 $\mu$ l 5x First Strand Buffer, 2 $\mu$ l 0.1M DTT, 1 $\mu$ l 10 mM dNTP Mix and 1 $\mu$ l SUPERSCRIPT II (200 units), mixed by pipetting gently up and down and incubated for 1-2 hours at 42 °C. The reaction was inactivated by heating at 70 °C for 15 min. The cDNA can now be used as a template for amplification in a PCR reaction.

Reaction mixture for Reverse Transcription

5 $\mu$ g	total RNA
1 $\mu$ l	Oligo (dT) <sub>12-18</sub> (500 $\mu$ g/ml)
4 $\mu$ l	5xFirst Strand Buffer
2 $\mu$ l	0.1M DTT
1 $\mu$ l	10 mM dNTP Mix (10mM each dATP, dGTP, dCTP and dTTP at neutral pH)
1 $\mu$ l	SUPERSCRIPT II (200 units)
x $\mu$ l	H <sub>2</sub> O

The PCR reaction was performed with the following conditions: pre-denaturation at 94°C for 3 min, 45 cycles (denaturation at 94°C for 30sec, 55°C for 30 sec for the annealing temperature of the primers and extension at 72 °C for 30 sec), and final extension at 72°C for 7 min.

PCR reaction mixture

5 $\mu$ l	cDNA (RT product)
4 $\mu$ l	10X buffer (Sigma)
1 $\mu$ l	10mM dNTPs
2 $\mu$ l	10 $\mu$ M forward primer
2 $\mu$ l	10 $\mu$ M backward primer
0.5 $\mu$ l	Taq polymerase (Sigma)
25.5 $\mu$ l	H <sub>2</sub> O

Primer pairs for RT-PCR were BG081305-F1 and BG081305-B10, and for nested RT-PCR were BG081305-F7 and BG081305-B2. RT-PCR products were subcloned in a pGem-TEasy vector.

#### **2.9.2.4 Synthesis of digoxigenin-labeled riboprobes**

Boehringer Dig RNA labeling kit was used to generate antisense riboprobes. Antisense riboprobes are synthesized as run-off transcripts from linearized templates, using bacteriophage polymerases and template DNA consisting of the DNA fragment of interest cloned in a vector containing the promoter appropriate for RNA polymerase (SP6, T7 or T3). RNA synthesis is carried out in the presence of a digoxigenin-substituted ribonucleotide. The procedure was



performed as follows: the template DNA was prepared by linearizing the plasmid with the appropriate enzyme(s). 2-3µg DNA was digested in 40µl reaction mixture at 37 °C for 1-2 hours. Linearized DNA was precipitated with 1/2 vol 7.5 M NH<sub>4</sub> OAc + 2.5 vol 100% ethanol, washed with 300µl 70% ethanol and eluted in 20-30 µl TE buffer. Then, 1-4µg of linearized template DNA was incubated in the following transcription reaction mixture for 2 hours at 37 °C.

Transcription reaction mixture

1-4 µg	DNA (1-13 µl linearized template)
2µl	10Xtranscription buffer
2µl	NTPs (Dig RNA labeling mix)
2µl	RNA polymerase (SP6, T7 or T3)
1µl	RNase inhibitor
x µl	H <sub>2</sub> O to 20 µl final volume (no DEPC- H <sub>2</sub> O)

After incubation, 2µl of RNase-free DNaseI was added into the reaction mixture tube and incubated for 15 min at 37 °C. Subsequently, for precipitation: 1µl tRNA (10 µg/µl), 100 µl DEPC- H<sub>2</sub>O, 33 µl 7.5M NH<sub>4</sub> OAc and 300 µl 100% EtOH were added to the reaction, incubated for 30 min at -80°C, centrifugated at 4000 rpm for 10 min and washed with 300 µl 70% EtOH. The riboprobe was rehydrated in 100µl 50% formamide/inDEPC-H<sub>2</sub>O and stored at -80°C. To estimate the amount of transcript against tRNA, 1 % agarose was runned for 5-10 min at 150V.

### **2.9.2.5 Whole-Mount in Situ Hybridization and detection of RNAs in mouse embryos**

Whole-Mount in Situ Hybridization (WISH) was performed following a standard procedure with digoxigenin-labeled antisense riboprobes (Wilkinson 1992) with minor modifications, to detect RNA transcripts in embryos.

To performe the WISH, the embryos were rehydrated through 75%, 50%, 25% methanol/PBS 10 min each on ice and washed 2 x 10 min in PBT on ice. Subsequently, the embryos were bleached with 6% hydrogen peroxide in PBT for 1 h on ice and washed 3x with PBT for 10 min, 3x with RIPA buffer for 5 min and 3x with PBT for 5 min. The fixation was performed with 4%PFA/0.2% glutaraldehyde in PBT for exactly 20 min. Embryos were washed 3x with PBT for 5 min, 1x with hybe-buffer/PBT (1:1) at RT for 10 min, 1x with hybe-buffer at RT for 10 min and incubated with hybe-buffer at 65°C for 1-3 hours. DIG labeled riboprobe was denatured in

hybe-buffer at 80 °C for 3 min and embryos were hybed in a hybe-buffer with: tRNA (100 µg/ml) and 1:100 dilution of Dig labeled probe (previously denatured 0.1-1 µg/ml; usually 0.25 µg/ml) at 65 °C overnight.

To remove the unbound probe, the embryos were washed 2x with hybe buffer for 30 min at 65 °C, 1x with hybe buffer /RNase solution (1:1) for 5 min at RT, incubated 2x with RNase solution containing 100µg/ml RNaseA for 30 min at 37°C and 1x with RNase solution/SSC/FA/Tween20 (1:1) for 5 min at RT. Embryos were heated from RT to 65 °C and washed 2x with SSC/FA/Tween20 for 5 min, 3 x for 10 min, 1 x for 30 min, 5 x for 1h. Afterwards, the embryos were cooled down, washed 1x with SSC/FA/Tween20 /TBST (1:1) for 5 min, 2x with TBST for 10 min at RT, 2x with MABT for 10 min at RT and then incubated for 1h at RT in 5% blocking solution/MABT. At the same time, Dig antibodies (1:5000 dilution) were preadsorbed at 4 °C for 1h in 1% blocking solution/MABT. Subsequently, the embryos were incubated in this antibody solution at 4 °C overnight while shaking gently.

To remove the unbound antibody, the embryos were washed 3x with TBST for 5 min at RT, 8x for 1h at RT and left in TBST on shaker overnight at 4 °C.

For staining, the embryos were washed 3x with alkaline phosphatase buffer for 20 min at RT and developed (at 37°C or at RT or at 4°C) in staining solution from Boehringer BM purple AP substrate (#1442074) to detect bound digoxigenin-11-dUTP labeled riboprobes with alkaline phosphatase conjugated anti-digoxigenin antibodies (Roche). After staining, the embryos were washed 2-3x with alkaline phosphatase buffer for 10 min and fixed in 4% PFA/PBS overnight at 4°C. The embryos were stored at 4°C. For photographic records, embryos were cleared in 50% glycerol.

All solutions used before and for hybridization should be treated with diethylpyrocarbonate (DEPC) and autoclaved to inhibit RNase activity.

<b>Solution</b>	<b>composition</b>
DEPC- H <sub>2</sub> O	0.01% DEPC (50 µg/500ml) autoclaved
PBS	30ml NaCl (5M), 15mL Na-Ph buffer (1M;ph7.3) add to 1liter water
4% PFA/PBS	4g PFA, 100ml DEPC water, a several drops of NaOH (10N), heat at 55°C until PFA is dissolved, cool on ice, adjust pH to 6-7 with HCl.

PBT	PBS, 0.1% Tween20
tRNA	10 µg/µl (from Boehringer #109517) in DEPC water, phenolize 2x and store as aliquots at -20°C
RIPA	2.5ml SDS (10%), 15ml NaCl (5M), 5ml NP40, 25 ml Deoxycholate (10%), 1ml EDTA (0.5M), 25ml 1MTris pH 8, add water to 500ml
20x SSC	17.53g NaCl, 8.82g sodium citrate, dissolve in 80ml water, adjust to pH 7 with a several drops of conc. HCl, adjust to 100ml
1M Citric acid	in DEPC water
Hybe buffer	5ml deionized formamide (FA), 2.5ml 20 X SCC, 10µl Tween20, 2.05ml water, adjust to pH6 with 1 M citric acid (ca. 450µl/10ml)
SSC/Formamid/Tween20	5ml SSC (20x), 25ml deionized formamid, 50µl Tween20, add to 50 ml with water
10x TBST	8g NaCl, 0.2g KCl, 25 ml Tris (1M; ph 7.5), 10 ml Tween, add to 100ml with water
RNase solution	1ml NaCl (5M), 100µl Tris HCl (1M;ph 7.5), 10µl Tween20, 8.89ml water
RNase A	dissolve RNase A (from Sigma R-4875) at a concentration of 10mg/ml in 0.01 sodium acetate (pH 5.2), heat to 100 °C for 15 min, cool to RT, adjust by adding 0.1 volumes of Tris HCl 1M pH 7.4, store as aliquots at -20 °C
MAB	11.6g maleic acid (0.1 mol/l), 8.8g NaCl (0.15mol/l), add 800 ml water, adjust with solid NaOH to pH 7.5, add water to 1liter
MABT	MAB, 0.1% Tween20
Blocking stock solution	5 % (w/v) blocking reagent (Boehringer/Ingelheim) was dissolved in MAB solution by heating in a microwave oven. This stock solution is autoclaved and stored as aliquots at -20 °C
Alkaline phosphatase buffer	1ml NaCl (5M), 2.5ml MgCl <sub>2</sub> (1M), 50µl Tween20, 5ml Tris (1M; pH9.5), add to 50ml with water
Staining solution	Boehringer BM purple AP substrate (#1442074)

## **2.10 Cell Biology Methods**

### **2.10.1 Cell culture conditions**

The environment in which the HEK293 cultures were kept, typically a water-jacketed 5%CO<sub>2</sub> incubator, must provide a constant temperature of 37°C, humidity to prevent evaporation of medium, O<sub>2</sub> for respiration and CO<sub>2</sub> for the maintenance of the pH of bicarbonate-buffered medium. Additionally, all solutions and equipment coming into contact with living cells were sterilized and all cell culture work was performed under aseptic conditions.

### **2.10.2 Trypsinizing and subculturing cells**

A primary culture of HEK293 cells was grown to confluency in a 6-cm petri plate containing 5ml culture medium. Cells were washed with EDTA-saline, were dispersed by trypsin treatment and then reseeded into secondary cultures, where a fresh medium was added.

<b>Solution</b>	<b>Composition</b>
EDTA-Saline	137 mM NaCl, 2,7 mM KCl, 4,3 mM Na <sub>2</sub> HPO <sub>4</sub> , 1,4 mM KH <sub>2</sub> PO <sub>4</sub> , 0,537 mM EDTA, pH 7,56, autoclaved
10x Trypsin-Lösung	0,5% Trypsin in EDTA-Saline, sterilized by filtration

### **2.10.3 Freezing cells**

A culture of HEK293 cells was grown to confluency in a 6-cm petri plate containing 5ml culture medium. Cells were dispersed from the plate by trypsin treatment, transferred to a sterile 5-ml falcon tube containing 2 ml of fresh medium, centrifugated for 3 min at 1000 rpm and the supernatant was removed. The cells were resuspended in 800µl fresh DMEM medium, 100µl FCS and 100µl DMSO and stored into 2-ml cryovials at -80°C.

#### **2.10.4 Thawing and recovering cells**

When cryopreserved HEK293 cells were needed, the vial was placed into 37°C water bath and agitated continuously until the medium was thawed. The thawed cell suspension was transferred into a sterile 5-ml falcon tube, centrifuged for 3 min at 1000 rpm and the supernatant was removed. The cells were gently resuspended in 1 ml fresh DMEM medium, transferred to 10-cm petri plate containing 10 ml of fresh medium and incubated at 37°C.

#### **2.10.5 Calcium-Phosphate-mediated transfection of HEK293 cells**

The transient transfection of DNA into HEK293 cells was performed by the Calcium-Phosphate-method. HEK293 cells were plated onto a 6-cm petri plate for tissue culture and grown to 80% confluency. Approximately, 2h before the transfection, the medium was changed and 4ml fresh DMEM medium was added. For the transfection, the following components were added to a sterile microcentrifuge tube: 200 µl 2x Hebs, 200 µl 2.5M CaCl<sub>2</sub> diluted (1:10), x µg DNA, pipetted up and down until a precipitate containing calcium phosphate and DNA was formed, added to the cells and incubated overnight at 37°C in a water-jacketed CO<sub>2</sub> incubator. The cells were washed 2x with 1x Hepes, (or with 1x PBS) and 4 ml fresh DMEM medium was added. After 30 h incubation, the cells were harvested.

<b>Solution</b>	<b>composition</b>
2.5M CaCl <sub>2</sub>	18.38g CaCl <sub>2</sub> , 50 ml H <sub>2</sub> O, and sterilized by filtration
10x Hepes	67 mM KCl, 1.42 M NaCl, 100 mM HEPES, adjust pH 7.3
10x Hebs	1.37 M NaCl, 0.21 M HEPES, 48 mM KCl, 7.5 mM Na <sub>2</sub> HPO <sub>4</sub>
2x Hebs	dilute 10x Hebs with water (1:5), adjust pH 7.1, and sterilized by filtration
10x PBS	80g NaCl, 2g KCl, 6.1g Na <sub>2</sub> HPO <sub>4</sub> , 1.9g KH <sub>2</sub> PO <sub>4</sub> , adjust pH 7.3

## **2.11 Biochemical Methods**

### **2.11.1 Transactivation Assay**

30h after the Calcium-Phosphate-mediated transfection of HEK293 cells, the cells were washed 2x with 1xPBS, 400 µl of Extraction buffer was added followed by incubation for 10 min at RT. The lysated cells were harvested together with the extraction buffer from the plate, transferred into a microcentrifuge tube and centrifugated for 5 min at 10,000 rpm. The lysate was transferred to a new tube and the measurements were then taken. The transfection studies were conducted in at least triplicate on two-to-three separate occasions.

<b>Solution</b>	<b>composition</b>
5x Extraction buffer	125mM Tris pH7.8 (adjusted with H <sub>3</sub> PO <sub>4</sub> ), 10 mM EDTA, 10 mM, DTT, 50% Glycerol, 5% Tritonx-100
10x PBS	80g NaCl, 2g KCl, 6.1g Na <sub>2</sub> HPO <sub>4</sub> , 1.9g KH <sub>2</sub> PO <sub>4</sub> , adjust pH 7.3

#### **2.11.1.1 Measurement of Luciferase activity**

To measure the luciferase activity: 50µl lysate, 300 µl Mess buffer, and then injected 100 µl 0.25M of luciferin solution by using a luminometer apparatus Lumat (Berthold, LB 9501). The luciferase activity is presented as relative light units.

<b>Solution</b>	<b>composition</b>
Mess -buffer	25mM Glygylglycin, 15mM MgSO <sub>4</sub> , 5mM ATP
Luciferin solution	100 mg luciferin in 14,27 ml of 25 mM NaOH (if required add some drops of NaOH until the sol. appears clear)

### 2.11.1.2 Measurement of $\beta$ -galactosidase activity

The  $\beta$ -Galactosidase activity was determined to normalize levels of the luciferase activity in the lysates. To measure the  $\beta$ -galactosidase activity: 40  $\mu$ l lysate, 400  $\mu$ l Z-buffer, 100  $\mu$ l ONPG (4 mg/ml in Z-buffer), incubated at RT until a clear yellow color was observed, then the reaction was stopped by adding 250  $\mu$ l 1M NaCO<sub>3</sub>. 100  $\mu$ l was used to measure the  $\beta$ -gal activity using a photometer Titertek-Multiskan-Plus-apparatus.

Solution	composition
Z-buffer	60 mM Na <sub>2</sub> HPO <sub>4</sub> , 40 mM NaH <sub>2</sub> PO <sub>4</sub> , 10 mM KCl, 1mM MgSO <sub>4</sub> , 50 mM $\beta$ -Mercaptoethanol

### 2.11.2 Whole-Mount histochemical detection of $\beta$ -galactosidase activity

The embryos were examined for *lacZ* expression by X-gal staining according to standard procedures, described as follows: the embryos were isolated, fixed for 5 min at room temperature in fixing solution, washed 2x for 5 -10 min at RT in washing solution and incubated overnight at 37°C in staining solution.

Solution	composition
Fixing solution	10 ml phosphat buffer (SPP), 80 $\mu$ l gluteraldehyde-solution (50% in H <sub>2</sub> O), 20 $\mu$ l 1M MgCl <sub>2</sub> , 100 $\mu$ l 0.5M EGTA pH 7.5
Washing solution	2ml 1M MgCl <sub>2</sub> , 10 ml 1% Na-desoxycholol, 10 ml 2 % NP40, and fill with SPP to 1000ml
Staining solution	100 $\mu$ l 0.5M K <sub>3</sub> FeCN <sub>6</sub> , 100 $\mu$ l 0.5M K <sub>4</sub> FeCN <sub>6</sub> , 200 $\mu$ l X-Gal (stock solution 50 mg/ml in Dimethylformamide), and 9.6 ml washing sol
Phosphat buffer pH 7.4	77.4 ml 1M Na <sub>2</sub> HPO <sub>4</sub> , 22.6 ml 1M NaH <sub>2</sub> PO <sub>4</sub> , and fill with H <sub>2</sub> O to 1000 ml
0.5M EGTA	19.02 g/ 100 ml, adjust to pH7.5 with 10N NaOH

## **2.12 Histology Methods**

### **2.12.1 Analysis of WISH-Paraffin-Sections after Eosin-staining**

After Whole-Mount In Situ Hybridization, the embryos E9.5 (which were previously fixed in 4% PFA) were washed 2x with PBS for 5 min at RT and dehydrated gradually into methanol: 1x in 25% methanol, 1x in 50% methanol, 1x in 75% methanol and 1x in 100% methanol. Embryos were transferred into paraffin as follows: 1x in isopropanol for 12 h, 1x in 50 % isopropanol/paraffin for 12 h, and 1x in paraffin overnight. Embryos were embedded in paraplast and cut 10 µm sections. After drying overnight at 42 °C, slides containing paraffin sections were placed in a slide holder and deparaffinized and stained as follows: incubation 2 x in Rotihistol for 1 min, 1x in 100% ethanol for 1 min, 1x in freshly made Eosin –staining solution for 5-15 sec, 1x in 90% ethanol for 30 sec, 1x in 100% ethanol for 1 min and 1x in Rotihistol for 1 min. Slides were covered with coverslips after using 2-3 drops of a VectaMount (H-5000) from Vector Laboratories, Inc., 60ml (permanent mounting medium).

<b>Solution</b>	<b>composition</b>
Eosin-staining solution	20 ml 2% Eosin Y-Certified (E4382) (Sigma) in H <sub>2</sub> O, 150 ml ethanol 100%, 2 ml glacial Acetic acid, 8 ml H <sub>2</sub> O

### **2.12.2 Skeleton preparation**

Newborn mice were eviscerated and placed in water overnight. The skeletons were immersed in a 65 °C water bath for 1 min and skinned. Subsequently, the skeletons were fixed in 100% ethanol for 4-7 days, changing the ethanol every 2 days. Then, incubated in acetone at room temperature for 3 days. After rinsing the skeletons in de-ionized water, they were incubated at RT in staining solution for 3-4 days. The skeletons were rinsed briefly with de-ionized water and were first cleared in 2 % KOH for 3-6 hours. The skeletons were further incubated in another clearing solution overnight or until the tissue surrounding the skeleton became clear. The skeletons were stored in 100% Glycerol.



<b>Solution</b>	<b>composition</b>
Staining solution	1 vol. 0.3% alcian blue 8GX (Sigma#3157) in 70% ethanol 1 vol. 0.3% alizarin red S (Sigma#5533) in 50% ethanol 1 vol. glacial acetic acid 17 vol. 100% ethanol
Clearing solution	1 vol. 50% glycerol 1 vol. 1% KOH

## 2.13 Embryology Methods

### 2.13.1 Embryo generation

Embryos were obtained from matings between wild type mouse strains or/and from matings between homozygous (*tc/tc*) mutant mice. The plaques were checked and the embryos were collected at the desired stage.

### 2.13.2 Fixation and storage of embryos

Embryos collected at different embryonic stages (6.5d until 13.5 d) were fixed in 4% PFA/PBS overnight at 4°C, washed 2x with 1xPBS for 10 min and dehydrated through 25%, 50%, 75% and 2x with 100% Methanol (DEPC- H<sub>2</sub>O) 10 min each on ice. These embryos can be stored at -20°C for up to 2 months or at -80°C for some years (2-3 years).

<b>Solution</b>	<b>composition</b>
DEPC- H <sub>2</sub> O	0.01% DEPC (50 µg/500ml) autoclaved
PBS	30ml NaCl (5M), 15mL Na-Ph buffer (1M;ph7.3) add to 1liter water
4% PFA/PBS	4g PFA, 100ml DEPC water, a several drops of NaOH (10N), heat at 55°C until PFA is dissolved, cool on ice, adjust pH to 6-7 with HCl.

## 2.14 Gene targeting by homologous recombination in ES cells

### 2.14.1 Construction of the Targeting vector

The replacement construct contains two regions of homology (5' and 3') to the target gene, positive selectable marker such as PGKpuro selection cassette flanked by *loxP* sites, and negative selectable marker such as Diphtheria ToxinA expression cassette (pKO SelectDT).

### 2.14.2 Isolation of genomic DNA from ES cells after electroporation

The targeting vector was electroporated into truncate ES cells and puromycin resistant ES cell clones were selected and expanded essentially as described (Schoor et al. 1999). The ES cells work has been done by the technical assistant Hannelore Burkhardt.

The genomic DNA was isolated from ES cells described as follows: the medium was removed from the 24 well-plates, in each well 500 µl of proteinase K buffer, containing 100µg/ml proteinase K, was added and the plates were incubated overnight at 37 °C. After incubation, 500 µl of cold isopropanol was added followed by another incubation of 6h at RT while shaking. The precipitated DNA of each clone was fished carefully with a needle and transferred into a fresh tube containing 200-400 µl TE buffer (pH 7.5). To dissolve the DNA, the tubes were incubated first for 15 min at 65 °C and afterwards, overnight at RT.

<b>Solution</b>	<b>composition</b>
Proteinase K buffer	100mM Tris-HCL pH8.5, 5mM EDTA, 200mM NaCL, 0.2% SDS
Proteinase K	stock solution 10 mg/ml
TE Buffer	10mM Tris pH 7.5, 1mM EDTA

### **2.14.3 Screen for the right targeted ES cells before cre expression**

Correctly targeted clones were identified by PCR using primers derived from the *puro* sequence puro3'Not-F1, and genomic sequences downstream of the targeting vector puro3'Not-B1 or puro3'Not-B2. The genotyping PCR cycling parameters were: 1 cycle 94°C for 2 min (for initial denaturation), 10 cycles (94°C for 15sec, 53°C for 30 sec and 68 °C for 4 min), 30 cycles (94°C for 15sec, 53°C for 30 sec and 68 °C for 4 min+50 sec) and 1 last cycle 72°C for 7 min (for final elongation).

The PCR reaction was performed using the Expand High Fidelity PCR system (Roche), which is composed of an enzyme mix containing thermostable Taq DNA polymerase and Tgo DNA polymerase, a thermostable DNA polymerase with proofreading activity. This Expand High Fidelity PCR system is designed to generate PCR products up to 5kb.

#### PCR reaction mixture

2µl	genomic DNA (250-500 ng)
5µl	10X Expand buffer 2 (Roche)
1µl	10mM dNTPs
1µl	10µM forward primer
1µl	10µM backward primer
1µl	Expand High Fidelity Enzyme mix (3.5U)(Roche)
40µl	H <sub>2</sub> O

The positive clones will generate a PCR product of 4.8-4.9kb. PCR-positive clones were verified by Southern blot analysis using labeled external probes located 3' and the 5' to the regions of homology in the vector.

### **2.14.4 Screen for the correct targeted ES cells after cre expression**

The removal of sequences between the *lox* sites is accomplished by transient expression of Cre recombinase. The *puro* cassette was excised by electroporating ES cells (positive clones previously identified by PCR and by Southern Blot) with supercoiled Cre expression plasmid Turbo-Cre (gift of the Embryonic Stem Cell Core of the Siteman Cancer Center, Washington University Medical School), and puromycin non-resistant ES cell clones were selected and expanded in 24 well-plates (each clone/per each well). The ES cells work has been done by the technical assistant Hannelore Burkhardt.

The genomic DNA was isolated from the ES cells (as described above) and *puro* excision was verified by Southern blot and by PCR ( $\Delta$ *puro* genotyping PCR) using the primers ca1 and ca2. The  $\Delta$ *puro* genotyping PCR cycling parameters were: 1 cycle 94°C for 3 min (for initial denaturation), 30 cycles (94°C for 30 sec for denaturation, 55°C for 30 sec annealing temperature for the primers and 72 °C for 30 sec for elongation) and 1 cycle 72°C for 7 min (for final extension).

#### PCR reaction mixture

1µl	genomic DNA (100-500 ng)
25µl	1x Lysis buffer
2.5µl	10x PCR buffer
1.5µl	40mM Mg Cl <sub>2</sub>
1µl	10mM dNTPs
2µl	10µM forward primer
2µl	10µM backward primer
1µl	Taq polymerase (5U)
14µl	H <sub>2</sub> O

The positives clones will generate two different PCR products: 236bp and 270bp that were checked by running 4% Metaphor gel.

### **2.14.5 Generation of tetraploid embryos**

To generate completely ES cell-derived embryos, ES cells were injected into tetraploid FVB/N morulae that were subsequently transferred to (C57BL/6 °— BALBc) F1 pseudopregnant females (this technique was performed by Dr.Karin Schuster-Gossler).

## **2.15 Transgene methods**

### **2.15.1 Construction of the promoter-*LacZ* reporter plasmid**

Promoter *LacZ* reporter construct contains 12kb upstream genomic region of *Not* containing the first exon and intron, fused in frame with the second exon of *Not* to *E.coli lacZ* gene containing SV40 and PGK polyadenylation signals.

### **2.15.2 Transgene generation by pronuclear injection**

The Promoter *LacZ* reporter construct was digested with NotI/XhoI to remove vector sequences. The linearized *lacZ* DNA was purified by gel electrophoresis and 2 ng/μl were microinjected into the pronucleus of FVB/N fertilized mouse egg. The injected embryos were transferred into pseudopregnant recipients and were recovered at E9.5 (this technique was performed by Dr.Karin Schuster-Gossler).

### **2.15.3 Genotyping of *LacZ* transgene**

The transgene integration was examined by PCR using genomic DNA from the yolk sac of the embryos at stage E9.5. The primers used for the genotyping were Ex2-F2 and LacZ4. Ex2-F2 derived from the genomic sequence of *Not* locus and LacZ4 derived from the *LacZ* sequence. The PCR cycling parameters were: 1 cycle 94°C for 3 min (for pre-denaturation), 30 cycles (94°C for 30 sec for denaturation, 56°C for 30 sec annealing temperature for the primers and 72 °C for 1 min for elongation) and 1 cycle 72°C for 7 min (for final extension). The PCR product size expected is 600 bp.

## 3. Results

### 3.1 Truncate phenotype

#### 3.1.1 Skeletal defects in truncate mutant mice

The vertebral column is the defining feature of vertebrates. Truncate is a mouse spontaneous recessive mutation, which leads to abnormalities of the vertebral column (Theiler 1959).

Previously, in the published data from Theiler, he described the morphological defect in homozygous truncate animals and pointed out that the affected tail of these animals was shortened or showed a thinned out segment of variable length. However in his study, he did not report that additionally some truncate mutant mice showed the total absence of a tail. Therefore, skeletal phenotypes of homozygous truncate newborn mice were analyzed by performing an alcian blue-alizarin red staining.

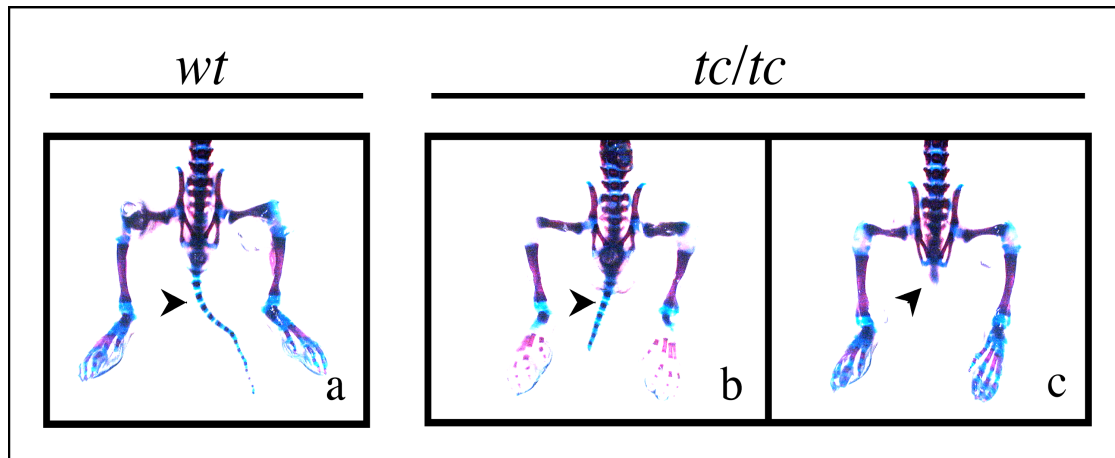


**Figure 1.** Skeletal defects in truncate mutant mice. Skeletal preparations of homozygous truncate newborn mice, showing axial skeleton defects in the caudal region with variable expressivity. Some mice had a normal tail as in the wild type (a), others exhibiting varying degrees of tail reduction like a short tail (b), or no tail (c).

This analysis revealed, that truncate mutant mice showed axial skeleton defects with variable expressivity that were confined to the caudal and sacral region (Fig. 1; and data not shown) Some mice exhibited a normal tail like in wild type case (a), others exhibited varying degrees of tail

reduction like a short tail (b), or no tail at all (c). Another typical defect seen in truncate mutants were thin or constricted tails (data not shown). This variable expressivity concerning the skeletal defects observed in homozygous truncate mice is characteristic of the truncate phenotype.

### 3.1.2 Notochord defects in truncate mutant embryos

In homozygous *tc/tc* embryos, the notochord formation was normal until around E9.5, but shortly after between E9.5-10 it failed to grow caudally and with abrupt ends (Theiler 1959; Dietrich et al. 1993). Notochord defects in homozygous truncate embryos were visualized by performing a whole-mount in situ hybridization to analyse the expression of some notochord markers like *Foxa2*, *Shh* and *T* (Fig. 2) in the wild type (a, b, c) and in the mutants (d, e, f, g) at embryonic stage E11.5. *Foxa2*, *Shh* and *T* are genes expressed in the notochord but also in other tissues (such as presomitic mesoderm, neural tube, gut...), which are not relevant in this analysis. The purpose of this analysis was also to investigate whether the expression pattern of these notochord markers was changed in the truncate mutants.

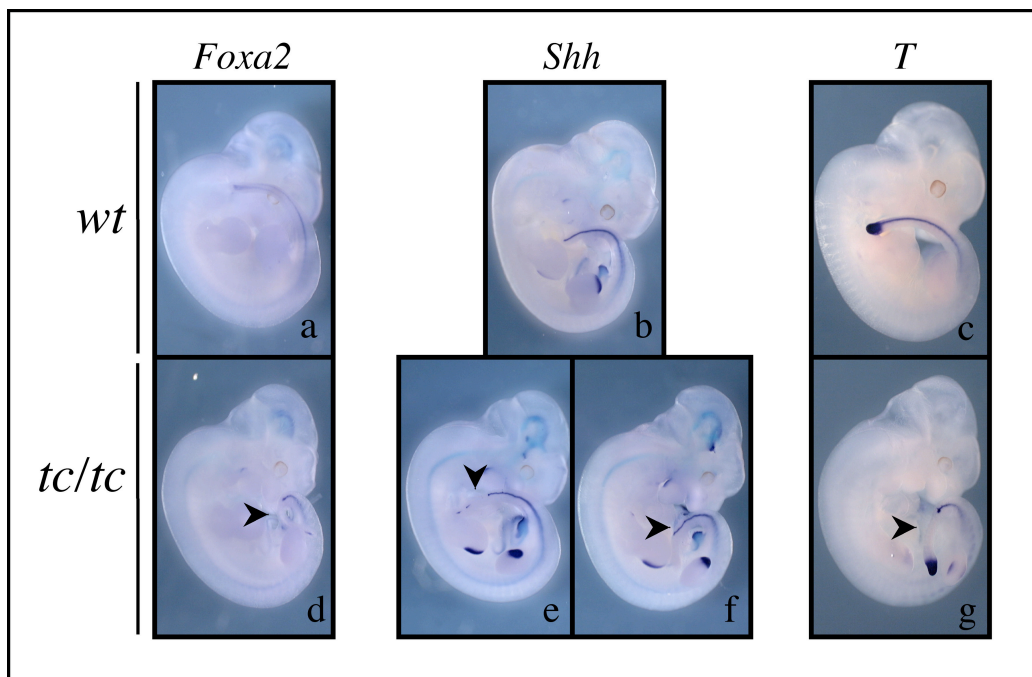


**Figure 2.** Notochord defects in truncate mutant embryos. Expression analysis of notochord markers *Foxa2*, *Shh* and *T* in wild type (a, b, c) and in homozygous truncate mutant (d, e, f, g) embryos at stage E11.5. Wild type embryos showed an intact continuous notochord while in truncate embryos discontinuous (f, g) or disrupted (d, e) caudal notochord was observed indicated by arrowheads.

Wild type embryos showed an intact continuous notochord (a, b, c) along the entire axis while in truncate embryos a discontinuous (f, g) or disrupted (d, e) caudal notochord was observed, indicated by arrowheads. These abnormalities, observed in the posterior portion of the developing notochord of the truncate mutant embryos, will lead later to malformations in the axial skeleton of the truncate mutant mice. The expression profile of notochord markers, used in this analysis such as *Foxa2*, *Shh* and *T* in the truncate mutant embryos, was not affected compared to the pattern of these markers in the wild type embryos.

### 3.2 Identification of *Not* as a candidate gene for truncate mutation

The predicted gene in the *tc* interval which represented a potential candidate for truncate mutation referred as *Not* gene was further analyzed.

#### 3.2.1 Expression pattern of the candidate gene *Not*

To determine whether *Not* gene was a good candidate for the truncate mutation, its expression was analyzed in wild type embryos by performing a whole-mount in situ hybridization using as a probe an EST clone, named AU00642.



**Figure 3.** Expression pattern of the candidate gene *Not* for the truncate mutation. Expression analysis was performed by whole-mount in situ hybridization of wild type embryo at embryonic stage E10 using as a probe an EST clone AU022460. This gene was specifically expressed in the posterior portion of the notochord

Effectively, the candidate gene *Not* showed a specific expression in the posterior notochord at embryonic stage E10 (Fig. 3). The expression pattern of this gene resembles the expression of *Gnot* (now *Gnot1*) in the chick embryo (Stein.S and Kessel.M, 1995). Truncate is a mouse mutation, which affects only a posterior portion of the notochord and the expression profile of



this mouse *Not* gene provided experimental evidence supporting that this gene is a potential candidate for the gene affected by the truncate mutation.

### 3.2.2 Cloning of *Not* cDNAs

*Not* cDNAs were cloned by reverse transcriptase-polymerase chain reaction (RT-PCR) using RNA of wild type or truncate embryos at stage E9.5 or E10.5 as a template (Fig. 4; and data not shown). The RT-PCR products were cloned and analyzed after sequencing.

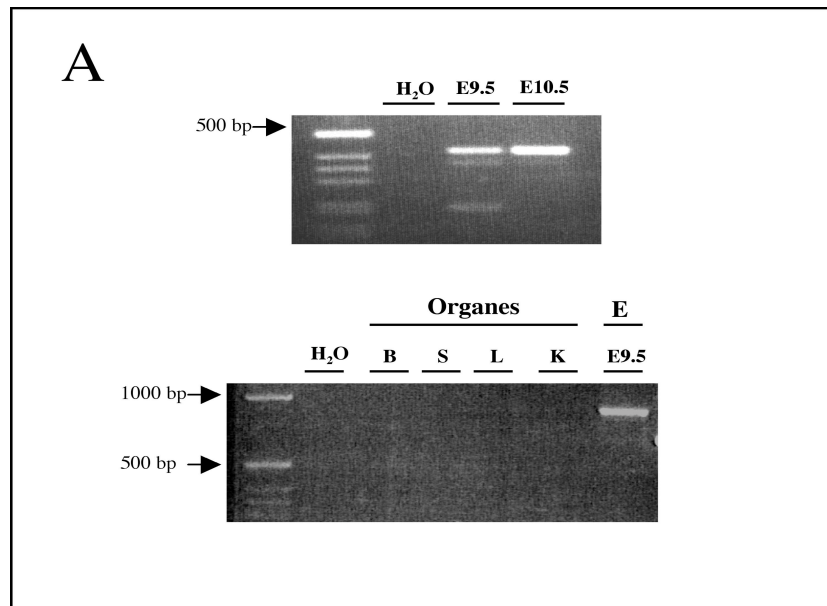


**Figure 4.** Cloning of *Not* cDNAs by Reverse-Transcription PCR. (A) RT-PCR was performed using RNA of wild type embryo E9.5 or E10.5 as a template. *Not* was expressed at both embryonic stages E9.5 and E10. No *Not* expression was observed when RNA from adult organs like brain “B”, spleen “S”, liver “L” or kidney “K” of wild type mice was used for RT-PCR.

Two different transcripts were obtained by RT-PCR, using a primer pair within exon1 and exon3 one transcript containing the predicted exon2 and one deprived from the 2<sup>nd</sup> exon (Fig. 4B c, d); while using primer pairs spanning the entire coding region, only one transcript containing the three predicted exons was obtained (Fig. 4B c), and this transcript represents the longest cDNA. The EST clones available in the RZPD also did not contain the second exon. These EST clones were identical to one of the transcripts obtained by RT-PCR, which was considered as a product of a splicing process. The interpretation of this result is still unclear.

No *Not* transcript was amplified when RNA from brain, spleen, liver, or kidney of wild type mice was used for RT-PCR (Fig. 4A).

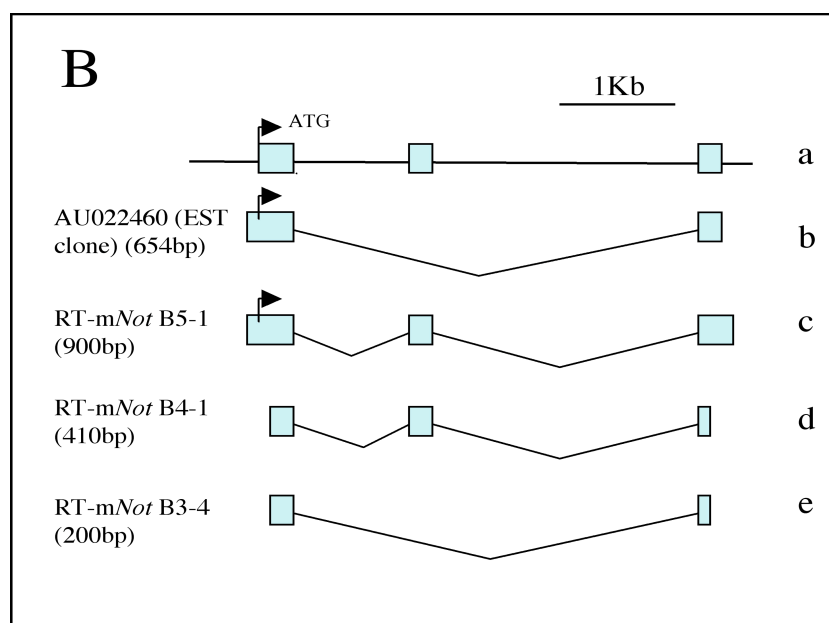


**Figure 4.** Cloning of *Not* cDNAs by Reverse-Transcription PCR. (B) Schematic representation of (a) genomic sequence with the predicted exon/intron structure of the candidate gene *Not*, (b) EST clone AU022460 obtained from RZPD, (c, d, e) two different transcripts obtained by RT-PCR the first one (c) long cDNA (d) short cDNA containing the three predicted exons and the second one (e) short cDNA deprived from the 2<sup>nd</sup> exon.

### 3.2.3 *Not* genomic organization, cDNA, encoded protein and similarity to other vertebrate *Not* genes

The localization of mouse *Not* gene is indicated in the physical map of truncate region in Fig.5A. The longest *Not* transcript isolated by RT-PCR from mRNA of day 9.5 embryos previously shown (Fig. 4B c) contained a cDNA covering the three predicted exons of *Not* (Fig. 5B). Comparison of the cDNA with the genomic sequence confirmed the predicted exon/intron structure, which is highly similar to chicken *Cnot2* (Stein et al. 1996). The mouse *Not* cDNA encodes a protein consisting of 240 amino acids (Fig. 5C). Similarities with previously characterized *Not* proteins were restricted to the homeodomain and a short octapeptide located upstream of the homeodomain (Fig. 5C; and data not shown). Sequence comparisons between canonical *Not* proteins and the murine candidate *Not* protein confirmed the very high divergence

level of the candidate proteins over the homeodomain, since the level of identity between these sequences did not exceed 61% as observed between human *Not* and chick *Not1* (data not shown).

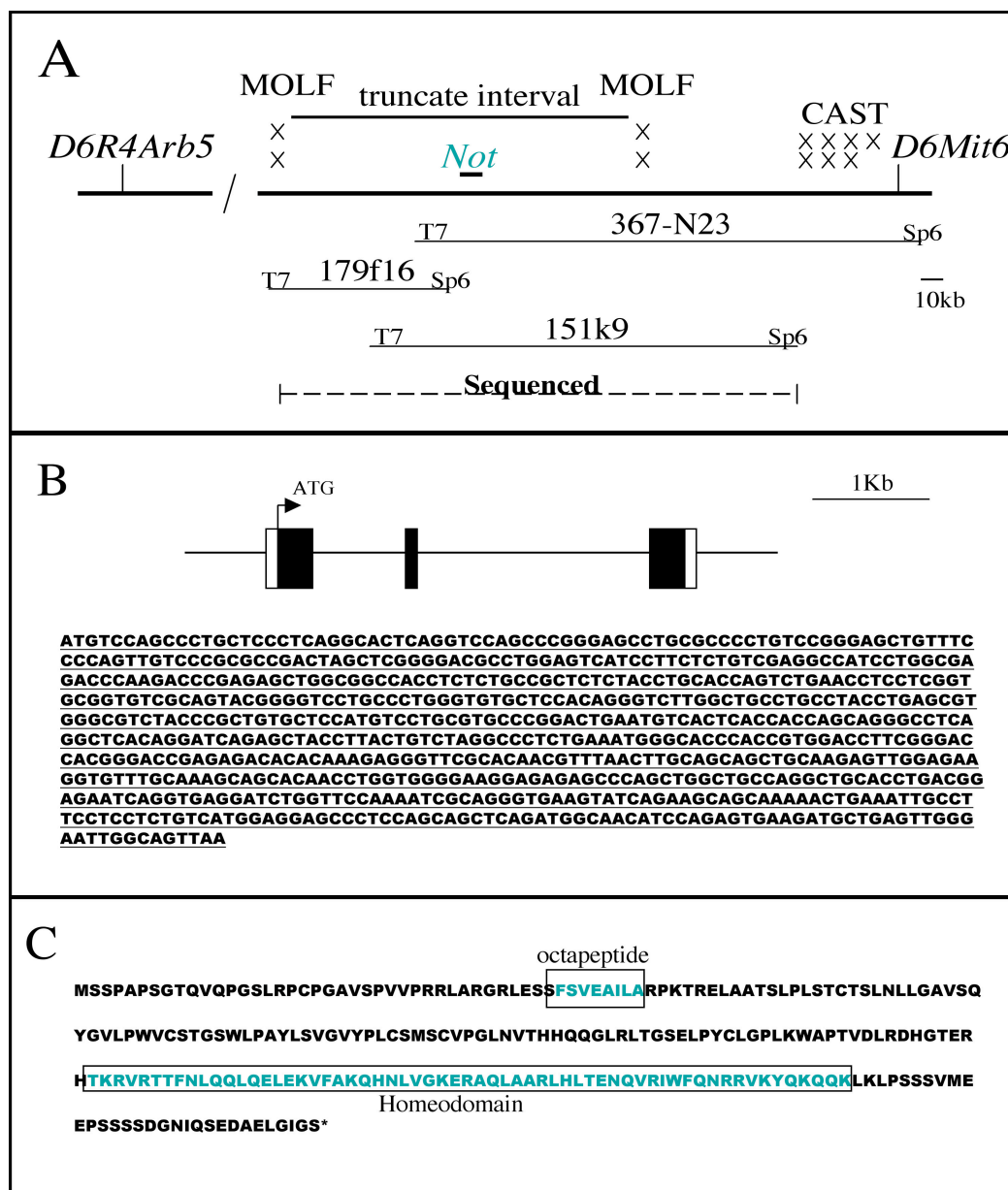


**Figure 5.** *Not* localization, structure and similarity to other vertebrate *Not* genes. (A) Localization of *Not* gene in the physical map of truncate region. (B) Genomic structure of the mouse *Not* gene. Exons are indicated by boxes and filled boxes (in black) depict the coding region whose sequence is shown below. (C) Amino acid sequence of mouse *Not* gene. The octapeptide and the homeodomain are indicated in boxes.

The homeodomain of mouse *Not* shared 56%–60% identity with the homeodomains of the

chicken, *Xenopus* and zebrafish genes (Fig. 5D), the most closely related vertebrate *Not* genes being *Cnot2* and ZF *flh* (Fig. 5E). These results highlight the very high rate of divergence of *Not* orthologs and mammals during evolution.

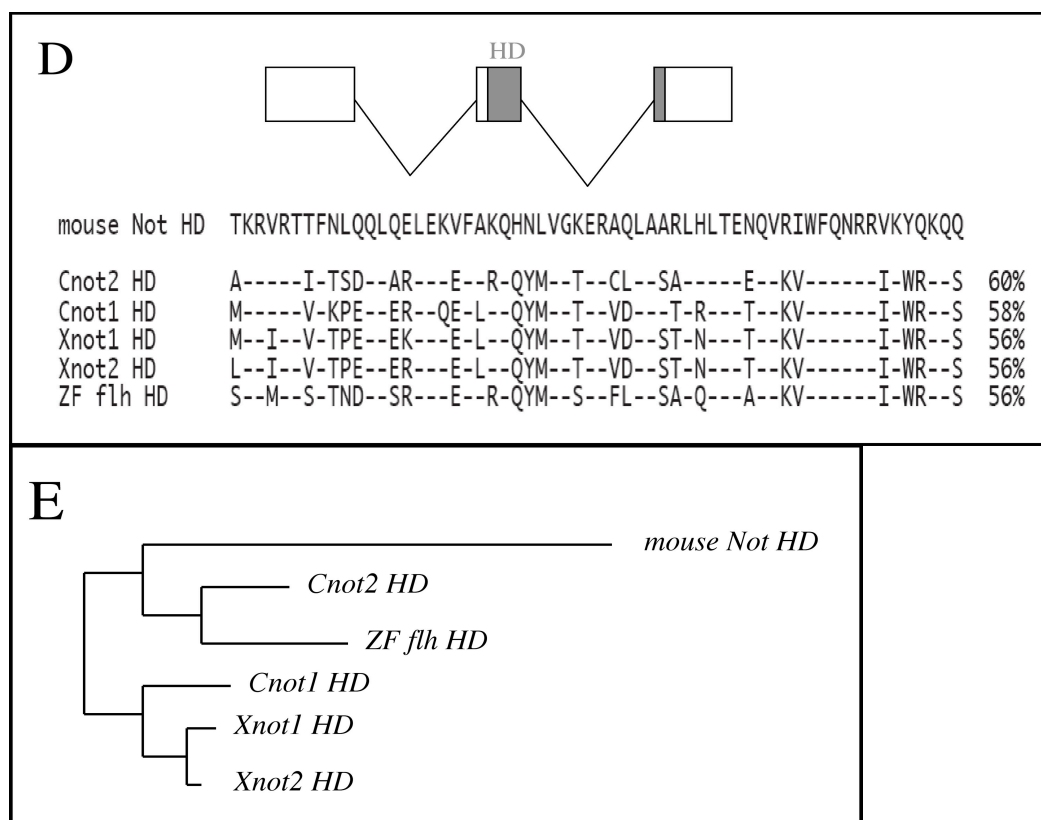


**Figure 5.** *Not* localization, structure and similarity to other vertebrate *Not* genes. (D) Alignment of mouse *Not* homeodomain with homeodomains of other *Not* family members. The percentage of identical amino acids is shown on the right. (E) Midpoint rooted phylogenetic tree of vertebrate *Not* genes based on ClustalW aligned homeodomains.

### 3.3 Expression of *Not*

#### 3.3.1 *Not* expression in the wild type during embryogenesis

The spatial pattern of *Not* expression during embryonic development was analyzed by whole-mount in situ hybridization of wild type embryos (Fig. 6), using an antisense riboprobe derived from the *Not* cDNA (covering the *Not* open reading frame) previously cloned by RT-PCR (shown in Fig. 4B c).

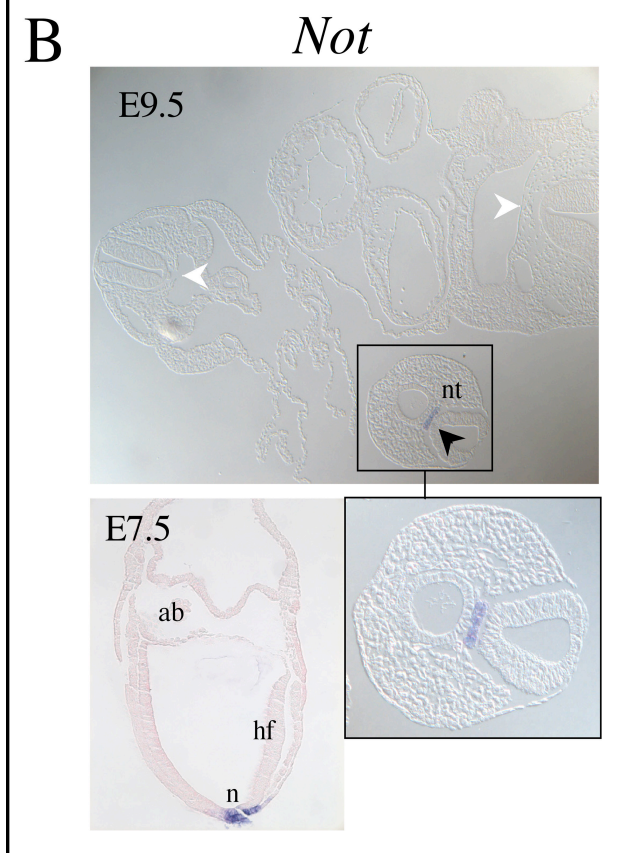
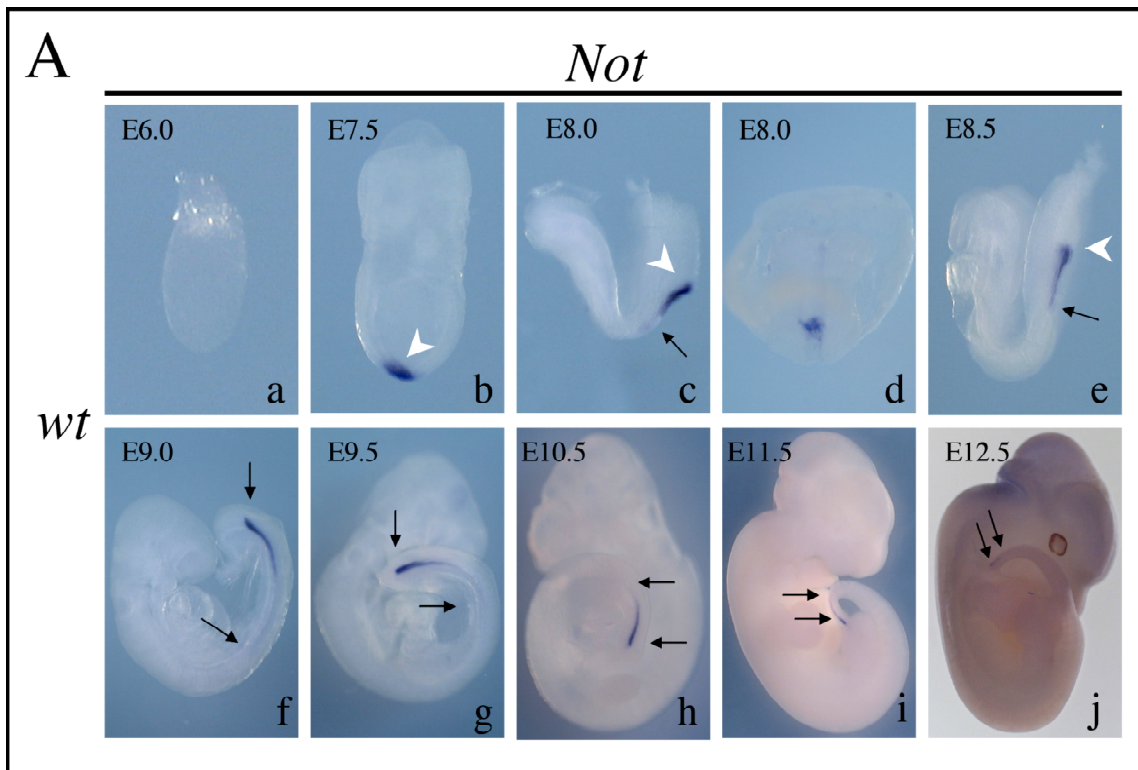


**Figure 6.** *Not* Expression in the wild type during embryonic development. (A) Expression analysis performed by whole-mount in situ hybridization using an antisense riboprobe derived from *Not* cDNA (covering *Not* ORF). (B) Sections of wild type embryos after WISH with the same *Not* cDNA probe.

No expression of *Not* was detected in E6.0 embryos (Fig.A a). *Not* transcripts were first detected in the node, and were subsequently restricted to the node (Fig.A. arrowheads in b, c, d, e) and caudal portions of the notochord (arrows in c, d, e, f, g, h, i, j). Sections (Fig.B) of hybridized embryo E7.5 showing the node “n” and embryo E9.5 showing restriction of *Not* transcripts to the caudal notochord “nt”.

No other expression domains were detected. White arrowheads in (Fig.B) point to the notochord in non-expressing regions, the black arrowheads indicate the caudal *Not*-expressing notochord and the boxed region shows an enlarged view of caudal notochord. ab, allantoic bud; hf, headfold.

No *Not* transcripts were detected in E6.0 embryos prior to the formation of the primitive streak and the onset of gastrulation (Fig. 6A a). At the extended primitive streak stage on E7.5, *Not* transcripts were detected in the node at the distal tip of the egg cylinder (Fig. 6A b) and were largely confined to the ventral node (Fig. 6B). Between E8.0 and E8.5, *Not* transcripts were abundant in the node and newly formed notochord, whereas more anterior, older notochord showed no expression (Fig. 6A c–e). During subsequent development until E12.5, *Not* expression was confined to the notochordal plate and caudal portion of the notochord (Fig. 6A f–j and Fig. 6B). No *Not* transcripts were detected in E13.5 embryos (data not shown).

Thus, *Not* expression was restricted to the node and notochord cells during gastrulation and axis elongation, closely resembling *Not* gene expression in the axial mesoderm of zebrafish, *Xenopus*, and chick embryos (von Dassow et al. 1993; Stein and Kessel 1995; Talbot et al. 1995; Melby et al. 1997).

### 3.3.2 *Not* expression in the truncate mutants during embryogenesis

The spatial pattern of *Not* expression during the development was analyzed by whole-mount in situ hybridization of truncate mutant embryos (Fig. 7), using an antisense riboprobe derived from *Not* cDNA (covering *Not* open reading frame) previously cloned by RT-PCR (shown in Fig. 4B c).

As in the wild type, no expression of *Not* was detected in E6.0 embryos prior to the formation of the primitive streak and the onset of gastrulation (Fig. 7 a). At the embryonic stage E7.5, *Not* transcripts were detected in the node (Fig. 7 b), and subsequently, expression of *Not* was observed in the node and caudal portions of the notochord (Fig. 7 c, d, e, f, g, h, i, j).

*Not* transcripts were detected in the node and posterior notochord of homozygous *tc* embryos at levels similar to wild type (Fig. 7). In contrast to wild type embryos, *Not* transcripts persisted temporarily at high levels in the head process and anterior notochord of mutant E7.75 -E8.5 embryos (Fig. 7 c, d, e, f). Similarly, at later stages, expression extended further anteriorly than in wild type embryos (Fig. 7 g, h, i, j), suggesting that downregulation in the notochord was delayed. In older stages, *Not* expression in the posterior notochord of truncate mutant embryos was discontinuous and reflected the loss or disruptions of the notochord (white arrowhead in Fig. 7 h, i).

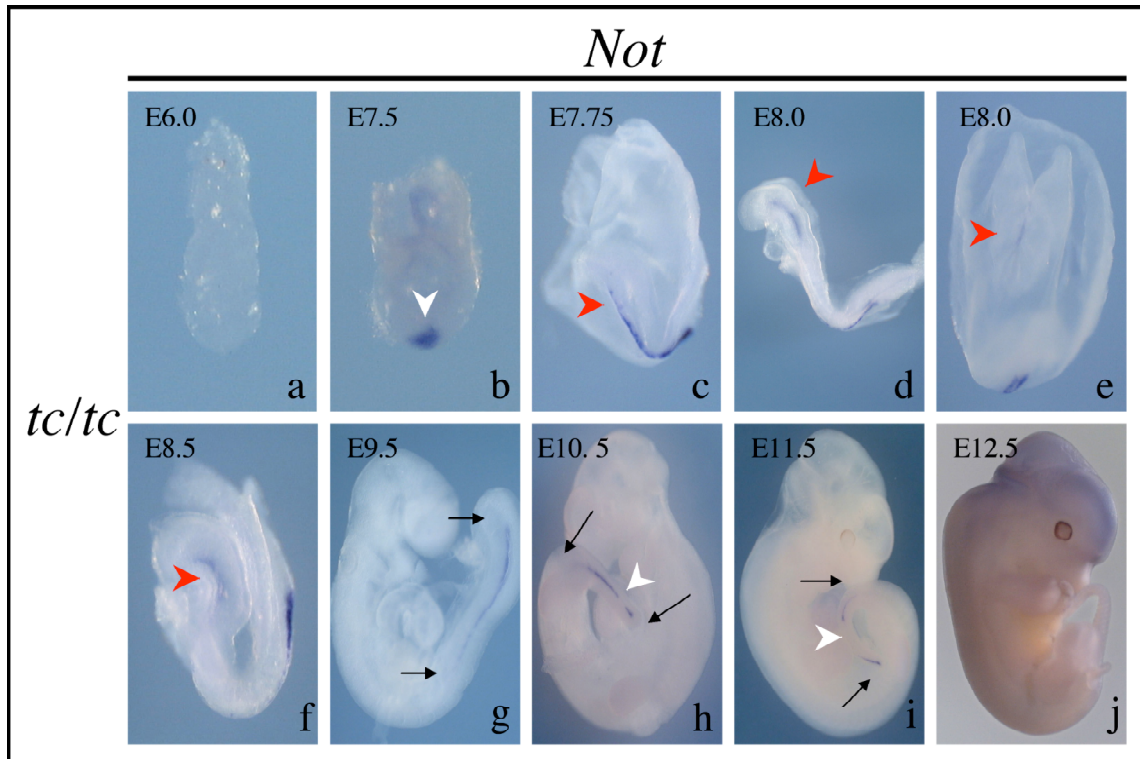


**Figure 7.** *Not* Expression in the truncate mutants during embryonic development. Expression analysis was performed by whole-mount in situ hybridization using an antisense riboprobe derived from *Not* cDNA (covering *Not* ORF). No expression of *Not* was detected in E6.0 embryos (a). *Not* transcripts were first detected in the node (b) at E7.5, and subsequently, expression of *Not* was observed in the node and caudal portions of the notochord (c, d, e, f, g, h, i, j). Ectopic transcripts were detected in the head process and anterior notochord (red arrowheads in c, d, e, f) and in the expression domain in the notochord (g, h, i, j) of mutant embryos. The white arrowheads in (h, i) point to gaps in the notochord reflecting the *tc* phenotype.

### 3.4 Transcription of *Not*

The analysis of a gene expression by in situ hybridization using a cDNA probe reflects the presence of the total mRNA (both before and after splicing process). While, the analysis of the transcription of a gene can be investigated by using an intron probe, which reflects the active transcription process.

Therefore, transcriptional activity of *Not* was analyzed further by performing whole-mount in situ hybridization with an intron *Not* probe of wild type embryos E9.0 and compared to the embryos hybridized with a cDNA *Not* probe (Fig. 8).

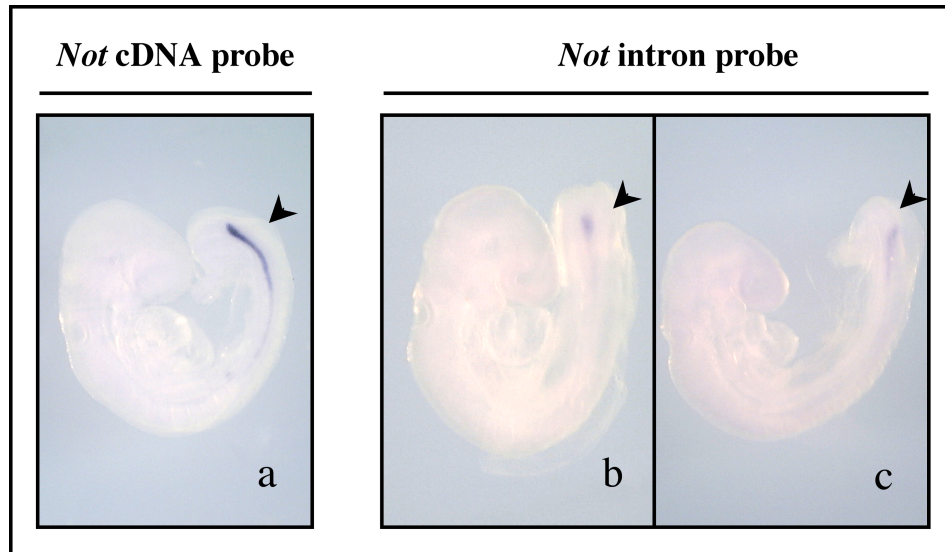


**Figure 8.** *Not* Transcriptional activity. Expression of *Not* was visualized by whole-mount in situ hybridization with an intron *Not* probe of wild type embryo E9.0 compared to a cDNA *Not* probe. Weaker and shorter expression domain was observed in embryos hybridized with intron probe (b, c), which indicated that *Not* RNA was relatively stable.

Notably, weaker and shorter expression domain in the caudal notochord was observed in embryos hybridized with the intron probe (Fig. 8 b, c), compared to those ones hybridized with the cDNA probe (Fig. 8 a). This result showed that *Not* RNA was relatively stable after the transcriptional process, and that *Not* transcription was highly restricted to the newly formed notochord in the caudal region of the embryo.

### 3.5 Truncate allele is a point mutation in the homeobox of *Not*

#### 3.5.1 Identification of a point mutation in the *tc* allele

Since, the expression levels of *Not* detected in *tc* mutant embryos were similar of the ones seen in wild type embryos, the possibility that the *tc* phenotype could be due to a reduction of *Not* transcripts was discarded. To test whether potential mutations in the coding region of *Not* in *tc* mutants account for the *tc* phenotype, the three exons were amplified by PCR from genomic DNA of six homozygous *tc* mice, and from DNA of C57BL/6, 129Sv/ImJ, FVB/N and CD1 wild type mice strains, respectively, subcloned into pGemTEasy and sequenced. The comparison of these different genomic DNAs showed that exon/intron junctions and the first exon and the third



exon of wild type and mutant DNAs were identical. The only difference detected between the sequences of six independent clones from different individual mutant DNAs and the sequences of wild type clones of the different strains was a single base change (T ↔ G) in the 2<sup>nd</sup> exon (Fig. 9A, 9B).

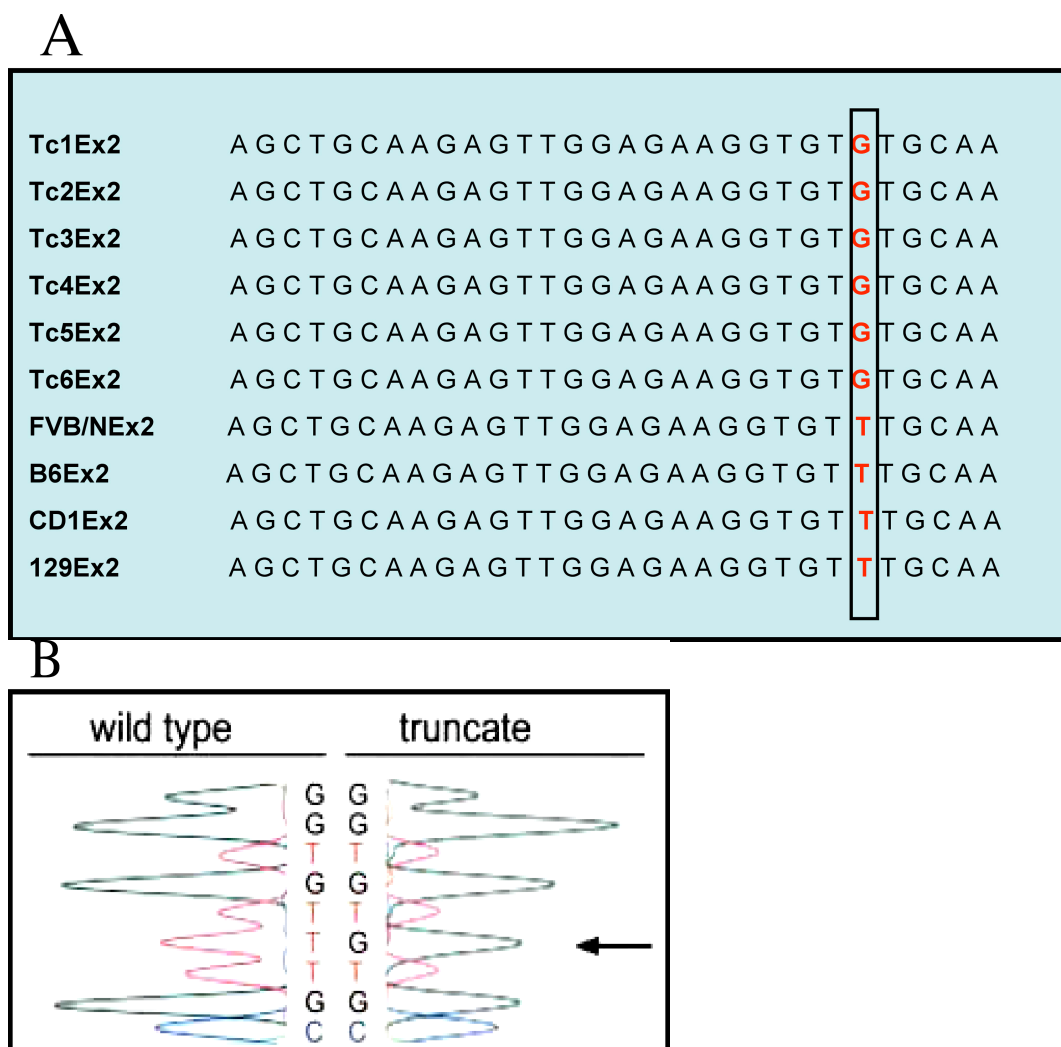


**Figure 9.** Identification of a point mutation in the *tc* allele.

(A) Partial nucleotide sequence of six different individual homozygous *tc* mice and of C57BL/6, 129Sv/ImJ, FVB/N and CD1 wild type strain mice, where the point mutation is indicated by a black box. (B) Example from chromatogramme of partial sequence of wild type and truncate *Not* allele around the T↔G mutation.

Consequently, this point mutation in the nucleotide sequence leads to a substitution of

Phenylalanine by Cysteine in position 20 of helix1 of the homeodomain protein designed as (F20C) shown in Fig. 9C.

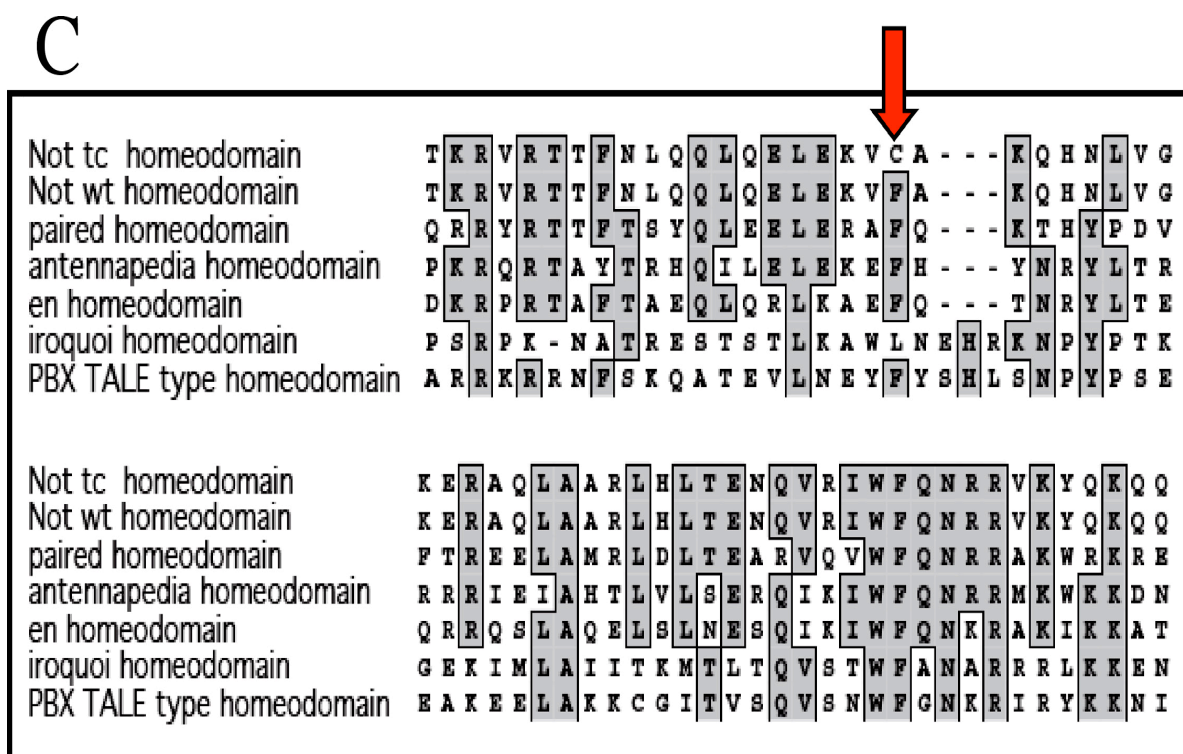


**Figure 9.** Identification of a point mutation in the *tc* allele. (C) Alignment of Not homeodomain with other related homeodomain sequences. The red arrow points to the substitution of phenylalanine by a cysteine in *tc* as a consequence of this point mutation.

### 3.5.2 Stability of Not homeodomain

Phenylalanine in position 20 represents a conserved amino acid among related *Not* genes (Fig. 9C). In homeodomains of other homeobox genes, a Phenylalanine residue or another hydrophobic amino acid is normally found in this position (<http://www.sanger.ac.uk/cgi-bin/Pfam/getalignment.pl?name=homeobox&acc=PF00046&format=link>; and see examples in Fig. 9C). This suggests that the substitution of Phenylalanine by Cysteine could affect the biochemical or physicochemical properties of the homeodomain. To analyze the effect of the F20C mutation on the Not homeodomain protein properties, the wild type and mutant Not homeodomains were subcloned in expression vectors (Fig. 10A), then expressed as GST fusion proteins, the circular dichroism was measured and the thermal denaturation curve of the purified wild type and truncate Not homeodomains was determined.

This experiment has been done in collaboration with Dr. Rolando Rivera-Pomar (Max-Planck-Institute for Biophysical Chemistry, Göttingen). First, the wild type and truncate *Not* homeoboxes were amplified from *Not* wt and *Not* tc cDNAs using the primers not-homeo-F1 and not-homeo-B1 in which BamHI and EcoRI sites were introduced, were subcloned, and posteriorly were sent to Dr. Rolando Rivera-Pomar for further analysis.

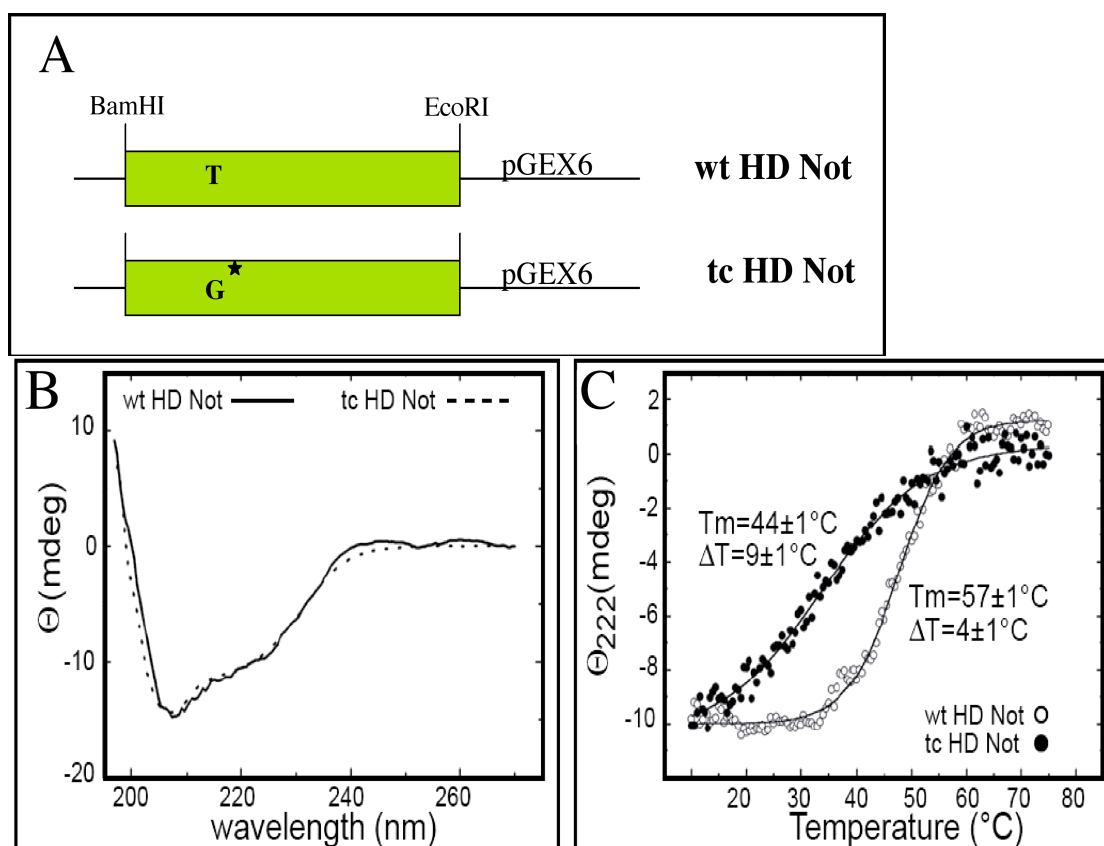


**Figure 10.** F20C mutation caused a significant destabilization of *Not* homeodomain in vitro. (A) *Not* homeoboxes cloned into pGEX6 expression vector. (B) UV-CD spectra obtained from HD NOT-WT (solid line) and HD-NOT-F20C (broken line). (C) Thermal denaturation curves obtained from HD-NOT-WT (open circles) and HD-NOT-F20C (filled circles) monitored by the ellipticity of the absorption signal at 222 nm indicate a significant reduction of the melting temperature of HD-Not F20C ( $\approx 44^{\circ}\text{C}$  compared with  $57^{\circ}\text{C}$  of the wild type homeodomain).

The pattern of circular dichroism of the wild type and mutant protein in the far UV was equivalent at  $25^{\circ}\text{C}$  (Fig. 10B), and similar to that observed in other homeodomains (Ades and Sauer 1994; Subramaniam et al. 2001), indicating that the helical structure of the *Not* homeodomain was not altered by the F20C change. However, measuring the helical content of

the homeodomains as a function of the temperature showed that the F20C mutation caused a significant destabilization of the Not homeodomain in vitro (Fig. 10C) that could affect *Not* function in vivo.

### 3.5.3 Generation of *Not*<sup>tc/tc</sup> ES cells and reversion of the *tc* mutation

Since, the point mutation (T ↔ G) caused a significant destabilization of *Not* homeodomain in the in-vitro assay, a rescue experiment was designed with the purpose of restoring this point mutation in one *Not* allele in the tetraploid embryos.

To address whether the F20C mutation leads to the *tc* phenotype, *Not*<sup>tc/tc</sup> embryonic stem (ES) cells were generated by Dr. Karin Schuster-Gossler, and the F20C mutation in one *Not* allele of these cells was corrected by homologous recombination using a replacement vector that contained the wild type exon2 sequence in its 5' region of homology (Fig. 11A). 11kb of genomic DNA of the *Not* locus including the three exons were used to make the targeting construct. A Diphtheria ToxinA expression cassette (pKO SelectDT; Lexicon Genetics) was cloned upstream of the 5' homology arm. A PGKpuro selection cassette flanked by *loxP* sites was cloned in intron2 into *SspI* site, approximately 180bp downstream of exon2 (Fig. 11A).

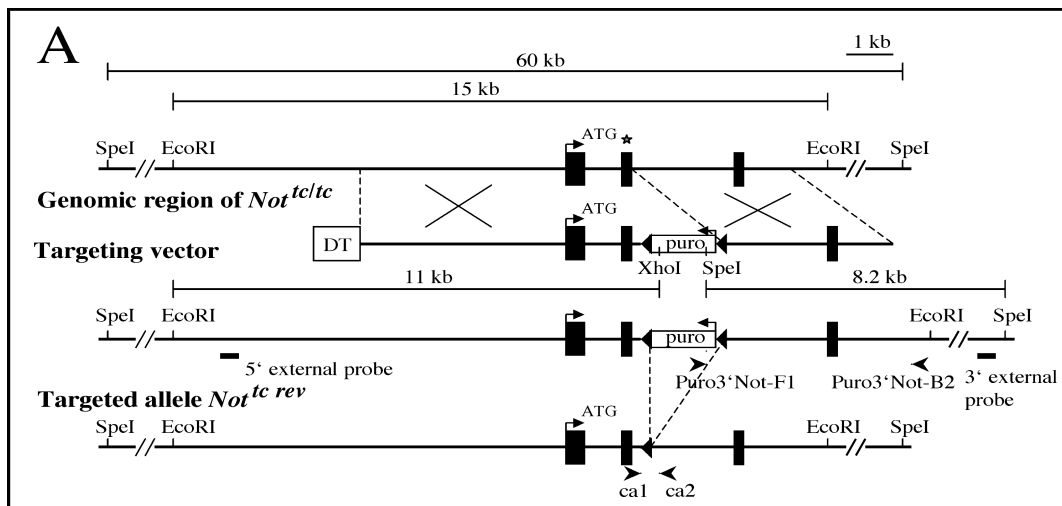


**Figure 11.** Reversion of the *tc* mutation. (A) Targeting strategy for reverting F20C, with schematic representation of the genomic *Not* locus targeting vector and reverted targeted allele. Exons are indicated by black boxes, relevant restriction sites and restriction fragments, as well as the probes used for genotyping, are shown above and below. The asterisk in exon 2 of the genomic locus indicates the point mutation.

Positive targeted clones containing puro cassette, were identified by PCR with the primers Puro3'Not-F1 and Puro3'Not-B2 and by Southern blot analysis using 5' and 3' probes (Fig. 11A, 11B a). The selection cassette "puro" was removed by transient expression of Cre in correctly targeted cells containing puro. Positive targeted clones deprived from puro cassette, were identified by PCR with the primers ca1 and ca2 and by Southern blot analysis using 5' probe (Fig. 11A, 11B b). Additionally, the reversion to wild type (*tc<sup>rev</sup>*) was verified by cloning and sequencing exon 2 from the targeted allele (data not shown).

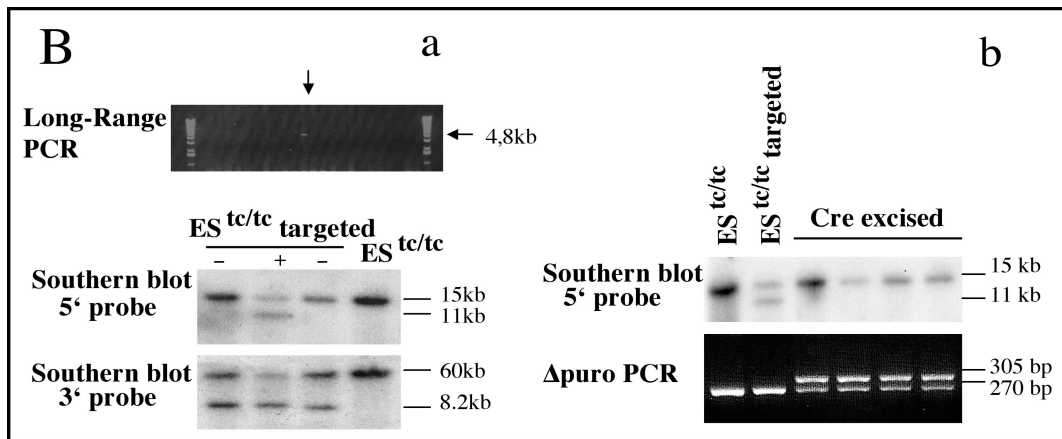


**Figure 11.** Reversion of the *tc* mutation. (B) Screen for targeted clones before (Ba) and after Cre-mediated excision of puro (Bb) by Southern blot and by PCR. Negative and positive targeted clones are indicated in Ba with – and +, respectively.

*Not<sup>tc/tc</sup>* and finally *Not<sup>tc/tc<sup>rev</sup></sup>* ES cells were used to generate completely ES-derived embryos by injection of tetraploid morulae (Nagy et al. 1990). This technique allows the generation of an embryo from ES cells. The injection of tetraploids was performed by Dr. Karin Schuster-Gossler. To visualize the eventual defects in the notochord, a *Brachyury (T)* probe was used as a specific marker for the notochord in this analysis (Fig. 11C; Table1).

**Table 1.** Summary of the number of embryos and tetraploids from different genotypes used in the Rescue experiment

Genotype	Number of embryos “E” or tetraploides “tetra” hybridized with Brachyury ( <i>T</i> ) probe
<i>wt</i>	5 E
<i>Not<sup>tc/tc</sup></i>	10 E
ES <i>Not<sup>tc/tc</sup></i>	11 tetra (2 tetra shows truncate phenotype)
ES <i>Not<sup>tc/tcrev</sup></i>	20 tetra (with puro) and 15 tetra (without puro)

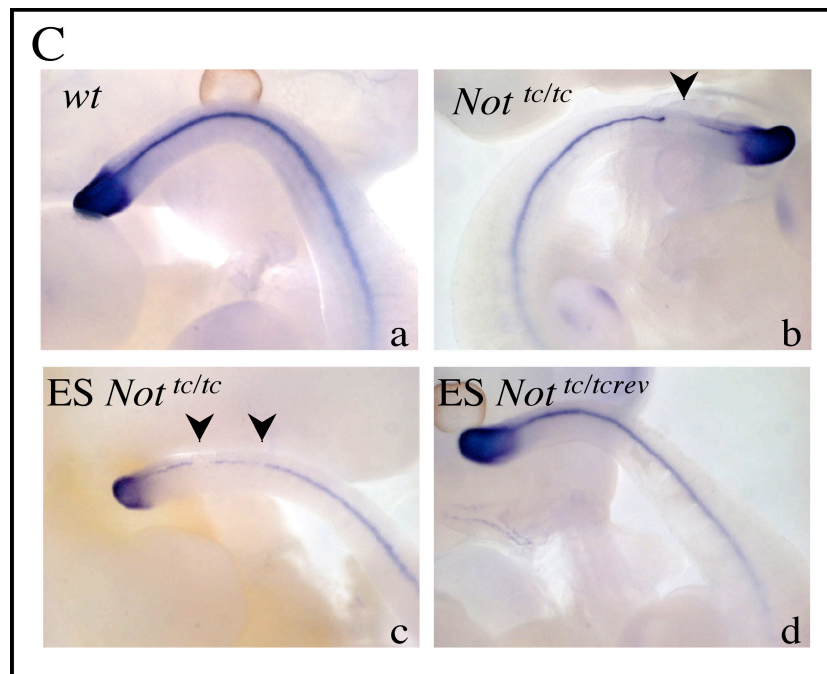


**Figure 11.** Reversion of the *tc* mutation. (C) Glycerol cleared wild type *wt* (panel a) and *Not<sup>tc/tc</sup>* mutant (panel b) embryos collected from natural matings, and completely ES cell-derived embryos obtained with *Not<sup>tc/tc</sup>* (panel c) and *Not<sup>tc/tcrev</sup>* (panel d) cells, respectively, after in situ hybridization with a brachyury probe. Arrowheads in (panels b,c) point to gaps in the notochord.

The result revealed that two out of eleven completely *Not*<sup>*tc/tc*</sup> ES cell-derived E11–E11.5 embryos showed disruptions in the caudal notochord, reflecting the typical phenotype of *tc* mutant embryos (Fig. 11C, panel c). This low frequency is very likely attributed to the incomplete penetrance and highly variable expressivity of the *tc* phenotype. In contrast, all embryos ( $n=35$ ) obtained with *Not*<sup>*tc/tcrev*</sup> ES cells either with ( $n=20$ ) or without ( $n=15$ ) the puro cassette showed a normal intact notochord (Fig. 11C, panel d; and data not shown) which was identical to the wild type pattern (Fig. 11C, panel a). This finding indicated that the restoration of one allele in *Not*<sup>*tc/tc*</sup> ES cells was able to rescue the truncate phenotype.

These data provided direct evidence that the F20C mutation is effectively responsible for the notochordal defects seen in *tc* mutant embryos.

## 3.6 Regulation of *Not*

### 3.6.1 *Not* act downstream of both *Foxa2* and *T*

In previous studies, it has been reported that both transcription factors *Foxa2* and *T* play a prominent role in notochord formation during development. To determine which position fulfills *Not* gene in the genetic cascade involved in notogenesis process, with respect to *Foxa2* and *T* genes, *Not* expression in *Foxa2* and *T* mutant embryos was analyzed by performing whole-mount in situ hybridization.

This experiment was done in collaboration with Dr. Janet Rossant (Samuel Lunenfeld Research Institute, Canada) and with Dr. Bernhard G. Herrmann (Max-Planck-Institute, Berlin) who provided *T* mutant embryos.

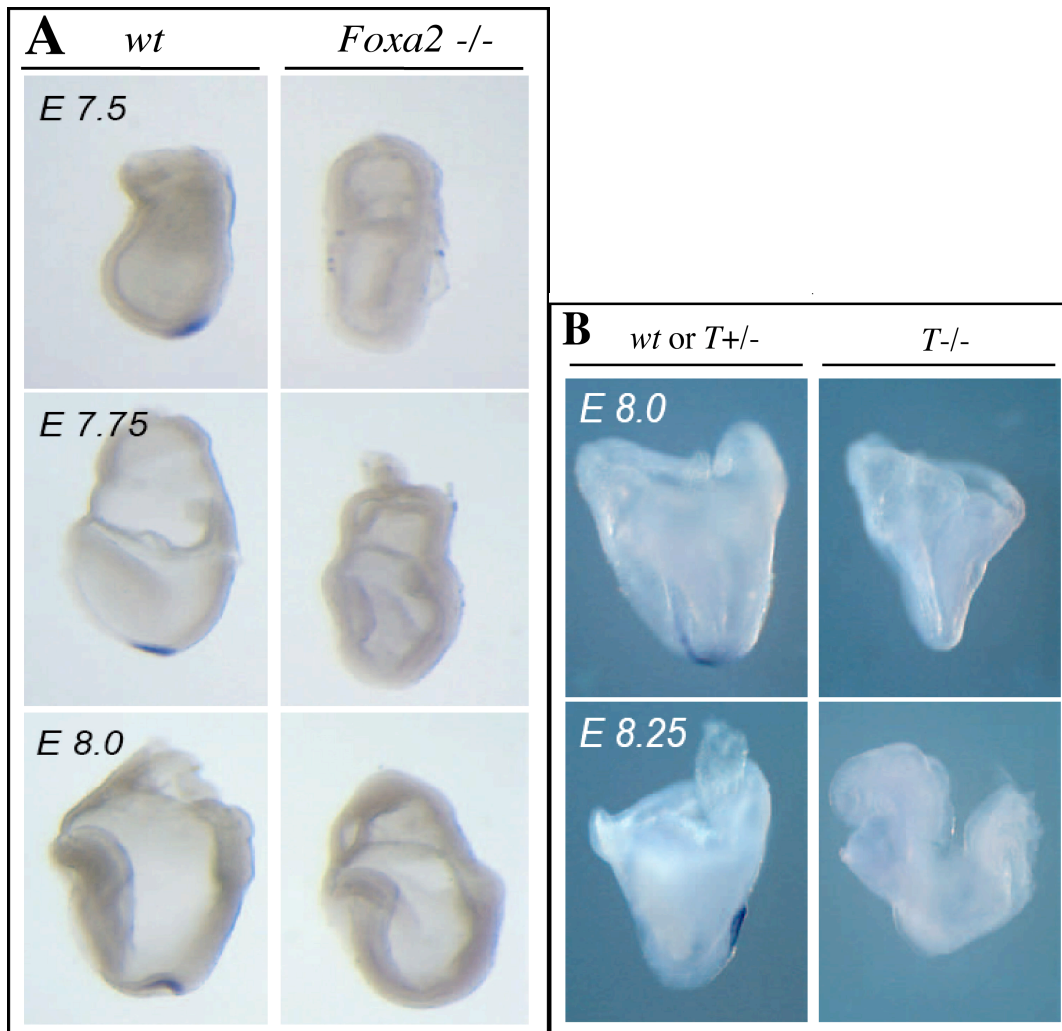


**Figure 12.** *Not* Expression in *Foxa2*<sup>-/-</sup> and *T*<sup>-/-</sup> mutant embryos. The expression of *Not* was visualized by whole-mount in situ hybridization. Absence of *Not* transcripts in both *Foxa2*<sup>-/-</sup> (A) and *T*<sup>-/-</sup> (B) mutants.

In the case of *Foxa2*, chimeras between homozygous *Foxa2* null ES cells and tetraploid embryos were used to generate the mutants. In these embryos, node and notochord are defective as in *Foxa2* null mutants, but streak morphogenesis is restored (Dufort et al. 1998). The results showed that *Not* transcripts were abolished in *Foxa2* tetraploid chimeras between embryonic stage E7.5 and E8 (Fig. 12A), suggesting that *Foxa2* is required for *Not* expression and thus, *Not* acts genetically downstream of *Foxa2*. Likewise, in 6 of 28 E8–E8.25 embryos obtained from matings between heterozygous *T* mutants (Dobrovolskaia-Zavadskaia 1927), *Not* transcripts were absent, except in one embryo, *Not* expression was severely reduced compared to the usual mRNA levels of *Not* observed in the wild type (Fig. 12B; and data not shown). These data suggest that *T* is also required for *Not* expression and thus, *Not* acts genetically also downstream of *T*.



### 3.6.2 *Not* is most likely a direct target of *Foxa2*

*Foxa2* is a transcription factor, which plays a pivotal role during notogenesis. Since no *Not* expression was detected in homozygous *Foxa2* mutants, these could suggest that *Not* is a direct transcriptional target of *Foxa2*, but these also can simply reflect the lack of notochordal cells in these mutants. To investigate whether *Not* is a target of *Foxa2*, the transactivation effect of *Not* promoter by *Foxa2* was analyzed in vitro by a luciferase reporter construct. Approximately 12kb upstream genomic region of *Not* containing the first exon and intron was fused in frame with the second exon of *Not* to the luciferase reporter gene to generate *Not* promoter reporter luciferase construct (*Not* pr Luc) (Fig. 13A). Also, expression plasmids for *Foxa2* and *Not* were cloned (Fig. 13B). Then, the *Not* pr luc construct was cotransfected together with the expression plasmids into HEK293 cells and the luciferase activity was measured. All transfections experiments shown in (Fig. 13C) were independently repeated five times and the results were reproducible. The statistical significance of this experiment was assessed using the student *t*-test. Strong activation (about  $5,2 \pm 0,9$  folds;  $P < 0,05$ ) of the transcriptional activity of *Not* pr Luc was observed when *Foxa2* was transfected. These results are statistically significant. These data suggest that *Foxa2* is a direct regulator of *Not*. This observation was supported by sequence analysis showing that putative binding sites for *Foxa2* were located upstream of the first exon of the *Not* gene and in the first intron (indicated in Fig. 13A; and Table2).

In homozygous truncate mutants a transient ectopic expression of *Not* was observed suggesting that *Not* contributes to its own regulation. To investigate a potential autoregulatory effect of *Not* gene, a cotransfection of an expression plasmid for *Not* and *Not* reporter construct was performed. No activation of transcriptional activity of *Not* promoter was detected when *Not* was cotransfected.

Since *Foxa2* and *Not* share in part overlapping expression domains this could suggest that *Foxa2* and *Not* cooperates in the transcription of *Not*. This would validate the possibility that *Not* contributes directly to its own regulation in vivo. Therefore, a possible potential of *Not* to enhance the transactivation properties of *Foxa2* was investigated by performing transactivation assay. No change was detected on *Not* promoter transcriptional activity when *Not* was cotransfected with *Foxa2* (about  $5,2 \pm 1,5$  folds) compared to the one with cotransfection of *Foxa2* alone.



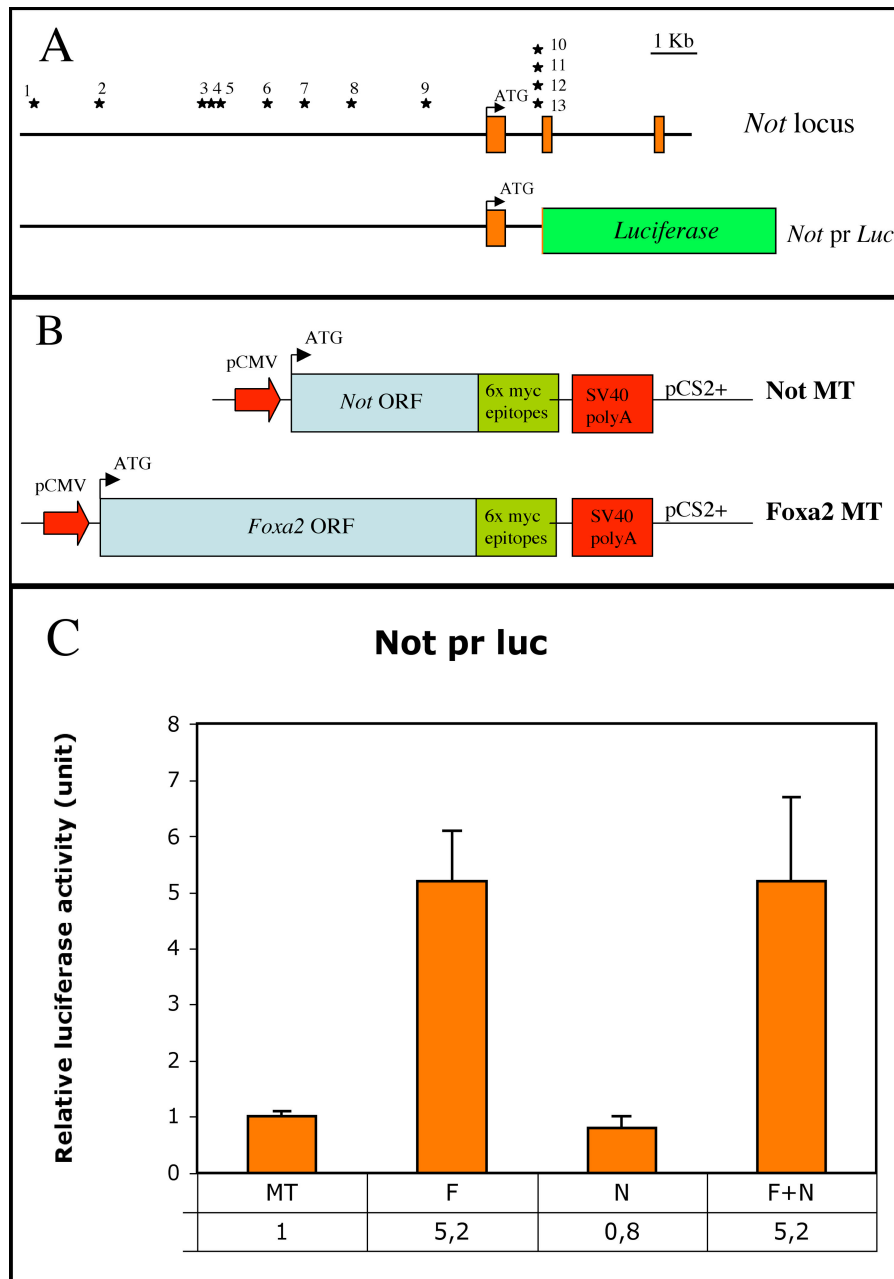


**Figure 13.** Transactivation effect of Foxa2 or/and Not in vitro on *Not* promoter. (A) Schematic representation of *Not* promoter luciferase reporter construct (*Not*pr Luc), about 12kb upstream genomic region of *Not* containing the first exon and intron were fused with luciferase reporter gene. The asterisk indicates potential binding sites for Foxa2. (B) Schematic representation of expression plasmids for Foxa2 and Not cloned in myc-tagged pCS2+ vector. (C) Transactivation effect on *Not* promoter by Foxa2 and Not in vitro. The *Not* pr luc construct was cotransfected together with the expression plasmids into HEK293 cells and the luciferase activity was measured. As a control empty plasmid myc tagged pCS2+ (MT) was used and also an appropriate amount of empty plasmid was used to keep total DNA constant. The results indicated strong activation of the transcriptional activity of *Not* pr Luc with transfection of Foxa2. No activation of transcriptional activity of *Not* promoter was detected when Not was transfected. No change was detected when Not is cotransfected together with Foxa2 on *Not* promoter transcriptional activity compared to the transfection with Foxa2 alone. Luciferase activities were normalized by B-galactosidase activities. The data are the result of pooling five independent experiments. Error bars indicate standard deviation.

### 3.6.3 Analysis of the significance of predicted binding sites of *Not* promoter

Sequence analysis indicated the presence of putative binding sites for Foxa2 located upstream to the first exon of *Not* gene and/or in the first intron (shown in asterix in Fig. 14A). To investigate the significance of these predicted binding sites of the *Not* promoter, several 5' deletions of the *Not* promoter fused to the luciferase reporter gene were generated (Fig. 14A). These deletion constructs and the Foxa2 expression plasmid (shown in Fig. 13B) were cotransfected into HEK293 cells and luciferase activity was measured. All transfection experiments shown in (Fig. 14B) were independently repeated at least three times and the results were reproducible. The statistical significance of this experiment was assessed using the student *t*-test.

The result indicated strong activation of the transcriptional activity of all different *Not* promoter Luciferase constructs (*Not*pr Luc, *Not* fgIII luc, *Not* fgII luc, and *Not* ATGfgII luc) by Foxa2. These results are statistically significant ( $P < 0,05$ ). These data support the proposed idea previously, suggesting that Foxa2 is a direct regulator of *Not*.

However, a higher activation by Foxa2 was observed with *Not* fgII luc construct (about  $16,7 \pm 2$  folds;  $P < 0,05$ ) suggesting that the binding sites located in the additional fragment of *Not* pr luc (about  $5,3 \pm 0,9$  folds) or *Not* fgIII luc (about  $9,4 \pm 1,4$  folds) could have an antagonistic effect on transcription while those located in *Not* fgII luc have an activator effect.

The induction of *Not* ATGfgII luc (about  $10,7 \pm 2,6$  folds;  $P < 0,05$ ) was reduced compared to that of *Not* fgII luc (about  $16,7 \pm 2$  folds), suggesting that some of the four binding sites in the first intron of *Not* gene might have some relevant functional significance in *Not* regulation.

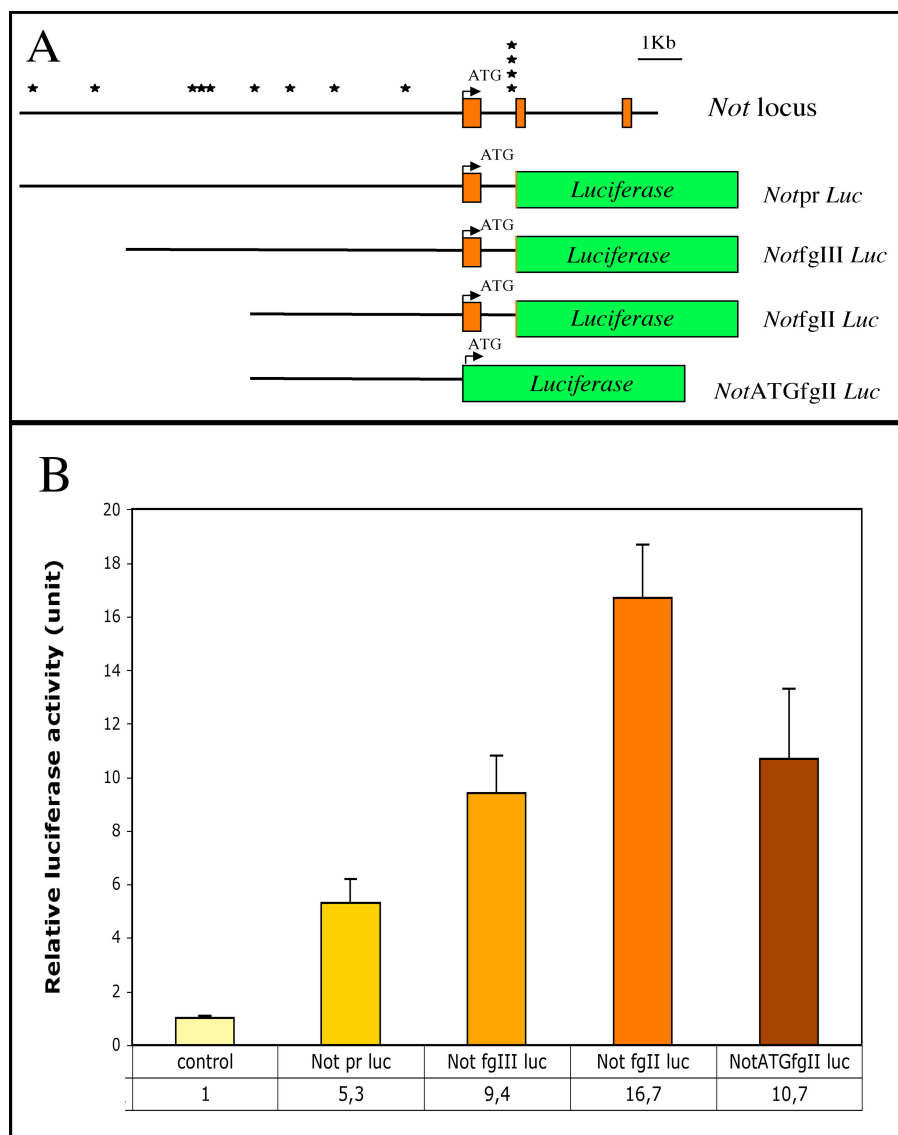


**Figure 14.** Transactivation effect of Foxa2 in vitro on different deletions *Not* promoter constructs. (A) Schematic representation of *Not* promoter luciferase reporter construct (*Notpr Luc*) and different deletions promoter luciferase constructs (*Not fgIII luc*, *Not fgII luc*, and *Not ATGfgII luc*). The asterisk indicates potential binding sites for Foxa2. (B) Transactivation effect on deletions *Not* promoter constructs by Foxa2, after cotransfection into HEK293 cells. The result showed strong activation of the transcriptional activity of all the different *Not* promoter Luciferase constructs by Foxa2. However, the highest activation was observed with *Not fgII luc* construct. The induction of *Not ATGfgII luc* was reduced compared to that of *Not fgII luc*. Luciferase activities were normalized by B-galactosidase activities. The data are the result of pooling at least three independent experiments. Error bars indicate standard deviation.

### 3.6.4 Analysis of the regulatory region required for *Not* expression in vivo in transgenic embryos

*Not* showed a highly restricted expression pattern during embryonic development, since the expression was confined to the node and notochord. To define the regulatory regions of *Not* promoter, which are essential for directing *Not* expression into the node and notochord, a promoter reporter construct in transient transgenic embryos was analyzed. To clone *Not* promoter reporter *LacZ* construct (*Not* pr *LacZ*), approximately 12kb upstream genomic region of *Not* containing the first exon and intron (the same region used for *Not*pr luc construct) was fused in frame with the second exon of *Not* to *E.coli lacZ* gene containing the SV40 and PGK polyadenylation signals (Fig. 15A).

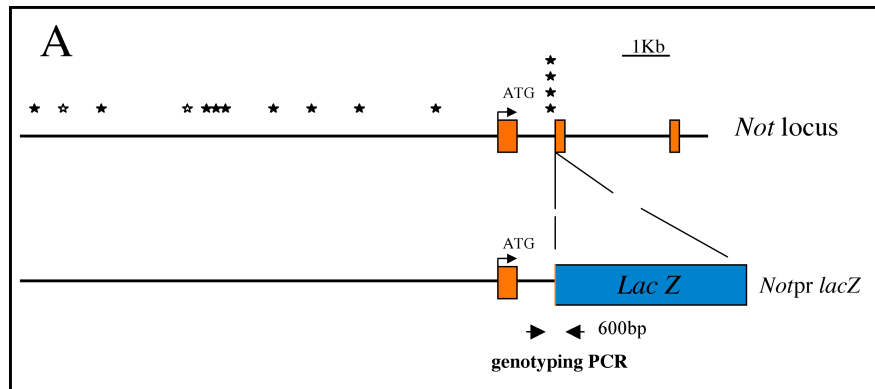


**Figure 15.** Promoter analysis of *Not* in transgenic embryos. (A) Schematic representation of *Not* promoter *lacZ* reporter construct (*Not*pr *LacZ*). About 12kb upstream genomic region of *Not* containing the first exon and intron were fused with *E.coli lacZ* gene with the SV40 and PGK polyadenylation signals. The asterix indicates potential binding sites for Foxa2.

The transgenic embryos were generated by pronuclear injection of *Not*pr *lacZ* construct performed by Dr.Karin Schuster-Gossler. The E9.5 embryos were examined for the presence of the transgene by PCR (Fig. 15B) and analyzed for *lacZ* expression by X-gal staining (Fig. 15C).

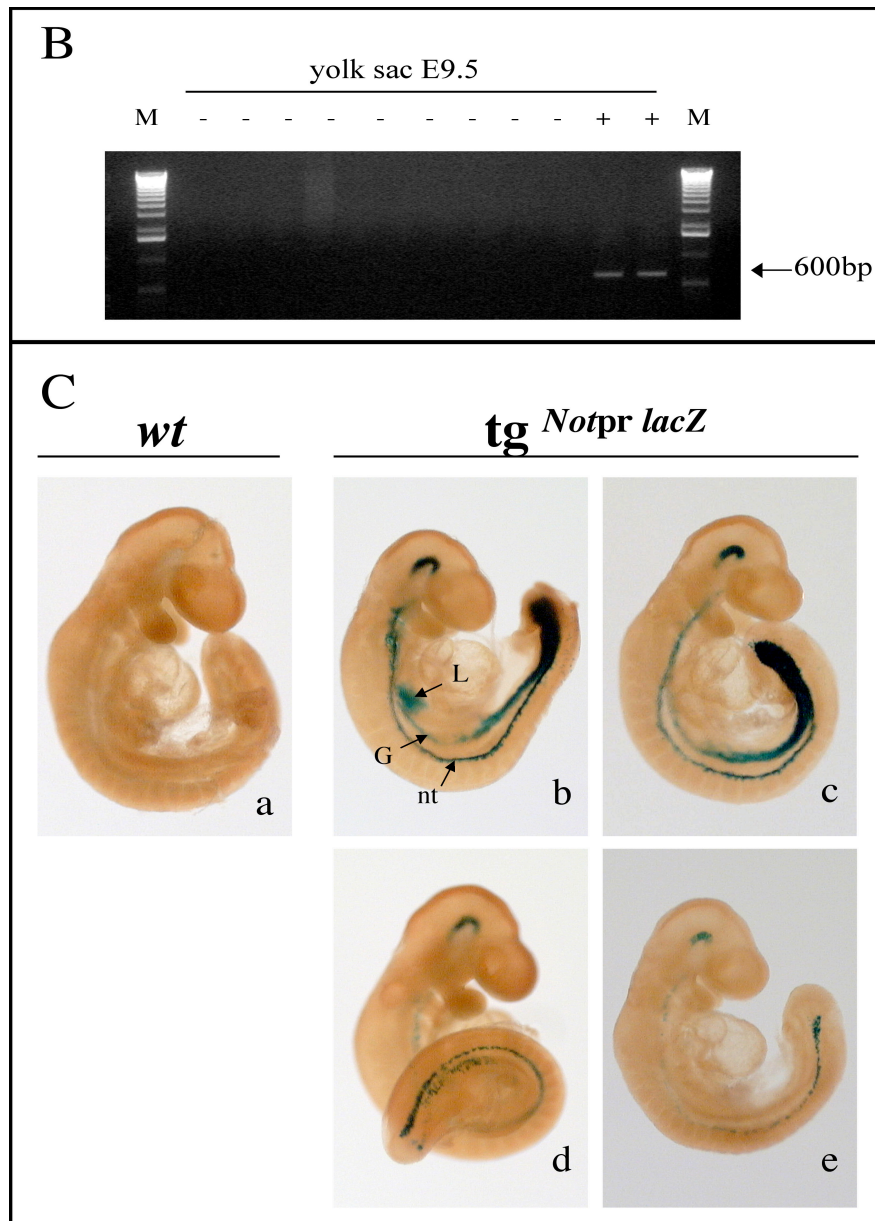


**Figure 15.** Promoter analysis of *Not* in transgenic embryos. (B) Genotyping PCR for the *lacZ* transgene. (C) Expression pattern of transgenic embryos E9.5 (*tg*<sup>*Notpr lacZ*</sup>) visualized by X-gal staining. *LacZ* expression was detected in notochord (b, c, d, e), gut (b, c, d, e) and developing liver (b).

The results showed that in transgenic embryos E9.5, *lacZ* expression was detected in notochord (Fig. 15C b, c, d, e), gut (Fig. 15C b, c, d, e) and developing liver (Fig. 15C b). Interestingly, the expression domains of the transgene reflected the endogenous expression pattern of *Foxa2*. The transgene (Fig. 15C) showed the same pattern but different expression levels, probably due to the

integration events of the reporter construct. This promoter analysis indicated that the genomic region (12kb) of *Not* locus used for *Notpr lacZ* construct is sufficient to drive *Not* expression in the notochord; however this region does not contain all the regulatory sequences that are necessary to recapitulate the endogenous expression pattern in transgenic embryos. This result also suggests that additional negative regulatory elements for the restriction of expression to notochord are located either upstream or downstream of the genomic region tested in the transgene (tg<sup>*Notpr lacZ*</sup>).

### 3.7 Left-right determination defects in truncate mutants

The notochord is required for the correct establishment of the left-right asymmetry during the development. Truncate is a mutation affecting the integrity of the caudal notochord. *Not* null mutants show defects in the left-right determination (A.Beckers and A.Gossler, unpublished data). Since truncate represents a strong hypomorph of *Not* (Ben Abdelkhalek et al, 2004) and the viability of *Not*<sup>*tc/tc*</sup> mice is reduced, the laterality specification in the truncate mutants was investigated.

#### 3.7.1 Randomization of embryonic turning in truncate mutants

One of the first morphological events leading to asymmetry between the left and right body halves in the developing embryo is the looping of the tubular heart to the right. In rodents, this process is accompanied by an anti-clockwise rotation of the lordotic embryo along its anteroposterior (AP) axis (Beddington and Robertson, 1999). In mice, this process occurs between E8.5-E9.5 and is referred to as embryonic turning. Therefore, the direction of turning in truncate mutant embryos at E9.5 of embryonic development was examined (Fig. 16).

100% of the wild type embryos E9.5 (n= 30) showed that the developing tail curves to the right side as a consequence of the anti-clockwise rotation (Fig. 16 b). In contrast, 50% of homozygous *Not*<sup>*tc/tc*</sup> mutant embryos (n= 30) showed positioning of the tail at E9.5 oriented to the left side indicating that axial rotation at E8.5 was clockwise in 50% (Fig. 16 a). These data showed that, in homozygous *Not*<sup>*tc/tc*</sup> mutant embryos, the direction of embryonic turning was randomized.



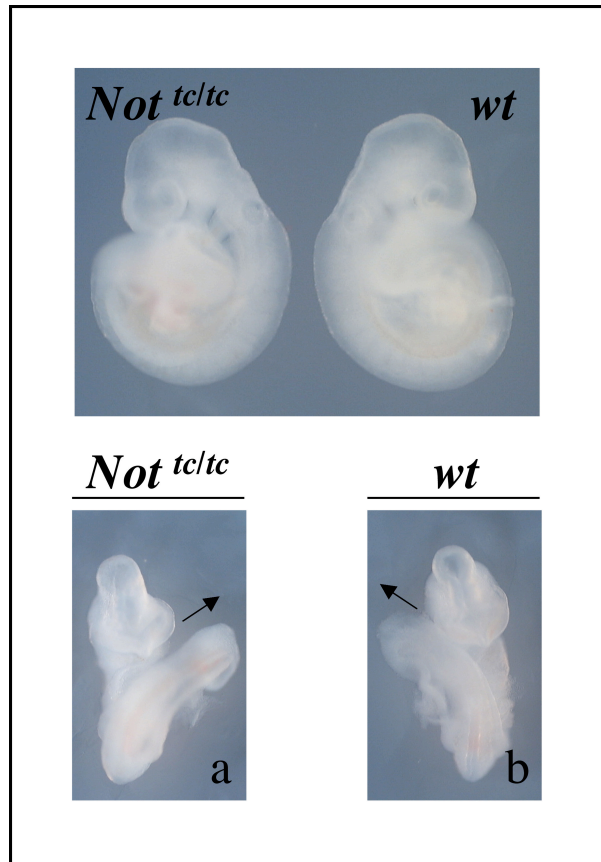


**Figure 16.** Embryonic turning in E9 truncate mutants. (b) As a result of an anti-clockwise rotation, the tail lies at the right body side of the wild type embryo (*wt*). (a) In half of the homozygous *Not<sup>tc/tc</sup>* mutants, the tail was left-sided, due to the randomization of the direction of axial rotation.

### 3.7.2 Left-right positional defects in visceral and thoracic organs in truncate mutants

A variable number of *Not<sup>tc/tc</sup>* newborns die shortly after birth. To determine the cause of postnatal mortality in *Not<sup>tc/tc</sup>* mice, the morphology of 18-18.5 dpc fetuses and neonates that were subjected to postmortems was examined (Fig. 17).

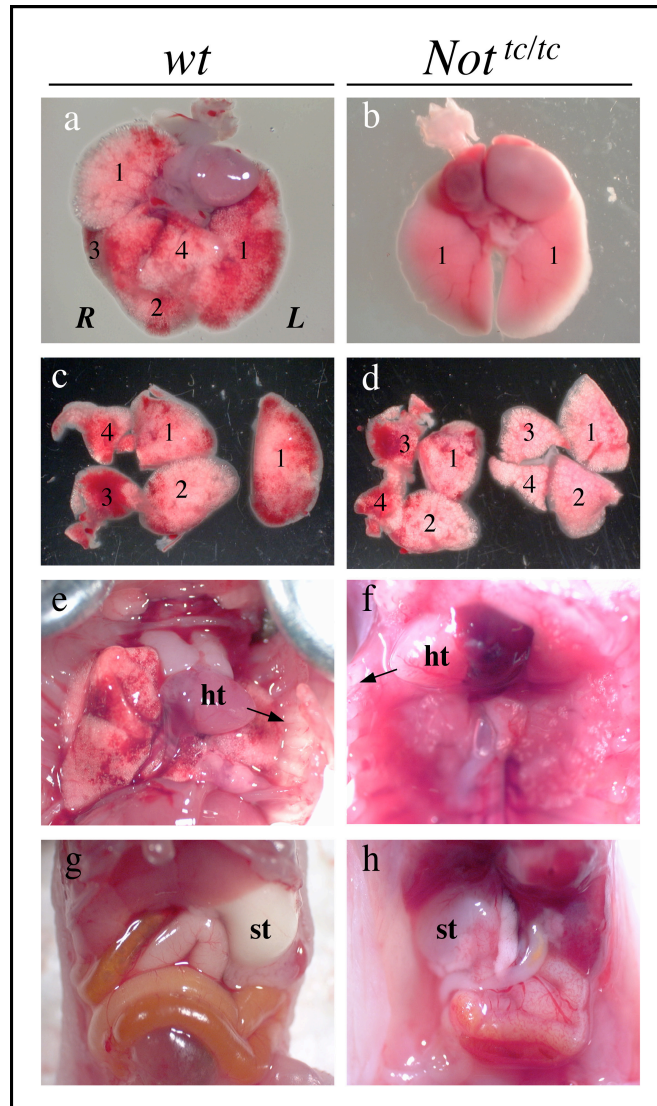


**Figure 17.** Left-right patterning defects of the organs in *Not<sup>1c/tc</sup>* mice. Visceral and thoracic organs of wild type *wt* and *Not<sup>1c/tc</sup>* mutants of pups E18-E18.5 (shortly before or after birth) were examined. Pattern of lung lobation showed that wild type have 4 lobes in the right lung and 1 lobe in the left lung (a, c) while *Not<sup>1c/tc</sup>* mutant have bilaterally monolobed lungs (b) or have 4 lobes in the right lung and 4 lobes in the left lung (d). Orientation of the heart apex showed that in the wild type the heart (ht) is oriented to the left while in some of *Not<sup>1c/tc</sup>* it was oriented to the right. The stomach (st) is normally located on the left side (g) but in some of *Not<sup>1c/tc</sup>* it was located on the right side (h).

A variety of positional defects were apparent in visceral and/or thoracic organs referred to as heterotaxia, which mean that many individuals exhibited partial situs inversion. Although the precise phenotype varied among individual animals, the most common features of the *Not<sup>tc/tc</sup>* mice were left pulmonary isomerism. In wild type mice, the right lung has four lobes, whereas the left lung has one (Fig. 17 a, c). The *Not<sup>tc/tc</sup>* mice, however, had bilaterally monolobed lungs (Fig. 17 b) indicating left pulmonary isomerism. The *Not<sup>tc/tc</sup>* mice also showed lungs with four lobes in the right and four lobes in the left indicating right pulmonary isomerism (Fig. 17 d). In normal littermates, the apex of the heart points to the left (Fig. 17 e), yet in *Not<sup>tc/tc</sup>* mutants the heart apex was ambiguously positioned such that a proportion pointed to the left, some to the middle and others to the right (Fig. 17 e, f; and data not shown). Other malformations apparent in *Not<sup>tc/tc</sup>* mice included random orientation of the stomach being normal, reversed, or ambiguous (Fig. 17 g, h; and data not shown).

In summary, from 50 mutant mice macroscopically analyzed at stage E18-18.5 dpc fetuses and neonates (Table3), only 30% showed clear L-R defects but the remaining 70% failed to show any apparent laterality defect.

**Table 3.** *L-R asymmetry defects in the organs of *Not<sup>tc/tc</sup>* mutants at birth*

	Lung lobation			Heart apex direction			Stomach position	
	Normal	LI	RI	Left	Middle	Right	Left	Right
<b><i>Wt</i></b>	(10/10)	0	0	(10/10)	0	0	(10/10)	0
<b><i>Not<sup>tc/tc</sup></i></b>	(39/50)	(7/50)	(4/50)	(41/50)	(5/50)	(4/50)	(48/50)	(2/50)

### 3.7.3 Randomized expression of *Nodal* as L-R marker in truncate mutants

To further investigate the determination of left-right asymmetry in *Not*<sup>tc/tc</sup> mutant embryos the expression pattern of *Nodal*, which is a molecular marker for L-R specification, was analyzed by performing whole-mount in situ hybridization (Fig. 18).

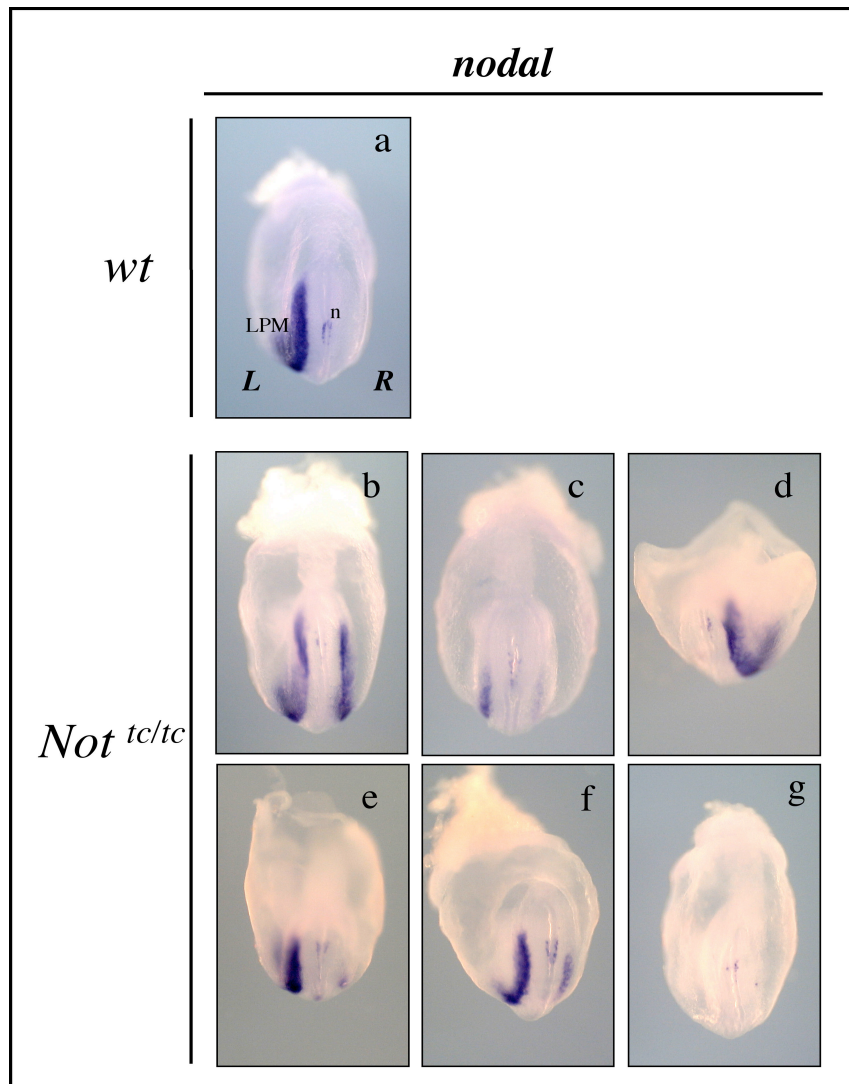


**Figure 18.** Randomization of *Nodal* expression pattern used as specific left-right marker at embryonic stage E8. (a) In the wild type embryos *Nodal* is expressed in the left lateral plate mesoderm (LPM) and lateral to the node (n). In *Not*<sup>tc/tc</sup> mutant embryos *Nodal* expression in the LPM was left-sided, right-sided (d), bilateral (b, c, e, f) or not detectable (g).

In wild type embryos at stage E8, nodal expression was confined to the left lateral plate mesoderm (LPM) and to small domains to the left and right of the node (n) (Fig. 18 a). In contrast, expression of *Nodal* in 50% of *Not<sup>tc/tc</sup>* homozygous mutant embryos was altered, with the expression either in the left LPM, in the right LPM (Fig. 18 d), bilateral expression (Fig. 18 b, c, e, f) or the expression was absent from the LPM (Fig. 18 g). However, the bilateral expression levels of nodal in the LPM of *Not<sup>tc/tc</sup>* was very variable showing equal strong expression (Fig. 18 b) or equal weak expression (data not shown) in both left and right LPM; or unequal expression level in the left and right LPM (Fig. 18 c, e, f).

The summary of *Nodal* expression pattern analysis in wild type and mutant embryos is indicated in Table 4.

**Table 4.** Expression pattern of *Nodal* a LR- Marker in *Not<sup>tc/tc</sup>* mutants

Genotype	LPM			
	Left	Right	bilateral	Absent
<i>wt</i>	25/25	0	0	0
<i>Not<sup>tc/tc</sup></i>	35/70	1/70	11/70 equal in both sides 15/70 unequal between the two sides	8/70

## 4. Discussion

### 4.1 Murine *Not* represents a new member of *Not* genes family

The *Not* genes represent a unique family of homeobox genes and their closest relatives, the *empty spiracles* genes of *Drosophila* (*ems*) or vertebrates (*Emx*), are only distantly similar. The vertebrate *Not* genes such as zebrafish *flh*, *Xenopus Xnot1/Xnot2*, and chicken *Cnot1/Cnot2*, belong to a subgroup of the *ems* homeobox gene family (von Dassow et al.1993; Talbot et al. 1995; Stein et al. 1996), and their homeodomain proteins share between 71% and 90% identity. In contrast, the mouse *Not* homeodomain sequence shares only 56-60% identical amino acids compared to the other vertebrate *Not* genes and seems more closely related by sequence to *Emx1/2* and *Drosophila ems*. Thus, the sequence comparisons between mouse *Not* protein and other *Not* proteins confirm the very high divergence level of the murine protein over the homeodomain. Nevertheless, there are remarkable similarities in the expression profile of murine *Not* gene and the pattern of the other vertebrate *Not* genes. The zebrafish, *Xenopus*, and chicken *Not* orthologs all share prominent expression domains in the organizer, the developing notochord with a graded pattern of expression, and at later stages in the tailbud and developing epiphysis (von Dassow et al.1993; Talbot et al. 1995; Ranson et al. 1995; Stein and Kessel, 1995; Stein et al. 1996). In the case of the mouse *Not*, all these expression features are conserved except for the brain which remains negative for the gene expression. Since, in mouse, *Not* is expressed during embryonic development in the node, later during the elongation of the body axis in the notochord with a posterior to anterior decreasing gradient of intensity, furthermore *Not* is required for notochord formation suggesting that functionally mouse *Not* represents a new member of the vertebrate *Not* gene family. These data are supported by other studies, which identified mammalian orthologs of *Not*, by using an *in silico* approach based on similarity searches in vertebrate genomes and subsequent bayesian phylogenetic analysis (Plouhinec et al. 2004). It has been reported that the comparison of the primary sequences from zebrafish, *Xenopus*, and chicken *Not* homeodomains revealed that *Not* genes fall into two significantly different subgroups comprised of *Cnot2/flh* and *Cnot1/Xnot*, respectively (Stein et al. 1996). Based on sequence analysis, the mouse *Not* homeodomain is most similar to *Cnot2*, having 60% amino acid identity. This finding suggests that *Not* constitutes the third member of this group becoming *Cnot2/flh/Not*. Additionally, the genomic organization of *Not* resembles *Cnot2* rather than *Cnot1* and the expression patterns of *Not* and *Cnot2* appear to be more closely related than expression of

*Not* and *Cnot1*, since the limb bud expression domain characteristic for *Cnot1* is abolished in *Cnot2* and *Not* profiles. Clustered homeobox genes are present in all vertebrates, such as *Cnot1/Cnot2* which is also considered as a genomic duplication during evolution, and it has been assumed that *Cnot2* represents the original gene in chick and *Cnot1* a duplicated copy (Stein et al. 1996). However, in mouse no evidence for a second *Not* homeobox gene in the genomic contig on each side of *Not* locus or elsewhere in the genome is found. Similarly, in the zebrafish or human genome sequence, no second closely clustered *Not* gene is known, suggesting that the presence of tightly clustered *Cnot1* and *Cnot2* genes reflect a gene duplication specific for avians. Nevertheless, in both the mouse and human genomes *Emx1* is located approximately 250 kb next to *Not*. This might indicate that *Not* and *Emx1* represent the results of a gene duplication and diverged with regard to both sequence and regulation, since *Emx1* expression is confined to the dorsal forebrain (Simeone et al. 1992a; Simeone et al. 1992b). Therefore, the high variability of the *Not*<sup>tc/tc</sup> phenotype cannot be attributed to the presence of a second *Not* gene but could be explained by the intervention of another regulatory protein(s). Since our analysis was done on a predominantly 129Sv/ImJ genetic background, it is unlikely that the segregating genetic modifiers could be linked to this variability.

#### 4.2 The truncate mutation and *Not* function

In zebrafish, *flh* mutant embryos have shown lower expression levels of *flh* transcripts, which suggested that *flh* positively regulates its own expression and thus acts as a transcriptional activator (Melby et al. 1997). In contrast, experiments in *Xenopus* embryos have shown that *Xnot1* acts as a transcriptional repressor in notochord formation (Yasuo and Lemaire 2001). In mouse, the transient ectopic expression of *Not*, observed in the head process and anterior notochord in *Not*<sup>tc/tc</sup> mutant embryos, suggests strongly that normal *Not* function is required to downregulate its own expression in the head process /anterior notochord. This is consistent with a repressor function also in mice, supported by the finding of a short octapeptide presence, located upstream of the homeodomain. This motif shows similarity to the conserved engrailed eh1 motif, which acts as a transcriptional repressor domain (Smith and Jaynes 1996) that was identified in *Xnot1* (Yasuo and Lemaire 2001), but also has been recognized in other homeodomains such as fork-head domain transcription factors (Williams and Holland, 2000).

Nevertheless, to clarify this question further experimental analysis is required. For example, one could investigate the transcriptional activity of Not homeodomain fused to a known transcriptional active domain like VP16 and of Not homeodomain fused to a known repressive domain like en1R. These fusion proteins are supposed to have similar properties compared to those of VP16-GAL4 and en1R-GAL4 proteins. If no induction by VP16-NotHD can be detected when compared to the effect of Not-HD, used as a control in the transactivation assay, it is very unlikely that Not binds directly to its own promoter and thereby regulates its own expression directly. But, this could be also due simply to the absence of some missing binding partners. In contrast, if induction by VP16-NotHD is detected, this will support the idea that Not binds its promoter and therefore can regulate itself. In addition, if no change in the transcriptional activity by en1R-NotHD compared to that of Not-HD is observed in the transactivation assay, this result means it is very likely that the fused putative antagonistic domain (en1R) and Not have the same properties.

In vertebrate *Not* genes homeodomains a phenylalanine in position 20 is conserved. Likewise, in homeodomains of other homeobox genes a phenylalanine residue or another hydrophobic amino acid is found in this position. The truncate allele carries a point mutation in the homeodomain that changes a highly conserved hydrophobic amino acid in position 20 in the first helix of the homeodomain to a polar amino acid. Previously, structural analysis have demonstrated that helix 1 and helix 2 play a critical role in helping to stabilize the folded structure of the homeodomain, and that this stabilization requires a hydrophobic core, to which a conserved Leucine in position 16 (L16) and phenylalanine in position 20 (F20) molecular residue in helix 1 contribute (Qian et al. 1989; Kissinger et al. 1990). This F20C mutation in the truncate allele represents the first natural point mutation in the homeodomain of a mouse homeobox gene so far known, affecting significantly the stability of the homeodomain in vitro. Finally, considering the combination of the different data such as the destabilisation of the homeodomain in the truncate allele in vitro, the severe loss-of-function phenotype of *Not*<sup>tc/tc</sup> mutant embryos in vivo showing abnormalities in notochord formation and the restoration of notochords in completely ES cell-derived E11.5 *Not*<sup>tc/tcrev</sup> embryos strongly support the importance of hydrophobic interactions between helix 1 and the recognition helix for the homeodomain stability. Thus, these data suggest that F20 is critical for this interaction under physiological conditions in vivo since this mutation has an remarkable impact on *Not* function in vivo.



### 4.3 The role of *Not* in notochord development

In zebrafish, *flh* is an essential gene for axial development during embryogenesis and is one of the earliest genes to be expressed in notochord precursors, since the loss of *Not/flh* function in these mutant embryos leads to the lack of a differentiated notochord along the entire anterior-posterior body axis (Halpern et al. 1995; Talbot et al. 1995). Molecular marker analysis indicated that *flh* mutants showed inappropriate expression of paraxial mesoderm markers in the axial midline during gastrulation, and therefore instead, muscle cells occupy the position normally filled by notochord. However, fate mapping in *flh* mutants has shown that notochord precursors, which originally express *flh* RNA, develop as muscle. This suggests that *flh* is required to maintain rather than to establish notochordal fate (Halpern et al. 1995). In *Xenopus* overexpression experiments of *Xnot* by injecting *Xnot1* or *Xnot2* mRNA to wild type embryos leads to increased development notochord tissue or to the formation of multiple notochords (Gont et al. 1996; Yasuo and Lemaire 2001) while expression of a VP16-transactivator /XNOT1 homeo domain fusion inhibits the formation of endogenous notochord formation (Yasuo and Lemaire 2001). Taken together, the data from studies in zebrafish and *Xenopus* embryos suggested that *Not* genes are necessary and sufficient for maintaining notochordal fate in these species and that their function is required for the entire anterior-posterior body axis during development. In contrast, in mouse embryos the restriction of *Not* expression domain to the caudal notochord suggests that *Not* function is required for notogenesis only in the posterior region of the body axis. This is supported by loss of *Not* function studies in mice (Ben Abdelkhalek et al. 2004). Thus, in mouse embryo the role of *Not* gene appears to have diverged.

### 4.4 The regulation of *Not* gene

In zebrafish, *Foxa2* homologue, *axial* acts upstream of *flh*. In contrast, *flh* appears to act upstream of *T* because the zebrafish brachyury homologue *ntl* is not expressed in notochord precursors of *flh* mutant embryos (Talbot et al. 1995) and *flh* transcripts are present in embryos lacking *ntl* function (Melby et al. 1997). In mouse, in *Foxa2* mutant embryos all notochord cells and an organised node are abolished, and *T* is expressed only in cells of the abnormal primitive streak (Ang and Rossant 1994; Weinstein et al. 1994), while in homozygous *T* mutant embryos node and trunk notochord are lacking but notochord cells of the head process are formed (Herrmann 1995), suggesting that *Foxa2* acts upstream of *T* in the genetic cascade involved in notogenesis.

Loss of *Not* expression in homozygous *Foxa2* embryos places *Foxa2* also upstream of *Not*. The lack of *Not* transcripts in homozygous *T* embryos suggests that *Not* acts downstream of *T* in the notogenesis. Since *Not* expression is transient in the notochord but *T* expression persists, *T* might be required to initiate *Not* transcription in the notochord and node, but is apparently not sufficient to maintain *Not* expression. Thus, in mouse the action of *T* upstream of *Not* during notochord formation differs from zebrafish. This finding further supports the notion that the role of *Not* during notochord development in mouse and zebrafish embryos has diverged.

Previous studies in zebrafish demonstrate that *flh* and *ntl* interact in a complex way, with each being required to maintain the expression of the other (Talbot et al. 1995; Melby et al. 1996; Halpern et al. 1997). In mouse, heterozygous *T* embryos show fragmented notochord in the posterior trunk and tail region (Herrmann 1995), closely resembling the *Not*<sup>tc/tc</sup> phenotype. Thus, both reduction of *T* or disturbance of normal *Not* function lead to similar defects. This could be explained by various possible interactions between *T* and *Not*. A reduction of *T* would decrease *Not* activity posteriorly below a certain level, which in turn would lead to a disrupted notochord formation. Alternatively, *T* and *Not* could cooperatively regulate genes critical for posterior notochord formation, and in the posterior region both high levels of *T* and full function of *Not* are required to maintain notogenesis. In both cases, *T* or another unknown regulatory protein might compensate for the lack of *Not* expression in the anterior notochord. The analysis of double heterozygous *T* and *Not* mutant embryos should help to further elucidate the relation and interaction of *T* and *Not*.

The Forkhead box DNA-binding domain and the homeodomain are highly conserved among winged-helix/Forkhead box transcription factors and homeoproteins, respectively. Since Fox proteins and homeoprotein can interact physically and functionally to regulate many distinct functions, from the earliest events of embryonic development throughout adulthood, it is proposed that interaction between Forkhead box transcription factors and homeoproteins is a general phenomenon (Foucher et al. 2003). Homeoproteins constitute a large family of transcription factors characterized by a highly conserved 60 amino acid-long DNA binding motif, the homeodomain (Gehring et al. 1994), and by specific spatiotemporal expression patterns during development (Krumlauf, 1994; Lumsden and Krumlauf, 1996; Stern and Foley, 1998). An important problem is the remarkable conservation of the homeodomain, making it difficult to understand how transcriptional specificity can be attained. This is probably why only a few direct target genes of distinct homeoproteins have so far been identified (Mannervik, 1999). A probable

explanation for homeoprotein specificity is their association with cofactors. Clearly, homeoproteins have shown associations with numerous proteins, including members of the same homeoprotein family, members of different homeoproteins and non-homeodomain proteins. Direct physical interactions between *Foxa2* and *En2*, *Gsc*, *Lim1*, *Hoxa5*, or *Otx2* have been reported (Foucher et al. 2003). In transactivation assays *Foxa2* strongly activates the transcription of *Not* promoter suggesting that *Foxa2* is most likely a direct regulator of *Not*. These data are supported by a sequence analysis showing that putative consensus binding sites for *Foxa2* are located on *Not* promoter region tested in the assays. The level of transcriptional induction by *Foxa2* varies with the different deletions of *Not* promoter in the transactivation experiments, indicating that at least some of these binding sites might play a role in this regulation.

Since *Foxa2* and *Not* share in part, overlapping expression domains, this could suggest a potential cooperation in the transcription between *Foxa2* and *Not*. This is supported by the finding that *Foxa2* is able to induce the transcriptional activity of *Not* promoter in vitro. Nevertheless, no change is detected on *Not* promoter transcriptional activity, when *Not* is cotransfected together with *Foxa2* and compared to the transfection of *Foxa2* alone. These could be due to a possible requirement of some cofactor(s) that are missing in this experiment since the cells used in these assays are not notochordal cells. Temporarily, persistent *Not* expression of *Not<sup>tc/tc</sup>* mutant embryos in the head process and in the anterior notochord suggests that *Not* contributes to its own regulation. Two possible mechanisms are imaginable for this autoregulation: either *Not* is a direct repressor of itself or it is an activator of mediating factor which represses *Not* transcription. The transgenic analysis of *cis*-regulatory elements in the *Not* promoter is an important step towards the identification of transcription factors that are required for the spatially and temporally regulated expression of this gene during development. This analysis has shown that approximately 12kb upstream genomic region of *Not*, containing the first exon and intron, contains essential regulatory sequences that drive the expression in the notochord. Nevertheless, this region does not contain all the regulatory sequences that are sufficient to reproduce the endogenous expression pattern of *Not* in transgenic embryos. Regulatory elements for restriction of expression to notochord are located either upstream or downstream of the genomic region tested in the transgene *tg<sup>Not pr lacZ</sup>*. Interestingly, the expression pattern of this transgene closely resembles the endogenous expression pattern of *Foxa2*. This finding also supports the proposed idea that *Foxa2* is a direct regulator of *Not*.

#### 4.5 The truncate mutation and L-R determination

A complex regulatory network of genes required for the initiation, formation and maintenance of LR asymmetry of vertebrates has been discovered so far (Bisgrove and Yost, 2001; Capdevila et al., 2000; Hamada et al., 2002; Wood, 1997). The TGFb family genes such as *Nodal*, which are the earliest asymmetrically expressed genes in mice described so far, play pivotal roles in this process. In 50% of the *Not<sup>tc/tc</sup>* mutant embryos, the expression pattern of *Nodal* is altered, being normal, reversed, bilateral or absent; suggesting that *Not* regulates directly or indirectly *Nodal* expression. The loss of the unilateral expression domain of *Nodal* is in accordance with the observed situs ambiguous phenotype (heterotaxia) in *Not<sup>tc/tc</sup>* mutants. Nevertheless, only 30% of the analyzed *Not<sup>tc/tc</sup>* mutant mice show clear L-R defects in the organs; in contrast, 50% of the mutant embryos show abnormal L-R marker expression. This can possibly be explained by the fact that this analysis was achieved macroscopically. Perhaps, a careful examination of these animals by histological analysis would reveal that some mice displayed defects such as cardiovascular malformations including incomplete atrial and ventricular septation. Thus, the expression analysis demonstrates that *Not* is required for the consistent asymmetrical expression of *Nodal*. These results provide convincing evidence that truncate is, so far unknown, a mutation affecting laterality.

Homozygous *Not<sup>tc/tc</sup>* mutants show structural abnormalities in midline tissues, such as a lack of notochordal cells and floorplate in some regions of the caudal notochord. Defects in axial midline tissues are also reported from mouse mutants such as no turning, *Shh<sup>-/-</sup>*, *Sil<sup>-/-</sup>* and *Dll1*. The midline defects in *Not<sup>tc/tc</sup>* mutant embryos are consistent with the observations that midline tissues may function as a physical barrier, which might be a prerequisite for normal development and/or maintenance of laterality in vertebrates (Klessinger and Christ, 1996; Levin et al., 1996; Lohr et al., 1997). However, the observed defect in the midline structure of *Not<sup>tc/tc</sup>* mutant embryos cannot fully explain the primary cause of the LR abnormalities. Based on previous studies of cellular movements in the node and fate maps of the node and primitive streak (Kinder et al., 2001; Sulik et al., 1994; Tam and Beddington, 1987), it is likely that the midline defects of *Not<sup>tc/tc</sup>* mutant embryos may be caused by earlier defects in the differentiation of node cells and node morphology. It is suggested that the shape of the node and the equal distribution of motile

cilia on its ventral surface are prerequisites to generate a nodal flow, which might transport a – not yet identified – morphogen that triggers the onset of asymmetric gene expression (Nonaka et al., 1998; Okada et al., 1999). Taken together, the defects in LR-axis formation in *Not*<sup>tc/tc</sup> mutant embryos may originate from a combination of altered node morphology and a defective midline. The identification of truncate as a spontaneous mouse mutation with laterality defects is important for the further understanding of LR-axis formation in vertebrates.

In summary, this study supports the concept of regional differences in the genetic control of notochord development, and identifies *Not* as one important regulator in this process acting downstream of *Foxa2* and *T* during mouse embryonic development and most likely regulated directly by *Foxa2*. Regionalized control of notochord development also appears to occur in other vertebrate species as suggested by the zebrafish *mom* mutation, which disrupts notochord formation in the trunk but not in the tail (Odenthal et al. 1996). However, the role of individual components of the genetic hierarchy, that governs notogenesis, appears to vary between different vertebrate species. Additionally, in this analysis truncate is identified as a mouse mutation affecting LR determination and *Nodal*, an earliest asymmetrically expressed gene in mouse is regulated by *Not*. Thus, the *Not* gene plays a crucial role in the notogenesis and the left-right specification processes during development.

## 5. References

- Adams, D. S., Keller, R., and Koehl, M. A. (1990). The mechanics of notochord elongation, straightening and stiffening in the embryo of *Xenopus laevis*. *Development* **110**, 115–130.
- Ades, S.E. and Sauer, R.T. 1994. Differential DNA-binding specificity of the engrailed homeodomain: The role of residue 50. *Biochemistry* **33**: 9187–9194.
- Altschul, S.F., Madden, T.L., Schaffer, A.A., Zhang, J., Zhang, Z., Miller, W., and Lipman, D.J. 1997. Gapped BLAST and PSI-BLAST: A new generation of protein database search programs. *Nucleic Acids Res.* **25**: 3389–3402.
- Amacher, S.L. and Kimmel, C.B. 1998. Promoting notochord fate and repressing muscle development in zebrafish axial mesoderm. *Development* **125**: 1397–1406.
- Ang, S.L. and Rossant, J. 1994. HNF-3b is essential for node and notochord formation in mouse development. *Cell* **78**: 561–574.
- Apweiler, R., Attwood, T.K., Bairoch, A., Bateman, A., Birney, E., Biswas, M., Bucher, P., Cerutti, L., Corpet, F., Croning, M.D., et al. 2001. The InterPro database, an integrated documentation resource for protein families, domains and functional sites. *Nucleic Acids Res.* **29**: 37–40.
- Barteczko, K., and Jacob, M. 1999. Comparative study of shape, course, and disintegration of the rostral notochord in some vertebrates, especially humans. *Anat. Embryol.* **200**: 345–366.
- Basler, K., Edlund, T., Jessell, T. M., and Yamada, T. 1993. Control of cell pattern in the neural tube: Regulation of cell differentiation by dorsalin-1, a novel TGF beta family member. *Cell* **73**: 687–702.
- Beddington RSP, Robertson EJ. 1999. Axis development and early asymmetry in mammals. *Cell* **96**:195–209.
- Ben Abdelkhalek, H., Beckers, A., Schuster-Gossler, K., Pavlova, M. N., Burkhardt, H., Lickert, H., Rossant, J., Reinhardt, R., Schalkwyk, L. C., Müller, I., Herrmann, B. G., Ceolin, M., Rivera-Pomar, R., and Gossler, A. 2004. The mouse homeobox gene *Not* is required for caudal notochord development and affected by the truncate mutation. *Genes & Dev.* **18**: 1725-1736.
- Berry, R.J. 1960. Genetical studies on the skeleton of the mouse XXVI. Pintail. *Genet. Res. Camb.* **1**: 439–451.
- Bisgrove, B. W., and Yost, H. J. 2001. Classification of left-right patterning defects in zebrafish, mice, and humans. *Am. J. Med. Genet.* **101**: 315-323.
- Bisgrove, B. W., Essner, J. J., and Yost, H. J. 2000. Multiple pathways in the midline regulate concordant brain, heart and gut left-right asymmetry. *Development* **127**: 3567-3579.
- Bober, E., Brand-Saberi, B., Ebensperger, C., Wilting, J., Balling, R., Paterson, B. M., Arnold, H. H., and Christ, B. 1994. Initial Steps of myogenesis in somites are independent of influence from axial structures. *Development* **120**: 3073–3082.
- Brand-Saberi, B., and Christ, B. 2000. Evolution and development of distinct cell lineages derived from somites. *Current Topics in Developmental Biology* **48**:1-42.

- Bumcrot, D.A. and McMahon, A.P. 1995. Somite differentiation. Sonic signals somites. *Curr. Biol.* **5**: 612–614.
- Capdevila J, Vogan KJ, Tabin CJ, Izpisua-Belmonte JC. 2000. Mechanisms of left-right determination in vertebrates. *Cell* **101**:9–21.
- Cheng, A. M., Thisse, B., Thisse, C., and Wright, C. V. 2000. The lefty-related factor Xatv acts as a feedback inhibitor of nodal signaling in mesoderm induction and L-R axis development in *Xenopus*. *Development* **127**: 1049-1061.
- Chiang, C., Litingtung, Y., Lee, E., Young, K., Corden, J. L., Westphal, H., and Beachy, P. A. 1996. Cyclopia and defective axial patterning in mice lacking Sonic hedgehog gene function. *Nature* **383**: 407-413.
- Chuang, P. T., and McMahon, A. P. 1999. Vertebrate Hedgehog signaling modulated by induction of a Hedgehog-binding protein. *Nature* **397**: 617–621.
- Clark, K. L., Halay, E. D., Lai, E., and Burley, S. K. 1993. Co-crystal structure of the HNF-3/fork head DNA recognition motif resembles histone H5. *Nature* **364**: 412-420.
- Clarke, D. J., Holder, N., Soffe, S. R., and Storm-Mathisen, J. 1991. Neuroanatomical and functional analysis of neural tube formation in notochordless *Xenopus* embryos: Laterality of the ventral spinal cord is lost. *Development* **112**: 499-516.
- Cleaver, O., Seufert, D. W., and Krieg, P. A. 2000. Endoderm patterning by the notochord: Development of the hypochord in *Xenopus*. *Development* **127**: 869–879.
- Cooke, J. 1985. Dynamics of the control of body pattern in the development of *Xenopus laevis*. III. Timing and pattern after u.v. irradiation of the egg and after excision of presumptive head endomesoderm. *J. Embryol. Exp. Morphol.* **88**: 135–150.
- Dale, K., Sattar, N., Heemskerk, J., Clarke, J. D., Placzek, M., and Dodd, J. 1999. Differential patterning of ventral midline cells by axial mesoderm is regulated by BMP7 and chordin. *Development* **126**: 397–408.
- Dalgleish, A. E. 1985. A study of the development of thoracic vertebra in the mouse assisted by autoradiography. *Acta Anatomica* **122**: 91-98.
- Dalton, D., Chadwick, R., and McGinnis, W. 1989. Expression and embryonic function of empty spirales: a *Drosophila* homeo box gene with two patterning functions on the anterior-posterior axis of the embryo. *Genes & Dev.* **3**: 1940-1956.
- Danos, M. C., and Yost, H. J. 1995. Linkage of cardiac left-right asymmetry and dorsal-anterior development in *Xenopus*. *Development* **121**: 1467-1474.
- Danos, M. C., and Yost, H. J. 1996. Role of notochord in specification of cardiac left-right orientation in zebrafish and *Xenopus*. *Dev. Biol.* **177**: 96-103.
- Davidson, B. P., Kinder, S. J., Steiner, K., Schoenwolf, G. C., and Tam, P. P. 1999. Impact of node ablation on the morphogenesis of the body axis and the lateral asymmetry of the mouse embryo during early organogenesis. *Dev. Biol.* **211**: 11-26.

- de Vries, W. N., Binns, L.T., Fancher, K.S., Dean, J., Moore, R., Kemler, R., and Knowles, B.B. 2000. Expression of Cre recombinase in mouse oocytes: A means to study maternal effect genes. *Genesis* **26**: 110–112.
- Devoto, S. H., Melancon, E., Eisen, J. S., and Westerfield, M. 1996. Identification of separate slow and fast muscle precursor cells in vivo, prior to somite formation. *Development* **122**: 3371–3380.
- Dias, M. S. and Schoenwolf, G. C. 1990. Formation of ectopic neuroepithelium in chick blastoderms: age-related capacities for induction and self-differentiation following transplantation of quail Hensen's node. *Anat. Rec.* **228**: 437–448.
- Dick, A., Meier, A., and Hammerschmidt, M. 1999. Smad1 and Smad5 have distinct roles during dorsoventral patterning of the zebrafish embryo. *Developmental Dynamics* **216**: 285–298.
- Dietrich, S., Schubert, F.R., and Gruss, P. 1993. Altered Pax gene expression in murine notochord mutants: The notochord is required to initiate and maintain ventral identity in the somite. *Mech. Dev.* **44**: 189–207.
- Dobrovolskaia-Zavadskaia, N. 1927. Sur la mortification spontanée de la queue chez la souris nouveau-née et sur l'existence d'un caractère héréditaire 'non viable'. *C.R. Soc. Biol.* **97**: 114–116.
- Dockter, J. L. 2000. Sclerotome induction and differentiation. *Current Topics in Developmental Biology* **48**: 77–127.
- Dodd, J., Jessel, T. M., and Placzek, M. 1998. The when and where of floor plate induction. *Science* **282**: 1654–1657.
- Dudley, A. T., and Robertson, E. J. 1997. Overlapping expression domains of bone morphogenetic protein family members potentially account for limited tissue defects in BMP7 deficient embryos. *Dev. Dyn.* **208**: 349–362.
- Dufort, D., Schwartz, L., Harpal, K., and Rossant, J. 1998. The transcription factor HNF3 $\beta$  is required in visceral endoderm for normal primitive streak morphogenesis. *Development* **125**: 3015–3025.
- Echelard, Y., Epstein, D. J., St-Jacques, B., Shen, L., Mohler, J., McMahon, J. A., and McMahon, A. P. 1993. Sonic hedgehog, a member of a family of putative signaling molecules, is implicated in the regulation of CNS polarity. *Cell* **75**: 1417–1430.
- Elliott, G. B., Tredwell, S. J., and Elliott, K. A. 1970. The notochord as an abnormal organizer in production of congenital intestinal defect. *Am. J. Roentgenol. Radium Ther. Nucl. Med.* **110**: 628–634.
- Ericson, J., Morton, S., Kawakami, A., Roelink, H., and Jessell, T. M. 1996. Two critical periods of Sonic Hedgehog signaling required for the specification of motor neuron identity. *Cell* **87**: 661–673.
- Eyal-Giladi, H. 1958. The notochord as inductor of the orohypophysis in urodeles (*Pleurodeles waltii*). *Proc. K. Med. Wet. (Amsterdam)* **61**: 224–234.
- Fallon, M., Gordon, A. R., and Lendrum, A. C. 1954. Mediastinal cysts of fore-gut origin associated with vertebral anomalies. *Br. J. Surg.* **41**: 520–533.
- Fan, C. M., and Tessier-Lavigne, M. 1994. Patterning of mammalian somites by surface ectoderm and notochord: Evidence for sclerotome induction by a hedgehog homolog. *Cell* **79**: 1175–1186.



- Fan, C. M., Porter, J. A., Chiang, C., Chang, D. T., Beachy, P. A., and Tessier-Lavigne, M. 1995. Long-range sclerotome induction by sonic hedgehog: Direct role of the amino-terminal cleavage product and modulation by the cyclic AMP signaling pathway. *Cell* **81**: 457–465.
- Fleming, A., Keynes, R., and Tannahill, D. 2003. A central role for the notochord in vertebral patterning. *Development* **131**: 873-880.
- Foucher, I., Montesinos, M. L., Volovitch, M., Prochiantz, A., and Trembleau, A. 2003. Joint regulation of the MAP1B promoter by HNF $\beta$ /Foxa2 and engrailed is the result of a highly conserved mechanism for direct interaction of homeoproteins and Fox transcription factors. *Development* **130**: 1867-1876.
- Fouquet, B., Weinstein, B. M., Serluca, F. C., and Fishman, M. C. 1997. Vessel patterning in the embryo of the zebrafish: Guidance by notochord. *Dev. Biol.* **183**: 37–48.
- Frishman, D., Mironov, A., Mewes, H.W., and Gelfand, M. 1998. Combining diverse evidence for gene recognition in completely sequenced bacterial genomes. *Nucleic Acids Res.* **26**: 2941–2947.
- Furthauer, M., Thiesse, B., and Thiesse, C. 1999. Three different noggin genes antagonize the activity of bone morphogenetic proteins in the zebrafish embryo. *Developmental Biology* **214**: 181-196.
- Furumoto, T. A., Miura, N., Akasaka, T., Misutani-Koseki, Y., Sudo, H., and Fukuda, K et al. 1999. Notochord-dependent expression of MFH1 and PAX1 cooperates to maintain the proliferation of sclerotome cells during the vertebral column development. *Developmental Biology* **210**: 15-29.
- Gallera, J. 1971. Primary induction in birds. *Adv. Morph.* **9**: 149-180.
- Gasca, S., Hill, D.P., Klingensmith, J., and Rossant, J. 1995. Characterization of a gene trap insertion into a novel gene, cordon-bleu, expressed in axial structures of the gastrulating mouse embryo. *Dev. Genet.* **17**: 141–154.
- Gehring, W. J., Qian, Y. Q., Billeter, M., Furokubo-Tokunaga, K., Shier, A. F., Resendez-Perez, D., Affolter, M., Otting, G., and Wüthrich, K. 1994. Homeodomain-DNA Recognition. *Cell* **78**: 211-223.
- Gleiberman, A. S., Fedtsova, N. G., and Rosenfeld, M. G. 1999. Tissue interactions in the induction of anterior pituitary: Role of the ventral diencephalon, mesenchyme, and notochord. *Dev. Biol.* **213**: 340–353.
- Gluecksohn-Schoenheimer, S. 1943. The morphological manifestations of a dominant mutation in mice affecting tail and urogenital system. *Genetics* **28**: 341–348.
- Goldstein, A. M., and Fishman, M. C. 1998. Notochord regulates cardiac lineage in zebrafish embryos. *Dev. Biol.* **201**: 247–252.
- Gont, L.K., Fainsod, A., Kim, S.H., and De Robertis, E.M. 1996. Overexpression of the homeobox gene Xnot-2 leads to notochord formation in *Xenopus*. *Dev. Biol.* **174**: 174–178.
- Gont, L.K., Steinbeisser, H., Blumberg, B., and de Robertis, E.M. 1993. Tail formation as a continuation of gastrulation: The multiple cell populations of the *Xenopus* tailbud derive from the late blastopore lip. *Development* **119**: 991–1004.

- Goulding, M. D., Lumsden, A., and Gruss, P. 1993. Signals from the notochord and floor plate regulate the region-specific expression of two Pax genes in the developing spinal cord. *Development* **117**: 1001–1016.
- Goulding, M., Lumsden, A., and Paquette, A. J. 1994. Regulation of Pax-3 expression in the dermomyotome and its role in muscle development. *Development* **120**: 957–971.
- Hall, B. K. 1977. Chondrogenesis of the somitic mesoderm. *Adv. Anat. Embryol. Cell Biol.* **53**: 3–47.
- Halpern, M. E. 1997. Axial mesoderm and patterning of the zebrafish embryo. *Am. Zool.* **37**: 311–322.
- Halpern, M. E., Ho, R. K., Walker, C., and Kimmel, C. B. 1993. Induction of muscle pioneers and floor plate is distinguished by the zebrafish no tail mutation. *Cell* **75**: 99–111.
- Halpern, M.E., Thisse, C., Ho, R.K., Thisse, B., Riggleman, B., Trevarrow, B., Weinberg, E.S., Postlethwait, J.H., and Kimmel, C.B. 1995. Cell-autonomous shift from axial to paraxial mesodermal development in zebrafish floating head mutants. *Development* **121**: 4257–4264.
- Hamada, H., Meno, C., Watanabe, D., and Saijoh, Y. 2002. Establishment of vertebrate left-right asymmetry. *Nat. Rev. Genet.* **3**: 103-113.
- Hammerschmidt, M., and McMahon, A. P. 1998. The effect of pertussis toxin on zebrafish development: a possible role for inhibitory G-proteins in hedgehog signalling. *Developmental Biology* **194**: 166-171.
- Hara, K. 1978. Spemann's organiser in birds. In *Organizer – a milestone of a half-Century since Spemann*. (ed. O. Nakamura and S. Toivonen). pp. 221- 265. Amsterdam: Elsevier/North Holland.
- Hebrok, M., Kim, S. K., and Melton, D. A. 1998. Notochord repression of endodermal Sonic hedgehog permits pancreas development. *Genes & Dev.* **12**: 1705–1713.
- Hemmati-Briuanlou, A., Kelly, O. G., and Melton, D. A. 1994. Follistatin, an antagonist of activin, is expressed in the Spemann organizer and displays direct neuralizing activity. *Cell* **77**: 283–295.
- Herrmann, B.G. 1995. The mouse *Brachyury (T)* gene. *Sem. Dev. Biol.* **6**: 385–394.
- Herrmann, B.G., Labeit, S., Poustka, A., King, T.R., and Lehrach, H. 1990. Cloning of the *T* gene required in mesoderm formation in the mouse. *Nature* **343**: 617–622.
- Hirano, S., Fuse, S., and Sohal, G. S. 1991. The effect of the floor plate on pattern and polarity in the developing central nervous system. *Science* **251**: 310–313.
- Holley, S. A., and Nusslein-Volhard, C. 2000. Somitogenesis in zebrafish. *Current Topics in Developmental Biology* **47**: 247-277.
- Holtzer, H. 1952. An experimental analysis of the development of the spinal column II. The dispensability of the notochord. *Journal of experimental Zoology* **121**: 573-591.
- Holtzer, H., and Detwiler, S. R. 1953. An experimental analysis of the development of the spinal column III. Induction of skeletogenous cells. *Journal of experimental Zoology* **123**: 335-366.
- Hornbruch, A., and Wolpert, L. 1986. Positional signalling by Hensen's node when grafted to the chick limb bud. *J. Embryol. Exp. Morph.* **94**: 257-265.

- Isaacs, H. V., Pownall, M. E., and Slack, J. M. 1995. eFGF is expressed in the dorsal midline of *Xenopus laevis*. *Int. J. Dev. Biol.* **39**: 575–579.
- Izpisúa-Belmonte, J. C., De Robertis, E. M., Storey, K. G. and Stern, C. D. 1993. The homeobox gene *gooseoid* and the origin of the organizer cells in the early chick blastoderm. *Cell* **74**: 645-659.
- Jessell, T. M., and Dodd, J. 1990–1991. Floor plate-derived signals and the control of neural cell pattern in vertebrates. *Harvey Lect.* **86**: 87–128.
- Johnson, R. L., Laufer, E., Riddle, R. D., and Tabin, C. 1994. Ectopic expression of Sonic hedgehog alters dorsal–ventral patterning of somites. *Cell* **79**: 1165–1173.
- Joseph, E. M., and Melton, D. A. 1997. *Xnr4*: A *Xenopus* nodal-related gene expressed in the Spemann organizer. *Dev. Biol.* **184**: 367–372.
- Jurand, A. 1974. Some aspects of the development of the notochord in mouse embryos. *J. Embryol. Exp. Morphol.* **32**: 1–33.
- Kaufmann, E., and Knoechel, W. 1996. Five years on the wings of fork head. *Mech. Dev.* **57**: 3-20.
- Kenny-Mobbs, T., and Thorogood, P. (1987). Autonomy of differentiation in avian branchial somites and the influence of adjacent tissues. *Development* **100**: 449–462.
- Kim, S. K., Hebrok, M., and Melton, D. A.. 1997. Notochord to endoderm signaling is required for pancreas development. *Development* **124**: 4243–4252.
- Kinder, S.J., Tsang, T.E., Wakamiya, M., Sasaki, H., Behringer, R.R., Nagy, A., and Tam, P.P. 2001. The organizer of the mouse gastrula is composed of a dynamic population of progenitor cells for the axial mesoderm. *Development* **128**: 3623–3634.
- Kintner, C. R., and Dodd, J. 1991. Hensen's node induces neural tissue in *Xenopus* ectoderm. Implications for the action of the organizer in neural induction. *Development* **113**: 1495-1505.
- Kissinger, C.R., Liu, B.S., Martin-Blanco, E., Kornberg, T.B., and Pabo, C.O. 1990. Crystal structure of an engrailed homeodomain–DNA complex at 2.8 Å resolution: A framework for understanding homeodomain–DNA interactions. *Cell* **63**: 579–590.
- Kitchin, I. C. 1949. The effects of notochordectomy in *Amblystoma mexicanum*. *Journal of experimental Zoology* **112**: 393-415.
- Klessinger, S. and Christ, B. 1996. Axial structures control laterality in the distribution pattern of endothelial cells. *Anat. Embryol.* **193**: 319-330.
- Knezevic, V., Ransom, M. and Mackem, S. 1995. The organizer-associated chick homeobox gene *Gnot1* is expressed before gastrulation and regulated synergistically by activin and retinoic acid. *Dev. Biol.* **171**: 458-470.
- Kondaiah, P., Taira, M., Vempati, U. D., and Dawid, I. B. 2000. Transforming growth factor-beta5 expression during early development of *Xenopus laevis*. *Mech. Dev.* **95**: 207–209.
- Krumlauf, R. 1994. Hox genes in vertebrate development. *Cell* **78**: 191-201.

- Lamers, W. H., Splet, W. G., and Langemeyer, R. A. 1987. The lining of the gut in the developing rat embryo. Its relation to the hypoblast (primary endoderm) and the notochord. *Anat. Embryol.* **176**: 259–265.
- Lassar, A. B., and Munsterberg, A. E. 1996. The role of positive and negative signals in somite patterning. *Curr. Opin. Neurobiol.* **6**: 57–63.
- Lawson, K.A. and Pedersen, R.A. 1992. Clonal analysis of cell fate during gastrulation and early neurulation in the mouse. *Ciba Found. Symp.* **165**: 3–21.
- Lawson, K.A., Meneses, J.J., and Pedersen, R.A. 1991. Clonal analysis of epiblast fate during germ layer formation in the mouse embryo. *Development* **113**: 891–911.
- Le Douarin, N. M., and Halpern, M. E. 2000. Discussion point. Origin and specification of the neural tube floor plate: Insights from the chick and zebrafish. *Curr. Opin. Neurobiol.* **10**: 23–30.
- Le Douarin, N. M., Teillet, M. A., and Catala, M. 1998. Neurulation in amniote vertebrates: A novel view deduced from the use of quail–chick chimeras. *Int. J. Dev. Biol.* **42**: 909–916.
- Leikola, A. 1976. Hensen’s node – the organizer of the amniote embryo. *Experientia* **32**: 269-277.
- Levin, M., Johnson, R. L., Stern, C. D., Kuehn, M. and Tabin, C. J. 1995. A molecular pathway determining left-right asymmetry in chick embryogenesis. *Cell* **82**: 803-814.
- Levin, M., Roberts, D. J., Holmes, L. B., and Tabin, C. 1996. Laterality defects in conjoined twins. *Nature* **384**: 321.
- Lohr, J. L., Danos, M. C., and Yost, H. J. 1997. Left-right asymmetry of a nodal-related gene is regulated by dorsoanterior midline structures during *Xenopus* development. *Development* **124**: 1465-1472.
- Lumsden, A., and Krumlauf, R. 1996. Patterning the vertebrate neuraxis. *Science* **274**: 1109-1115.
- Maatman, R., Zachgo, J., and Gossler, A. 1997. The Danforth’s short tail mutation acts cell autonomously in notochord cells and ventral hindgut endoderm. *Development* **124**:4019–4028.
- Mannervik, M. 1999. Target genes of homeodomain proteins. *Bioassays* **21**: 267-270.
- Marti, E. 2000. Expression of chick BMP-1/Tolloid during patterning of the neural tube and somites. *Mech. Dev.* **91**: 415–419.
- Marti, E., Bumcrot, D. A., Takada, R., and McMahon, A. P. 1995. Requirement of 19K form of Sonic hedgehog for induction of distinct ventral cell types in CNS explants. *Nature* **375**: 322–325.
- McMahon, J. A., Takada, S., Zimmerman, L. B., Fan, C. M., Harland, R. M., and McMahon, A. P. 1998. Noggin-mediated antagonism of BMP signalling is required for growth and patterning of the neural tube and somite. *Genes & Dev.* **12**: 1438-1452.
- Melby, A. E., Warga, R. M., and Kimmel, C. B. 1996. Specification of cell fates at the dorsal margin of the zebrafish gastrula. *Development* **122**: 2225-2237.

- Melby, A.E., Kimelman, D., and Kimmel, C.B. 1997. Spatial regulation of floating head expression in the developing notochord. *Dev. Dyn.* **209**: 156–165.
- Melloy, P. G., Ewart, J. L., Cohen, M. F., Desmond, M. E., Kuehn, M. R., and Lo, C. W. 1998. No turning, a mouse mutation causing left–right and axial patterning defects. *Dev. Biol.* **193**: 77–89.
- Monsoro-Burq, A. H., and Le Douarin, N. 2000. Duality of molecular signalling involved in vertebral chondrogenesis. *Current Topics in Developmental Biology* **48**: 43-75.
- Monsoro-Burq, A. H., Bontoux, M., Teillet, M. N., and Le Douarin, N.M. 1994. Heterogeneity of the development of the vertebra. *Proceedings of the national Academy of Sciences of the USA* **91**: 10435-10439.
- Monsoro-Burq, A. H., Duprez, D., Watanabe, Y., Bontoux, M., Vincent, C., and Brickell, P et al. 1996. The role of bone morphogenetic proteins in vertebral development. *Development* **122**: 3607-3616.
- Morin-Kensicki, E. M., and Eisen, J. S. 1997. Sclerotome development and peripheral nervous system segmentation in embryonic zebrafish. *Development* **124**: 159-167.
- Munsterberg, A. E., Kitajewski, J., Bumcrot, D. A., McMahon, A. P., and Lassar, A. B. 1995. Combinatorial signaling by Sonic hedgehog and Wnt family members induces myogenic bHLH gene expression in the somite. *Genes Dev.* **9**: 2911–2922.
- Nagy, A., Gocza, E., Diaz, E.M., Prideaux, V.R., Ivanyi, E., Markkula, M., and Rossant, J. 1990. Embryonic stem cells alone are able to support fetal development in the mouse. *Development* **110**: 815–821.
- Nicolet, G. 1970. Analyse autoradiographique de la localisation des différentes ébauches présomptives dans la ligne primitive de l’embryon de poulet. *J. Embryol. exp. Morph.* **23**: 79-108.
- Nicolet, G. 1971. Avian gastrulation. *Adv. Morphogen.* **9**: 231-262.
- Nonaka S, Tanaka Y, Okada Y, Takeda S, Harada A, Kanai Y, Kido M, Hirokawa N. 1998. Randomization of left-right asymmetry due to loss of nodal cilia generating leftward flow of extraembryonic fluid in mice lacking KIF3B motor protein. *Cell* **95**:829–837.
- Nornes, S., Mikkola, I., Krauss, S., Delghandi, M., Perander, M., and Johansen, T. 1996. Zebrafish Pax9 encodes two proteins with distinct C-terminal transactivating domains of different potency negatively regulated by adjacent N- terminal sequences. *Journal of Biological Chemistry* **271**: 26914-26923.
- Odenthal, J., Haffter, P., Vogelsang, E., Brand, M., van Eeden, F.J., Furutani-Seiki, M., Granato, M., Hammerschmidt, M., Heisenberg, C.P., Jiang, Y.J., et al. 1996. Mutations affecting the formation of the notochord in the zebrafish, *Danio rerio*. *Development* **123**: 103–115.
- Okada, Y., Nonaka, S., Tanaka, Y., Saijoh, Y., Hamada, H., and Hirokawa, N. 1999. Abnormal nodal flow precedes situs inversus in *iv* and *inv* mice. *Mol. Cell* **4**: 459-468.
- Pavlova, M. N., Clark, A.M., and Gossler, A. 1998. High-resolution mapping of the truncate (*tc*) locus on mouse Chromosome 6. *Mamm. Genome* **9**: 843–845.
- Peters, H., Doll, U., and Niessing, J. 1995. Differential expression of the chicken Pax1 and Pax9 gene: in situ hybridization and immunohistochemical analysis. *Developmental Dynamics* **203**: 1- 16.

- Placzek, M. 1995. The role of notochord and floor plate in inductive interactions. *Curr. Opin. Genet. Dev.* **5**, 499–506.
- Placzek, M., Dodd, J., and Jessell, T. M. 2000. Discussion point. The case for floor plate induction by the notochord. *Curr. Opin. Neurobiol.* **10**: 15–22.
- Placzek, M., Tessier-Lavigne, M., Yamada, T., Jessell, T., and Dodd, J. 1990. Mesodermal control of neural cell identity: Floor plate induction by the notochord. *Science* **250**: 985–988.
- Placzek, M., Yamada T., Tessier-Lavigne, M, Jessell, T., and Dodd, J. 1991. Control of dorsoventral pattern in vertebrate neural development: Induction and polarizing properties of the floor plate. *Development Suppl.* **2**: 105–122.
- Plouhinec, J. L., Granier, C., Le Mentec, C., Lawson, K. A., Saberan-Djoneidi, D., Aghion, J., Shi, D. L., Collignon, J., and Mazan, S. 2004. Identification of the mammalian Not via a phylogenomic approach. *Gene Expr. Patterns* **5**: 11-22.
- Pourquié, O., Coltey, M., Teillet, M.A., Ordahl, C., and Le Douarin, N.M. 1993. Control of dorsoventral patterning of somitic derivatives by notochord and floor plate. *Proc. Natl. Acad. Sci.* **90**: 5242–5246.
- Pownall, M. E., Strunk, K. E., and Emerson, C. P. 1996. Notochord signals control the transcriptional cascade of myogenic bHLH genes in somites of quail embryos. *Development* **122**: 1475–1488.
- Qian, Y.Q., Billeter, M., Otting, G., Muller, M., Gehring, W.J., and Wuthrich, K. 1989. The structure of the Antennapedia homeodomain determined by NMR spectroscopy in solution: Comparison with prokaryotic repressors. *Cell* **59**: 573–580.
- Ranson, M., Tickle, C., Mahon, K. A., and Mackem, S. 1995. Gnot1, a member of a new homeobox gene subfamily is expressed in a dynamic, region-specific domain along the proximodistal axis of the developing limb. *Mech. Dev.* **51**: 17-30.
- Rebagliati, M. R., Toyama, R., Fricke, C., Haffter, P., and Dawid, I. B. 1998. Zebrafish nodal-related genes are implicated in axial patterning and establishing left–right asymmetry. *Dev. Biol.* **199**: 261–272.
- Remak, R. 1850. *Untersuchungen über die Entwicklung der Wirbeltiere*. Berlin: Reimer
- Riddle, R. D., Johnson, R. L., Laufer, E. and Tabin, C. 1993. Sonic hedgehog mediates the polarizing activity of the ZPA. *Cell* **75**: 1401-1416.
- Roelink, H., Augsburger, A., Heemskerk, J., Korzh, V., Norlin, S., Ruiz i Altaba, A., Tanabe, Y., Placzek, M., Edlund, T., Jessell, T. M., and Dodd, J. 1994. Floor plate and motor neuron induction by vhh-1, a vertebrate homolog of hedgehog expressed by the notochord. *Cell* **76**: 761–775.
- Rosenquist, G. C. 1966. A radioautographic study of labeled grafts in the chick blastoderm. *Contr. Embryol. Carnegie Inst. Wash.* **38**: 71-110.
- Rosenquist, G. C. 1983. The chorda center in Hensen’s node of the chick embryo. *Anat. Rec.* **207**: 349-355.

- Ruiz i Altaba, A., Placzek, M., Baldassari, M., Dodd, J. and Jessell, T. M. 1995. Early stages of notochord and floor plate development in the chick embryo defined by normal and induced expression of HNF-3b. *Devl. Biol.* **170**: 299-313.
- Sasai, Y., Lu, B., Steinbeisser, H., Geissert, D., Gont, L. K., and De Robertis, E. M. 1994. Xenopus chordin: A novel dorsalizing factor activated by organizer-specific homeobox genes. *Cell* **79**: 779–790.
- Schoenwolf, G. C. 1992. Morphological and mapping studies of the paranodal and postnodal levels of the neural plate during chick neurulation. *Anat. Rec.* **233**: 281-290.
- Schoenwolf, G.C. 1984. Histological and ultrastructural studies of secondary neurulation in mouse embryos. *Am. J. Anat.* **169**: 361–376.
- Schoor, M., Schuster-Gossler, K., Roopenian, D., and Gossler, A. 1999. Skeletal dysplasias, growth retardation, reduced postnatal survival, and impaired fertility in mice lacking the SNF2/SWI2 family member ETL1. *Mech. Dev.* **85**: 73–83.
- Selleck, M. A. J. and Stern, C. D. 1991. Fate mapping and cell lineage analysis of Hensen’s node in the chick embryo. *Development* **112**: 615-626.
- Selleck, M. A. J. and Stern, C. D. 1992. Commitment of mesoderm cells in Hensen’s node of the chick embryo to notochord and somite. *Development* **114**: 403-415.
- Selleck, M.A. and Stern, C.D. 1991. Fate mapping and cell lineage analysis of Hensen’s node in the chick embryo. *Development* **112**: 615–626.
- Shamim, H., Mahmood, R., Logan, C., Doherty, P., Lumsden, A., and Mason, I. 1999. Sequential roles for Fgf4, En1 and Fgf8 in specification and regionalisation of the midbrain. *Development* **126**: 945–959.
- Simeone, A., Acampora, D., Gulisano, M., Stornaiuolo, A., and Boncinelli, E. 1992a. Nested expression domains of four homeobox genes in developing rostral brain. *Nature* **358**: 687– 690.
- Simeone, A., Gulisano, M., Acampora, D., Stornaiuolo, A., Rambaldi, M., and Boncinelli, E. 1992b. Two vertebrate homeobox genes related to the *Drosophila* empty spiracles gene are expressed in the embryonic cerebral cortex. *EMBO J.* **11**: 2541–2550.
- Smith, J. L., and Schoenwolf, G. C. 1989. Notochordal induction of cell wedging in the chick neural plate and its role in neural tube formation. *J. Exp. Zool.* **250**: 49–62.
- Smith, S. T., and Jaynes, J. B. 1996. A conserved region of engrailed, shared among all en-, gsc-, Nk1-, Nk2- and msh-class homeoproteins, mediates active transcription repression in vivo. *Development* **122**: 3141-3150.
- Smith, S.T. and Jaynes, J.B. 1996. A conserved region of engrailed, shared among all en-, gsc-, Nk1-, Nk2- and msh-class homeoproteins, mediates active transcriptional repression in vivo. *Development* **122**: 3141–3150.
- Smith, W. C., and Harland, R. M. 1992. Expression cloning of noggin, a new dorsalizing factor localized to the Spemann organizer in Xenopus embryos. *Cell* **70**: 829–840.
- Spemann, H. 1938. “Embryonic Development and Induction.” Yale Univ. Press, New Haven, CT.

- Spratt, N. T. 1955. Analysis of the organizer center in the chick embryo. I Localization of notochord and somite cells. *J. Exp. Zool.* **128**: 121-163.
- Stein, S. and Kessel, M. 1995. A homeobox gene involved in node, notochord and neural plate formation of chick embryos. *Mech. Dev.* **49**: 37-48.
- Stein, S., Niss, K., and Kessel, M. 1996. Differential activation of the clustered homeobox genes CNOT2 and CNOT1 during notogenesis in the chick. *Dev. Biol.* **180**: 519-533.
- Stern, C. D. 1994. The avian embryo: a powerful model system for studying neural induction. *FASEB J.* **8**: 687-691.
- Stern, C. D., and Foley, A. C. 1998. Molecular dissection of Hox gene induction and maintenance in the hindbrain. *Cell* **94**: 143-145.
- Stern, C. D., Yu, R. T., Kakizuka, A., Kintner, C. R., Mathews, L. S., Vale, W. W., Evans, R. M. and Umesono, K. 1995. Activin and its receptors during gastrulation and the later phases of mesoderm development in the chick embryo. *Dev. Biol.* **172**: 192-205.
- Stickney, H. L., Barresi, M. J., and Devoto, S. H. 2000. Somite development in zebrafish. *Developmental Dynamics* **219**: 287-303.
- Storey, K. G., Crossley, J. M., De Robertis, E. M., Norris, W. E. and Stern, C. D. 1992. Neural induction and regionalisation in the chick embryo. *Development* **114**: 729-741.
- Streit, A., Stern, C. D., Théry, C., Ireland, G. W., Aparicio, S., Sharpe, M. and Gherardi, E. 1995. A role for HGF/SF in neural induction and its expression in Hensen's node during gastrulation. *Development* **121**: 813-824.
- Streit, A., Théry, C. and Stern, C. D. 1994. Of mice and frogs. *Trends Genet.* **10**: 181-183.
- Strudel, G. 1955. L'action morphogène du tube nerveux et de la corde sur la différenciation des vertèbres et des muscles vertébraux chez l'embryon de poulet. *Archives d'Anatomie Microscopique et de morphologie Experimentale* **44**: 209-235.
- Subramaniam, V., Jovin, T.M., and Rivera-Pomar, R.V. 2001. Aromatic amino acids are critical for stability of the bicoid homeodomain. *J. Biol. Chem.* **276**: 21506-21511.
- Sulik, K., Dehart, D. B., Iangaki, T., Carson, J. L., Vrablic, T., Gesteland, K. and Schoenwolf, G. C. 1994. Morphogenesis of the murine node and notochordal plate. *Dev. Dyn.* **201**: 260-278.
- Sumoy, L., Keasey, J. B., Dittman, T. D., and Kimelman, D. 1997. A role for notochord in axial vascular development revealed by analysis of phenotype and the expression of VEGF-2 in zebrafish *flh* and *ntl* mutant embryos. *Mech. Dev.* **63**: 15-27.
- Talbot, W. S., Trevarrow, B., Halpern, M.E., Melby, A.E., Farr, G., Postlethwait, J.H., Jowett, T., Kimmel, C.B., and Kimelman, D. 1995. A homeobox gene essential for zebrafish notochord development. *Nature* **378**: 150-157.
- Tam, P. P. L., and Beddington, R. S. P. 1987. The formation of mesodermal tissues in the mouse embryo during gastrulation and early organogenesis. *Development* **99**: 109-126.



- Tam, P. P., Steiner, K.A., Zhou, S.X., and Quinlan, G.A. 1997. Lineage and functional analyses of the mouse organizer. *Cold Spring Harb. Symp. Quant. Biol.* **62**: 135–144.
- Tanabe, Y., Roelink, H., and Jessell, T. M. 1995. Induction of motor neurons by Sonic hedgehog is independent of floor plate differentiation. *Curr. Biol.* **5**: 651–658.
- Teillet, M. A., Lapointe, F., and Le Douarin, N. M. 1998. The relationships between notochord and floor plate in vertebrate development revisited. *Proc. Natl. Acad. Sci. USA* **95**: 11733–11738.
- Theiler, K. 1959. Anatomy and development of the ‘truncate’ (boneless) mutation in the mouse. *Am. J. Anat.* **104**: 319–343. ———. 1988. *Vertebral malformations*. Springer Verlag, Berlin, Heidelberg, New York.
- Tonegawa, A., Funayama, N., Ueno, N., and Takahashi, Y. 1997. Mesodermal subdivision along the mediolateral axis in chicken controlled by different concentrations of BMP-4. *Development* **124**: 1975–1984.
- van Straaten, H. W. M., and Drukker, J. 1987. Influence of the notochord on the morphogenesis of the neural tube. In *Mesenchymal-Epithelial interactions in neural Development* (J.R. Wolff et al., eds.). Berlin: Springer-Verlag. (NATO/ASI Series vol. H5) pp. 153–162.
- van Straaten, H. W., Hekking, J. W., Wiertz-Hoessels, E. J., Thors, F., and Drukker, J. 1988. Effect of the notochord on the differentiation of a floor plate area in the neural tube of the chick embryo. *Anat. Embryol. (Berlin)* **177**: 317–324.
- van Straaten, H.W. and Hekking, J.W. 1991. Development of floor plate, neurons and axonal outgrowth pattern in the early spinal cord of the notochord-deficient chick embryo. *Anat. Embryol. Berl.* **184**: 55–63.
- van Straaten, H.W.M., Thors, F., Wiertz-Hoessels, L., Hekking, J., and Drukker, J. 1985. Effect of a notochordal implant on the early morphogenesis of the neural tube and neuroblasts: Histometrical and histological results. *Dev. Biol.* **110**: 247–254.
- Verbout, A. J. 1976. A critical review of the ‘neugliederung’ concept in relation to the development of the vertebral column. *Acta Biotheoretica* **25**: 219–258.
- Verbout, A. J. 1985. The development of the vertebral column. *Advances in Anatomy Embryology and Cell Biology* **90**: 1–122.
- Vogel, G. 1998. Embryo’s organizational chart redrawn. *Science* **280**: 1838–1839.
- von Dassow, G., Schmidt, J.E., and Kimelman, D. 1993. Induction of the *Xenopus* organizer: Expression and regulation of Xnot, a novel FGF and activin-regulated homeo box gene. *Genes & Dev.* **7**: 355–366.
- Waddington, C. H. 1932. Experiments on the development of chick and duck embryos, cultivated in vitro. *Phil. Trans. R. Soc. Lond. B* **221**: 179–230.
- Waddington, C. H. 1933. Induction by the primitive streak and its derivatives in the chick. *J. Exp. Biol.* **10**: 38–46.
- Watanabe, Y., Duprez, D., Monsoro-Burq, A. H., Vincent, C., and Le Douarin, N. M. 1998. Two domains in vertebral development: Antagonistic regulation by SHH and BMP4 proteins. *Development* **125**: 2631–2639.

- Watterson, R. L., Fowler, I., and Fowler, B. G. 1954. The role of the neural tube and notochord in development of the axial skeleton of the chick. *American Journal of Anatomy* **95**: 337-399.
- Weinberg, E. S., Allende, M. L., Kelly, C. S., Abdelhamid, A., Murakami, T., Andermann P., Doerre, O. G., Grunwald, D. J., and Riggleman, B. 1996. Developmental regulation of zebrafish MyoD in wild-type, no tail and spadetail embryos. *Development* **122**: 271-280
- Weinstein, D.C., Ruiz i Altaba, A., Chen, W. S., Hoodless, P., Prezioso, V.R., Jessell, T.M., and Darnell Jr., J.E. 1994. The winged-helix transcription factor HNF-3 $\beta$  is required for notochord development in the mouse embryo. *Cell* **78**: 575-588.
- Wilkinson, D.G. 1992. Whole mount in situ hybridization of vertebrate embryos. In *In situ hybridization: A practical approach* (ed. D.G. Wilkinson), pp. 75-84. Oxford University Press, Oxford, UK.
- Williams, N. A., and Holland, P.W. 2000. An amphioxus Emx homeobox gene reveals duplication during vertebrate evolution. *Mol. Biol. Evol.* **17**: 1520-1528.
- Wilson, V. and Beddington, R.S.P. 1996. Cell fate and morphogenetic movement in the late mouse primitive streak. *Mech. Dev.* **55**: 79-89.
- Wolpert, L., Beddington, R., Jessel, T., Lawrens, P., Meyerowitz, E., and Smith, J. 2002. *Principles of Development*, 2<sup>nd</sup> edition. Oxford University Press, Oxford, UK.
- Wood, W. B. 1997. Left-right asymmetry in animal development. *Annu. Rev. Cell Dev. Biol.* **13**: 53-82.
- Xue, X. J., and Xue, Z. G. 1996. Spatial and temporal effects of axial structures on myogenesis of developing somites. *Mech. Dev.* **60**: 73-82.
- Yamada, T., Placzek, M., Tanaka, H., Dodd, J., and Jessell, T.M. 1991. Control of cell pattern in the developing nervous system: Polarizing activity of the floor plate and notochord. *Cell* **64**: 635-647.
- Yamagishi, T., Nakajima, Y., and Nakamura, H. 1999. Expression of TGFbeta3 RNA during chick embryogenesis: A possible important role in cardiovascular development. *Cell Tissue Res*, **298**: 85-93.
- Yasuo, H. and Lemaire, P. 2001. Role of Goosecoid, Xnot and Wnt antagonists in the maintenance of the notochord genetic programme in *Xenopus* gastrulae. *Development* **128**: 3783-3793.
- Youn, B. W., and Malacinski, G. M. 1981. Axial structure development in ultraviolet-irradiated (notochord-defective) amphibian embryos. *Dev. Biol.* **83**: 339-352.

## 6. Appendix

### 6.1 Abbreviations

(v/v)	(volume/volume)
(w/v)	(weight/volume)
%	percent
°C	Degree Centigrade
μ	micro= 10 <sup>-6</sup>
A <sub>260</sub>	Absorbance at 260
A <sub>280</sub>	Absorbance at 280
ATP	Adenosine Triphosphate
bp	base pair
BSA	Bovine Serum Albumin
cDNA	Complementary Deoxyribonucleic Acid
cpm	Counts per minute
DEPC	diethylpyrocarbonate
DMEM	Dulbecco's modified Eagle's medium
DMSO	Dimethyl sulfoxide
DNA	Deoxyribonucleic Acid
DNase	Deoxyribonuclease
dNTP	2'-deoxynucleotide-5'-triphosphate
DT	Diphtheria ToxinA
DTT	Dithiothreitol
EDTA	Ethylene diamine tetrasodium acetate
ES	Embryonic Stem
FCS	Fetal Calf Serum
g	gram(me)
h	hour(s)
HEPES	N-(2-Hydroxyethyl)piperazine-N-(2-Ethanesulfonic Acid)
IPTG	Isopropyl-β-D-thiogalactopyranosid
K	Kilo= 10 <sup>3</sup>

---

kb	kilobase
l	liter
LB	Luria-Bertani medium
m	milli= $10^{-3}$
M	Molar
min	minute
MOPS	3-(N-Morpholino)propanesulfonic Acid
n	nano= $10^{-9}$
OD	Optical Density
ORF	Open reading frame
p	pico= $10^{-12}$
PBS	Phosphate-Buffered Saline
PCR	Polymerase Chain Reaction
pH	Potentia hydrogenii
puro	<i>Puromycin</i>
RNA	Ribonucleic Acid
RNase	Ribonuclease
rpm	revolutions per minute
RT	Room Temperature
RT-PCR	Reverse Transcription-PCR
SDS	Sodium Dodecyl Sulfate
sec	second
T°	Temperature
TE	Tris-EDTA
TEMED	N,N,N',N'-Tetramethylethylenediamine
Tris	Tris-(hydroxymethyl)-aminomethane
t-RNA	transfer-RNA
U	unit
V	Volt (unit)
x g	g force
X-Gal	5-Brom-4-chlor-3-indolyl- $\beta$ -D-galactopyranosid

## 6.2 List of cloned constructs

### List of expression plasmids

**Not MT:** *Not* ORF was amplified by PCR with the primer pairs notORF-F3 and notORF-B3, generating BamHI in 5' and ClaI in 3' and cloned in a pGEM-TEasy vector. The insert BamHI/ClaI was subcloned into BamHI/ClaI in a pCS2-MT expression vector.

**Not tc MT:** *Not* ORF from the truncate mutant was amplified by PCR with the primer pairs notORF-F3 and notORF-B3, generating BamHI in 5' and ClaI in 3' and cloned in a pGEM-TEasy vector. The insert BamHI/ClaI was subcloned into BamHI/ClaI in a pCS2-MT expression vector.

**Foxa2 MT:** *Foxa2* ORF was amplified by PCR with the primer pairs Foxa2-F1 and Foxa2-B1, generating BamHI in 5' and ClaI in 3' and cloned in a pGEM-TEasy vector. The insert BamHI/ClaI was subcloned into BamHI/ClaI in a pCS2-MT expression vector.

**En2 MT:** *En2* ORF was amplified by PCR with the primer pairs En2-F1 and En2-B1, generating BamHI in 5' and Sall in 3' and cloned in a pGEM-TEasy vector. The insert BamHI/Sall blunted ends in Sall was subcloned into BamHI/ClaI blunted ends in ClaI in a pCS2-MT expression vector.

**Not pCS2:** *Not* ORF was amplified by PCR with the primer pairs notORF-F3 and notORF-B3, generating BamHI in 5' and ClaI in 3' cloned in a pGEM-TEasy vector. The insert BamHI/ClaI subcloned into BamHI/ClaI in pCS2 expression vector.

**Not tc pCS2:** *Not* ORF from truncate mutant was amplified by PCR with the primer pairs notORF-F3 and notORF-B3, generating BamHI in 5' and ClaI in 3' and cloned in a pGEM-TEasy vector. The insert BamHI/ClaI was subcloned into BamHI/ClaI in a pCS2 expression vector.

**Foxa2 pCS2:** *Foxa2* ORF was amplified by PCR with the primer pairs Foxa2-F1 and Foxa2-B1, generating BamHI in 5' and ClaI in 3' and cloned in a pGEM-TEasy vector. The insert BamHI/ClaI was subcloned into BamHI/ClaI in a pCS2 expression vector.

**En2 pCS2:** *En2* ORF was amplified by PCR with the primer pairs En2-F1 and En2-B1, generating BamHI in 5' and Sall in 3' and cloned in a pGEM-TEasy vector. The insert BamHI/Sall blunted ends in Sall was subcloned, into BamHI/ClaI blunted ends in ClaI, in a pCS2 expression vector.

**Not HA:** *Not* ORF was amplified by PCR with the primer pairs notORF-F3 and notORF-B3, generating BamHI in 5' and Sall in 3' and cloned in a pGEM-TEasy vector. The insert BamHI/Sall was subcloned into BamHI/Sall in a pQE30 expression vector.

**Not tc HA:** *Not* ORF from truncate mutant was amplified by PCR with the primer pairs notORF-F3 and notORF-B3, generating BamHI in 5' and Sall in 3' and cloned in a pGEM-TEasy vector. The insert BamHI/Sall was subcloned into BamHI/Sall in a pQE30 expression vector.

**Foxa2 HA:** *Foxa2* ORF was amplified by PCR with the primer pairs Foxa2-F1 and Foxa2-B1, generating BamHI in 5' and Sall in 3' and cloned in a pGEM-TEasy vector. The insert BamHI/Sall was subcloned into BamHI/Sall in a pQE30 expression vector.

**En2 HA:** *En2* ORF was amplified by PCR with the primer pairs En2-F1 and En2-B1, generating BamHI in 5' and Sall in 3' and cloned in a pGEM-TEasy vector. The insert BamHI/Sall was subcloned into BamHI/Sall in a pQE30 expression vector.

**Not GST:** *Not* ORF was amplified by PCR with the primer pairs notORF-F3 and notORF-B3, generating BamHI in 5' and Sall in 3' and cloned in a pGEM-TEasy vector. The insert BamHI/Sall was subcloned into BamHI/Sall in a pGEX4T-1 expression vector.

**Not tc GST:** *Not* ORF from truncate mutant was amplified by PCR with the primer pairs notORF-F3 and notORF-B3, generating BamHI in 5' and Sall in 3' and cloned in a pGEM-TEasy vector. The insert BamHI/Sall was subcloned into BamHI/Sall in a pGEX4T-1 expression vector.

**Foxa2 GST:** *Foxa2* ORF was amplified by PCR with the primer pairs Foxa2-F1 and Foxa2-B1, generating BamHI in 5' and Sall in 3' and cloned in a pGEM-TEasy vector. The insert BamHI/Sall was subcloned into BamHI/Sall in a pGEX4T-1 expression vector.

**En2 GST:** *En2* ORF was amplified by PCR with the primer pairs En2-F1 and En2-B1, generating BamHI in 5' and Sall in 3' and cloned in a pGEM-TEasy vector. The insert BamHI/Sall was subcloned into BamHI/Sall in a pGEX4T-1 expression vector.

**VP16 NotHDwt:** activator domain VP16 was amplified by PCR with the primer pairs VP16-F1 and VP16-B1, generating EcoRI and ATG in 5' and XhoI in 3' and cloned in a pGEM-TEasy vector. *Not* homeodomain from wild type was amplified by PCR with the primer pairs nHD-F1 and nHD-B1, generating XhoI in 5' and XbaI in 3' and cloned in a pGEM-TEasy vector. The VP16 insert EcoRI/ XhoI and *Not* wt homeodomain insert XhoI/XbaI were cloned into EcoRI/XbaI in a pCS2 expression vector.

**VP16 NotHDtc:** activator domain VP16 was amplified by PCR with the primer pairs VP16-F1 and VP16-B1, generating EcoRI and ATG in 5' and XhoI in 3' and cloned in a pGEM-TEasy

vector. *Not* homeodomain from truncate mutant was amplified by PCR with the primer pairs nHD-F1 and nHD-B1, generating XhoI in 5' and XbaI in 3' and cloned in a pGEM-TEasy vector. The VP16 insert EcoRI/XhoI and *Not* tc homeodomain insert XhoI/XbaI were cloned into EcoRI/XbaI in a pCS2 expression vector.

**ENG-N NotHDwt:** *Not* homeodomain from wild type was amplified by PCR with the primer pairs nHD-F2 and nHD-B1, generating SpeI in 5' and XbaI in 3' and cloned in a pGEM-TEasy vector. The insert *Not* wt homeodomain SpeI/XbaI was subcloned into SpeI/XbaI in a pCS2 expression vector containing Engrailed Repressor domain ENG-N.

**ENG-N NotHDtc:** *Not* homeodomain from truncate mutant was amplified by PCR with the primer pairs nHD-F2 and nHD-B1, generating SpeI in 5' and XbaI in 3' and cloned in a pGEM-TEasy vector. The insert *Not* tc homeodomain SpeI/XbaI was subcloned into SpeI/XbaI in a pCS2 expression vector containing Engrailed Repressor domain ENG-N.

#### **List of *Not* promoter-luciferase reporter plasmids**

**Not pr Luc:** 12kb of genomic DNA from 5' of *Not* locus ,where in 3' end was generated a HindIII site with the primer pairs not1LacZ-F1 and not1LacZ-B4, was cloned in pCR-XL-TOPO. The insert HindIII was subcloned in frame with Exon2 into HindIII in a pGL3-Basic vector.

**Not fgII Luc:** 6.3kb of genomic DNA from 5' of *Not* locus ,where in 3' end was generated a HindIII site with the primer pairs not1LacZ-F1 and not1LacZ-B4, was cloned in pCR-XL-TOPO. The insert HindIII was subcloned in frame with Exon2 into HindIII in a pGL3-Basic vector.

**Not fgIII Luc:** 9.3kb of genomic DNA from 5' of *Not* locus ,where in 3' end was generated a HindIII site with the primer pairs not1LacZ-F1 and not1LacZ-B4, was cloned in a pCR-XL-TOPO. The insert HindIII was subcloned in frame with Exon2 into HindIII in a pGL3-Basic vector.

**Not ATGfgII Luc:** 5kb of genomic DNA upstream of ATG from 5' of *Not* locus ,where in 3' end was generated XhoI site before ATG with the primer pairs not1LacZ-F1 and not1LacZ-B3, was cloned in a pCR-XL-TOPO. The insert MluI/XhoI was subcloned into MluI/XhoI in a pGL3-Basic vector.

**List of *Not* promoter-*Lac Z* reporter constructs**

**Not pr Lac Z:** 12kb of genomic DNA from 5' sequence of *Not* locus ,which contains a generated HindIII site in 3' end with the primer pairs not1LacZ-F1 and not1LacZ-B4, was cloned in a pCR-XL-TOPO. The insert SpeI/HindIII was subcloned in frame in Exon2 with *Lac Z* gene into SpeI/HindIII in a pBSKII.

To make a *lacZ* transgene: the insert was released with XhoI/NotI enzymes for microinjection.

**Not fgII Lac Z:** 6.3kb of genomic DNA from 5' sequence of *Not* locus ,where in 3' end was generated a HindIII site with the primer pairs not1LacZ-F1 and not1LacZ-B4, was cloned in a pCR-XL-TOPO. The insert SpeI/HindIII was subcloned in frame in Exon2 with *Lac Z* gene into SpeI/HindIII in a pBSKII.

**Not fgIII Lac Z:** 9.3kb of genomic DNA from 5' sequence of *Not* locus ,where in 3' end was generated a HindIII site with the primer pairs not1LacZ-F1 and not1LacZ-B4, was cloned in a pCR-XL-TOPO. The insert SpeI/HindIII was subcloned in frame in Exon2 with *Lac Z* gene into SpeI/HindIII in a pBSKII.

**Targeting Construct for Rescue Experiment**

The targeting vector for the rescue experiment was designed as follows: a replacement vector that contained the wild type exon2 sequence in its 5' region of homology. 11kb of genomic DNA of the *Not* locus including the three exons were used to make the targeting construct. A Diphtheria ToxinA expression cassette (pKO SelectDT; Lexicon Genetics) was cloned upstream of the 5'homology arm. A PGKpuro selection cassette flanked by *loxP* sites was cloned in intron2 into SspI site, approximately 180bp downstream of exon2 (Fig. 11A).



## Acknowledgements

*I would like to express my gratitude to Prof.Dr. Achim Gossler (Institute for Molecular Biology, Medical School of Hannover) for his direct supervision, continuous support, assistance and advice during my PhD.*

*I would also like to thank Dr.Janet Rossant (Samuel Lunenfeld Research Institute, Canada), Dr.Bernhard G. Herrmann (Max-Planck-Institute, Berlin) and Dr.Rolando Rivera-Pomar (Max-Planck-Institute for Biophysical Chemistry, Göttingen) for their collaboration in this work.*

*I would also like to thank Dr. T. Ley and the Embryonic Stem Cell Core of the Siteman Cancer Center (Washington University Medical School, St Louis, MO) for the Turbo-Cre plasmid.*

*I am very grateful to Dr.Karin Schuster-Gossler for the injections of ES cells and the transgene.*

*I am grateful for the excellent technical assistance of Ms. Hannelore Burkhardt in ES culture work.*

*I sincerely thank my colleague Dr. Katrin Serth who introduced me to my project at the beginning.*

*This work was supported by a grant from the German Research Council to A.G. (DGF Go449/6-1), and by the German Federal Ministry of Education and Research (BMBF) to R.R. (DHGP-2 Project 01 KW 0001).*

## **A token of appreciation**

*I am very grateful for the discussions and comments during the Seminars organized weekly by members of the Molecular Biology Institute and internal seminars organized weekly by members of our lab.*

*I would like to express my gratitude to Prof.Dr. Achim Gossler for comments and discussions. I appreciate his interest in different forms of expression (gene expression but also other forms of life expression such as Art and Music) with a touch of discretion.*

*I would also like to thank my colleagues Dr. Andre Schneider and especially Dr. Katrin Serth, Dr. Ralf Cordes and Dr. Natalia Schröder for comments and advice.*

*I sincerely thank Dr.Karin Schuster-Gossler and Prof. Dr. Achim Gossler for their nice invitations to all members of the lab. I also appreciate her gastronomic talent (at preparing cosmopolitan cuisine).*

*I sincerely thank my colleague Dr. Jürgen Mertsching for his friendship and for sharing ideas and comments concerning research. I will also remember the nice time enjoying good music in (Kanappe, Jazz-club).*

*I will also remember the nice time I had together with my colleague Dr. Katrin Serth and her partner, in (Plümecke, Steinhudermeer, Markt-halle).*

*I would also like to thank Ms. Ann Bochert for her help concerning burocratic matters.*

*I would also like to thank Herr. Anatoli Heiser for his help concerning mice.*

*I would like to thank my other colleagues Masami, Insa, Anja, Julia, Leonie, Juliana, Patricia (always smiling and having full power) and Hannelore Burkhardt (I will always remember her listening sometimes to classical music while working “I imagine the classical notes as microcentrifuge tubes“ and her dry sense of humor).*

*Thanks to my colleagues Stephan and especially Aravind for being positively special in both aspects (as a scientist and as a person).*

*I would like to thank Prof.Dr. Andreas Kispert for comments and discussions. I appreciate his perfectionism and his refined sense of humor. Thanks to all the members of his lab. Henner, Oliver, Markus, Rannar, Christian, Marianne and especially to Manvendra.*

*I would like to thank Dr. Nisar Malek for comments and discussions. I appreciate him being positive and his sense of humor with an American touch. Thanks to all the members of his lab. Kristine, Holly, Jörg, Nils, Sangita, Susanne, Inke and especially, to Uta for sharing many good times.*

*Special thanks to Dr. Utz Krug and his partner Dr. Katerin Sperveslage for their great friendship (being there in the good and in the bead times).*

*Special thanks to my partner for his patience, support and respect.*

*Special thanks to my lovely parents and lovely sisters for their support.*

# Curriculum Vitae

## Personal data:

**Name:** Hanaa Ben Abdelkhalek  
**Date of birth:** December 14<sup>th</sup>, 1970  
**Nationality:** Moroccan  
**Adresse:** Gerber str 3A, 30169 Hannover  
**Phone no.:** 0511 – 1691457

## Basic and academic education:

**1976-1981:** “Ibn Khaldoun” elementary school, Larache, Morocco.  
**1981-1985:** Junior high school, Larache, Morocco.  
**1985-1989:** “Moulay Abdellah” senior high school, Larache, Morocco. Concluded with the Bachelor of Natural Science.  
**1989-1993:** Studies in biological sciences at the faculty “Abdelmalek Essaadi”, **University of Tetuan**, Morocco. Concluded with the Degree of Biology.  
**1993-1996:** Studies in pharmaceutical sciences at the **University of Granada**, Spain.  
**1996-2000:** Ph.D. studies in microbiology and molecular biology focused on plants at the **University of Granada**, Spain.  
**2002-2005:** **Ph.D.** Research focused on developmental biology of the mouse (as a model), **Institute for Molecular Biology at Medical School of Hannover**, Germany.

## Postgraduate courses:

- **Molecular Biology of Plants** (1996-1997)
- **Genetic Manipulation Applied to Agricultural Development** (1996-1997)
- **Vegetable Biotechnology** (1996-1997)
- **Analysis and Nutritional Diagnostic of Plants** (1997-1998)
- **Models of Variation Analysis and Associated Problems** (1997-1998)
- **Agricultural Biotechnology and Applications: Environmental Risks** (1997-1998)
- **Purification of Proteins** (1997-1998)
- **Molecular-biological Advances in the Reproduction of Superior Plants: Agricultural Applications** (1998-1999)
- **Physiology of Plants under Extreme Conditions** (1998-1999)
- **Nitrogen Biology** (1998-1999)

## Other academic activities:

- Attendance to the “**Jornadas de Hongos y Setas**” (Conference on Fungi and Mushrooms), 1995, Faculty of Pharmacy, University of Granada, Spain.
- Participation at the IV. Reunion of the project ”**Nitrogen Fixation and Yield of Grain Legume in Saline Mediterranean Zones**”, organized by the FYSAME and FABAMED investigation groups, June 25<sup>th</sup> – 28<sup>th</sup>, 1997, Granada, Spain.
- Attendance to the “**I. Curso de Investigaciones Biotecnológicas**” (First Course on Biotechnological Investigation), March 2000, Faculty of Science, University of Granada, Spain.
- Attendance to the ”**Gene Technology Security Course**”, **State-approved Course § 15 Gen TSV for Project Leaders and Biosafety Officers**, September 13<sup>th</sup> – 14<sup>th</sup>, 2004, Medical School of Hannover, Germany

## Organization engagements:

- Member of the “**Sociedad Española de Microbiología**” (Spanish Microbiological Society), 1998-1999.
- Member of the “**American Society of Microbiology**”, 1998-2000.

## List of Main Publications:

- M. Soussi, **H. Ben Abdelkhalek**, C. Lluch and A. Ocaña. September 23<sup>rd</sup> – 26<sup>th</sup>, 1997. “Respuesta de la simbiosis *Cicer arietinum* – *Rhizobium ciceria* a distintas dosis de NaCl aplicadas en el crecimiento vegetativo” (Response of the *Cicer arietinum* – *Rhizobium ciceri* symbiosis to different NaCl doses applied to the vegetative growth). **V. Congreso Hispano-Luso de Fisiología Vegetal y XII. Reunión Nacional de la SEFV** (V. Spanish-Portuguese Congress on Vegetable Physiology / XII. National SEFV Reunion), Cordoba, Spain.
- M. Khadri, L. Pliego, **H. Ben Abdekhalek** and C. Lluch. September 25<sup>th</sup>, 1998. “Influencia del Nitrato en el contenido de Macronutrientes en la simbiosis *Phaseolus vulgaris* – *Rhizobium tropici*” (Influence of Nitrate on the content of Macronutrients in the *Phaseolus vulgaris* – *Rhizobium tropici* symbiosis). Communication at the **VII Simposio Nacional - III. Iberico sobre la Nutrición Mineral de las Plantas** (VII. National/III. Iberian Symposium about Mineral Nutrition of Plants), Madrid, Spain.
- **H. Ben Abdekhalek**, A. Ocaña, J. Sanjuan and C. Lluch. September 19<sup>th</sup> – 22<sup>nd</sup>, 1999. “Obtención de Cepas Isogénicas de *Rhizobium etlii* tolerantes a la sal: Contribución de la simbiosis en plantas de judía” (Obtainment of isogenic salt-tolerant strains of *Rhizobium etlii*: Contribution in the symbiosis of bean plants). **XIII. Reunión de la Sociedad Española de Fisiología Vegetal y VI. Congreso Hispano-Luso de Fisiología Vegetal** (XIII. Reunion of the Spanish Society of Vegetable Physiology/VI. Spanish-Portuguese Congress of Vegetable Physiology), Sevilla, Spain.

- **H. Ben Abdelkhalek**, C. Lluch, J. Olivares and J. Sanjuan. April 3<sup>rd</sup> – 5<sup>th</sup>, 2000. “Selection of rhizobial strains with increased tolerance to sodium chloride to improve symbiotic nitrogen fixation and plant growth”. **European Cost 830 Workshop on Selection Strategies for Plant-beneficial Microorganisms**, Nancy-Champenoux, France.
- J. Sanjuan, **H. Ben Abdelkhalek**, J. Nogales, R. Campos, J. Olivares and C. Lluch. July 9<sup>th</sup> – 13<sup>th</sup>, 2000. “*Rhizobium tropici* ciat899 genes involved in free-living tolerance to sodium chloride are also required for nitrogen fixation in symbiosis with *Phaseolus vulgaris*”. **Conférence Méditerranéenne de Rhizobiologie** (Mediterranean Conference of Rhizobiology), Montpellier, France.
- **Ben Abdelkhalek,H.\***, Beckers,A.\*, Schuster-Gossler,K.\*, Pavlova,M.N., Burkhardt,H., Lickert,H., Rossant,J., Reinhardt,R., Schalkwyk,L.C., Muller,I., Herrmann,B.G., Ceolin,M., Rivera-Pomar,R. and Gossler,A. 2004. **The mouse homeobox gene Not is required for caudal notochord development and affected by the truncate mutation**. *Genes & Dev.* **18**:1725-1736.

\* (equal contribution)

## **Language skills:**

<b>Arabic/French:</b>	Bilingual education since the age of five.
<b>Spanish:</b>	Two years of studies at the Centre of Spanish Culture of Tetuan, Morocco, and seven years of residence in Granada, Spain. Fluently.
<b>English:</b>	Four years of studies at the junior high school, followed by two summers in England to practice. Nearly fluently.
<b>German:</b>	Good knowledge.